NSIDE TRACK with
KYWORKS'
AVID
LDRICH p28

SIZING UP
RF/MICROWAVE
SEMICONDUCTORS p37

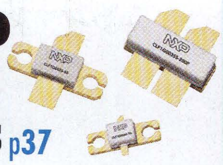

RECEIVER
SERVES MANY
STANDARDS p50

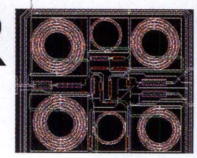

MicroWaves&RF

EBRUARY 2013 TRUSTED ENGINEERING RESOURCE FOR 50 YEARS www.MWRF.com

SEMICONDUCTOR ISSUE

DROs Drop Phase-Noise Levels

A PENTON PUBLICATION Periodicals Postage Paid • USPS 100 Approved Poly

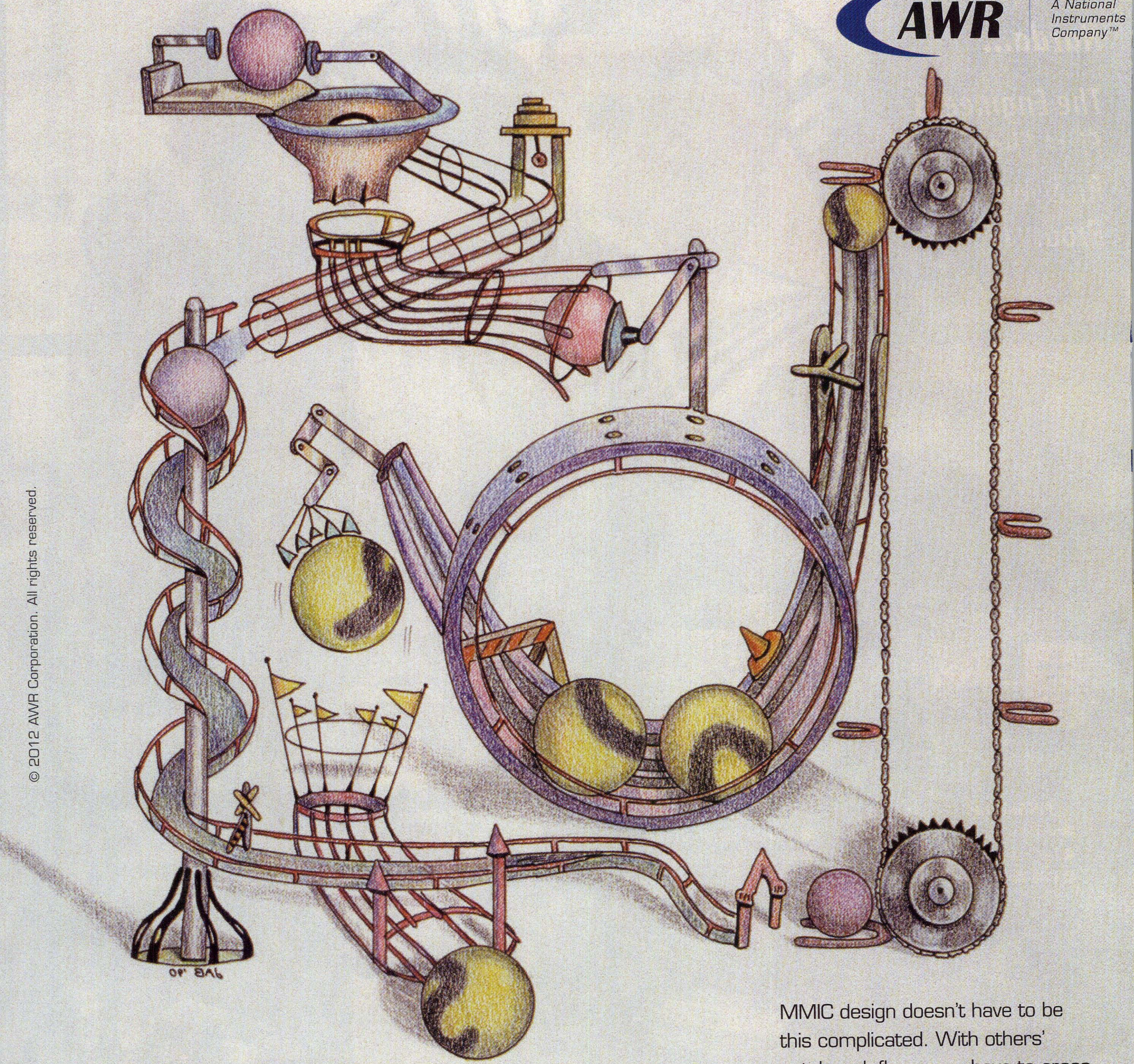

FEBRUARY | 2013
Volume 52, Issue 2

MicroWaves&RF

CONTENTS

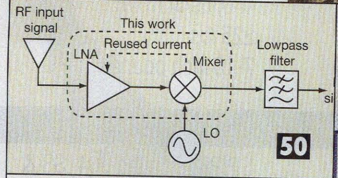

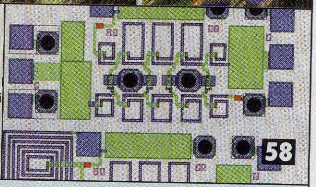

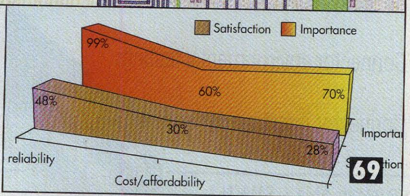

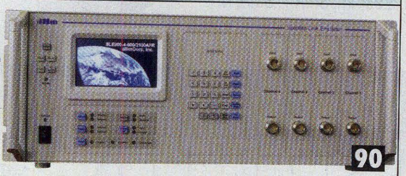

INDUSTRY TRENDS AND ANALYSIS

DESIGN FEATURES

PRODUCT TECHNOLOGY

COVER STORY

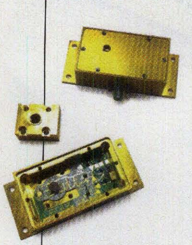

NEWS & COLUMNS

Penton
Design Engineering & Sourcing Group

Rosenberger® Rmor™ Cables Assembly

PHASE STABLE THROUGH 70GHz

Rosenberger Rmor™ cables are designed for rugged environments for indoor and outdoor applications. Each shielded coaxial cable is protected with flexible, SPIRAL-wound 304 Stainless Steel armor coated with extruded Polyurethane. The connector ends are sealed and encapsulated with a pressure injection-molded polymer strain relief.

This combination of materials and technology provides superior ruggedization, environmental resistance, RF shielding effectiveness and stability under flexure and vibration.

Additional connector interfaces and armor/cable diameters are available on request.

DESCRIPTION

Rosenberger connectors, cable assembly, standard length 915mm or 36 inches

GENERAL ELECTRICAL SPECIFICATIONS

Impedance:	50 +/- 1 Ohms
Operating frequency:	DC to 70 GHz
Return loss:	14 dB minimum up to 70 GHz
Cable insertion loss:	.67 dB/ft @ 10.0 GHz
Velocity of propagation (%):	78 % nominal
Capacitance:	24.7 pf/ft. nominal
Shielding effectiveness:	< -90 dB
Dielectric withstand voltage:	1000 Vrms
Amplitude & phase stable:	+/- .03dB & +/- 1° @10GHz

MECHANICAL SPECIFICATION

Cable jacket & armor outer diameter:	092 inches nominal & .250 inches nominal
Minimum bend radius:	.5 inches
Armor crush strength:	450 lbs/in (min)
Connector retention:	≥25 lbs.
Mating torque:	7-10 inch pounds

MATERIALS AND FINISHES

Armor type:	SPIRAL-wound 304 SS & Polyurethane blue jacket
Connector environmental testing:	Per MIL-STD-202, Meth 101,106,107,204 & 213
Connector interface dimension:	IEC 60169-17 Per MIL-PRF-39012 DINEN122200

Note: Cable assemblies also available with interfaces such as 1.85mm, 2.4mm, 2.92mm, SMA +, SMA, N.

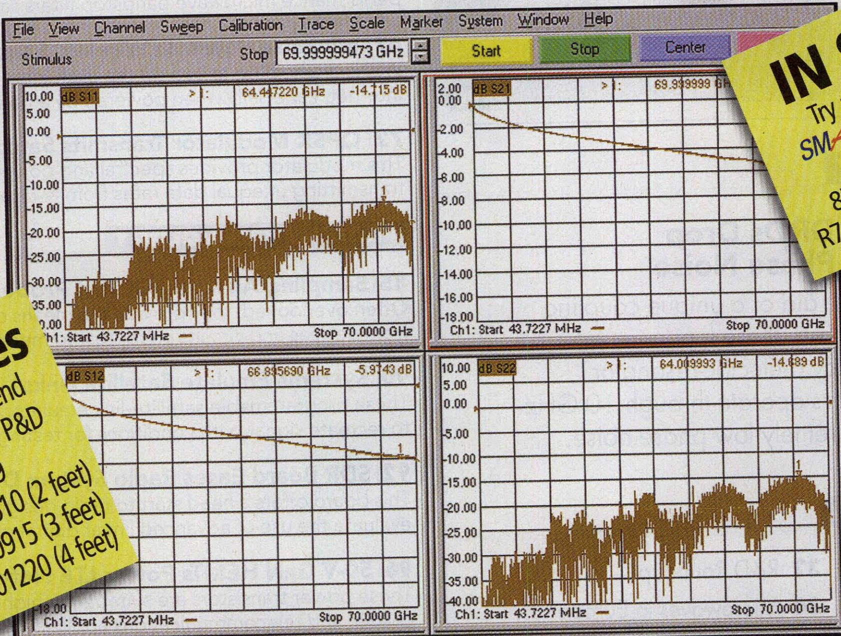

Example of typical 36 inches assembly up to 70 GHz

IN STOCK!
Try an Rmor cable with SMA+ (operates to 36 GHz)
Call RFMW today
877.367.7369. Ask for p/n
R71-32+S132+S1-00457 (18")

70GHz Cables
1.85mm males each end
Call RFMW today for P&D
877.367.7369
RU5-08S1-08S1-00610 (2 feet)
RU5-08S1-08S1-00915 (3 feet)
RU5-08S1-08S1-01220 (4 feet)

RFMW

RFMW is the exclusive stocking distributor for **Rosenberger**® Connectors and Cable Assemblies
RFMW, 188 Martinvale Lane, San Jose, CA 95119
PH: 408.414.1450 or 877.367.7369 Email: sales@rfmw.com
Website: www.rfmw.com/Rosenberger

RF Amplifiers and Sub-Assemblies for Every Application

Delivery from Stock to 2 Weeks ARO from the catalog or built to your specifications!

- Competitive Pricing & Fast Delivery
- Military Reliability & Qualification
- Various Options: Temperature Compensation, Input Limiter Protection, Detectors/TTL & More
- Unconditionally Stable (100% tested)

ISO 9001:2000 and AS9100B CERTIFIED

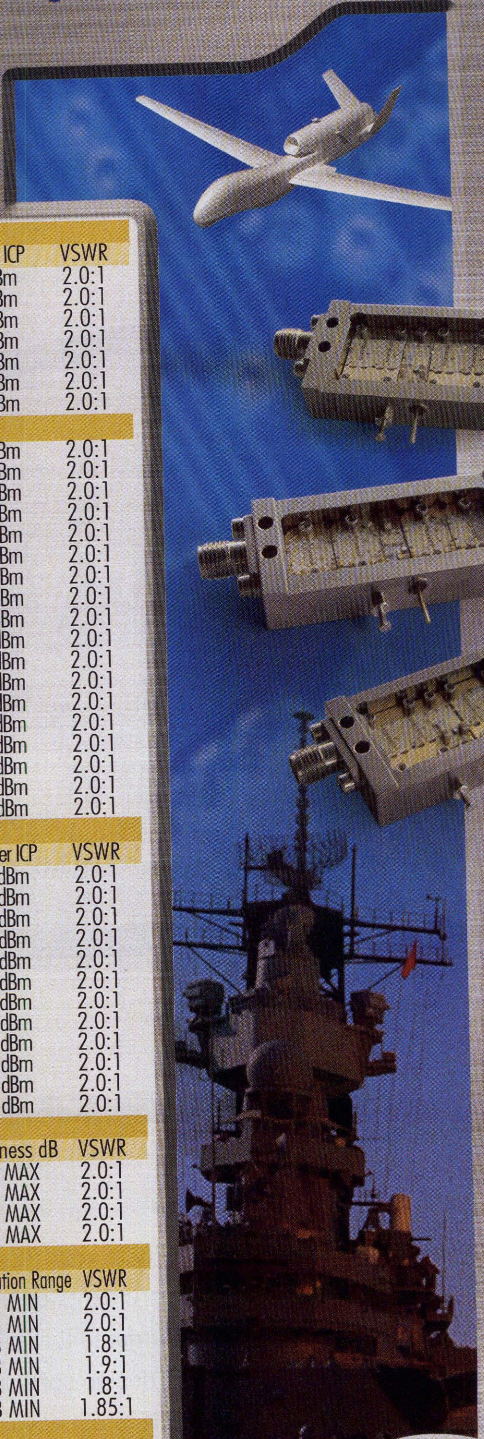

OCTAVE BAND LOW NOISE AMPLIFIERS

Model No.	Freq (GHz)	Gain (dB) MIN	Noise Figure (dB)	Power-out @ P1-dB	3rd Order ICP	VSWR
CA01-2110	0.5-1.0	28	1.0 MAX, 0.7 TYP	+10 MIN	+20 dBm	2.0:1
CA12-2110	1.0-2.0	30	1.0 MAX, 0.7 TYP	+10 MIN	+20 dBm	2.0:1
CA24-2111	2.0-4.0	29	1.1 MAX, 0.95 TYP	+10 MIN	+20 dBm	2.0:1
CA48-2111	4.0-8.0	29	1.3 MAX, 1.0 TYP	+10 MIN	+20 dBm	2.0:1
CA812-3111	8.0-12.0	27	1.6 MAX, 1.4 TYP	+10 MIN	+20 dBm	2.0:1
CA1218-4111	12.0-18.0	25	1.9 MAX, 1.7 TYP	+10 MIN	+20 dBm	2.0:1
CA1826-2110	18.0-26.5	32	3.0 MAX, 2.5 TYP	+10 MIN	+20 dBm	2.0:1

NARROW BAND LOW NOISE AND MEDIUM POWER AMPLIFIERS

Model No.	Freq (GHz)	Gain (dB) MIN	Noise Figure (dB)	Power-out @ P1-dB	3rd Order ICP	VSWR
CA01-2111	0.4 - 0.5	28	0.6 MAX, 0.4 TYP	+10 MIN	+20 dBm	2.0:1
CA01-2113	0.8 - 1.0	28	0.6 MAX, 0.4 TYP	+10 MIN	+20 dBm	2.0:1
CA12-3117	1.2 - 1.6	25	0.6 MAX, 0.4 TYP	+10 MIN	+20 dBm	2.0:1
CA23-3111	2.2 - 2.4	30	0.6 MAX, 0.45 TYP	+10 MIN	+20 dBm	2.0:1
CA23-3116	2.7 - 2.9	29	0.7 MAX, 0.5 TYP	+10 MIN	+20 dBm	2.0:1
CA34-2110	3.7 - 4.2	28	1.0 MAX, 0.5 TYP	+10 MIN	+20 dBm	2.0:1
CA56-3110	5.4 - 5.9	40	1.0 MAX, 0.5 TYP	+10 MIN	+20 dBm	2.0:1
CA78-4110	7.25 - 7.75	32	1.2 MAX, 1.0 TYP	+10 MIN	+20 dBm	2.0:1
CA910-3110	9.0 - 10.6	25	1.4 MAX, 1.2 TYP	+10 MIN	+20 dBm	2.0:1
CA1315-3110	13.75 - 15.4	25	1.6 MAX, 1.4 TYP	+10 MIN	+20 dBm	2.0:1
CA12-3114	1.35 - 1.85	30	4.0 MAX, 3.0 TYP	+33 MIN	+41 dBm	2.0:1
CA34-6116	3.1 - 3.5	40	4.5 MAX, 3.5 TYP	+35 MIN	+43 dBm	2.0:1
CA56-5114	5.9 - 6.4	30	5.0 MAX, 4.0 TYP	+30 MIN	+40 dBm	2.0:1
CA812-6115	8.0 - 12.0	30	4.5 MAX, 3.5 TYP	+30 MIN	+40 dBm	2.0:1
CA812-6116	8.0 - 12.0	30	5.0 MAX, 4.0 TYP	+33 MIN	+41 dBm	2.0:1
CA1213-7110	12.2 - 13.25	28	6.0 MAX, 5.5 TYP	+33 MIN	+42 dBm	2.0:1
CA1415-7110	14.0 - 15.0	30	5.0 MAX, 4.0 TYP	+30 MIN	+40 dBm	2.0:1
CA1722-4110	17.0 - 22.0	25	3.5 MAX, 2.8 TYP	+21 MIN	+31 dBm	2.0:1

ULTRA-BROADBAND & MULTI-OCTAVE BAND AMPLIFIERS

Model No.	Freq (GHz)	Gain (dB) MIN	Noise Figure (dB)	Power-out @ P1-dB	3rd Order ICP	VSWR
CA0102-3111	0.1-2.0	28	1.6 Max, 1.2 TYP	+10 MIN	+20 dBm	2.0:1
CA0106-3111	0.1-6.0	28	1.9 Max, 1.5 TYP	+10 MIN	+20 dBm	2.0:1
CA0108-3110	0.1-8.0	26	2.2 Max, 1.8 TYP	+10 MIN	+20 dBm	2.0:1
CA0108-4112	0.1-8.0	32	3.0 MAX, 1.8 TYP	+22 MIN	+32 dBm	2.0:1
CA02-3112	0.5-2.0	36	4.5 MAX, 2.5 TYP	+30 MIN	+40 dBm	2.0:1
CA26-3110	2.0-6.0	26	2.0 MAX, 1.5 TYP	+10 MIN	+20 dBm	2.0:1
CA26-4114	2.0-6.0	22	5.0 MAX, 3.5 TYP	+30 MIN	+40 dBm	2.0:1
CA618-4112	6.0-18.0	25	5.0 MAX, 3.5 TYP	+23 MIN	+33 dBm	2.0:1
CA618-6114	6.0-18.0	35	5.0 MAX, 3.5 TYP	+30 MIN	+40 dBm	2.0:1
CA218-4116	2.0-18.0	30	3.5 MAX, 2.8 TYP	+10 MIN	+20 dBm	2.0:1
CA218-4110	2.0-18.0	30	5.0 MAX, 3.5 TYP	+20 MIN	+30 dBm	2.0:1
CA218-4112	2.0-18.0	29	5.0 MAX, 3.5 TYP	+24 MIN	+34 dBm	2.0:1

LIMITING AMPLIFIERS

Model No.	Freq (GHz)	Input Dynamic Range	Output Power Range Psat	Power Flatness dB	VSWR
CLA24-4001	2.0 - 4.0	-28 to +10 dBm	+7 to +11 dBm	+/- 1.5 MAX	2.0:1
CLA26-8001	2.0 - 6.0	-50 to +20 dBm	+14 to +18 dBm	+/- 1.5 MAX	2.0:1
CLA712-5001	7.0 - 12.4	-21 to +10 dBm	+14 to +19 dBm	+/- 1.5 MAX	2.0:1
CLA618-1201	6.0 - 18.0	-50 to +20 dBm	+14 to +19 dBm	+/- 1.5 MAX	2.0:1

AMPLIFIERS WITH INTEGRATED GAIN ATTENUATION

Model No.	Freq (GHz)	Gain (dB) MIN	Noise Figure (dB)	Power-out @ P1-dB	Gain Attenuation Range	VSWR
CA001-2511A	0.025-0.150	21	5.0 MAX, 3.5 TYP	+12 MIN	30 dB MIN	2.0:1
CA05-3110A	0.5-5.5	23	2.5 MAX, 1.5 TYP	+18 MIN	20 dB MIN	2.0:1
CA56-3110A	5.85-6.425	28	2.5 MAX, 1.5 TYP	+16 MIN	22 dB MIN	1.8:1
CA612-4110A	6.0-12.0	24	2.5 MAX, 1.5 TYP	+12 MIN	15 dB MIN	1.9:1
CA1315-4110A	13.75-15.4	25	2.2 MAX, 1.6 TYP	+16 MIN	20 dB MIN	1.8:1
CA1518-4110A	15.0-18.0	30	3.0 MAX, 2.0 TYP	+18 MIN	20 dB MIN	1.85:1

LOW FREQUENCY AMPLIFIERS

Model No.	Freq (GHz)	Gain (dB) MIN	Noise Figure dB	Power-out @ P1-dB	3rd Order ICP	VSWR
CA001-2110	0.01-0.10	18	4.0 MAX, 2.2 TYP	+10 MIN	+20 dBm	2.0:1
CA001-2211	0.04-0.15	24	3.5 MAX, 2.2 TYP	+13 MIN	+23 dBm	2.0:1
CA001-2215	0.04-0.15	23	4.0 MAX, 2.2 TYP	+23 MIN	+33 dBm	2.0:1
CA001-3113	0.01-1.0	28	4.0 MAX, 2.8 TYP	+17 MIN	+27 dBm	2.0:1
CA002-3114	0.01-2.0	27	4.0 MAX, 2.8 TYP	+20 MIN	+30 dBm	2.0:1
CA003-3116	0.01-3.0	18	4.0 MAX, 2.8 TYP	+25 MIN	+35 dBm	2.0:1
CA004-3112	0.01-4.0	32	4.0 MAX, 2.8 TYP	+15 MIN	+25 dBm	2.0:1

CIAO Wireless can easily modify any of its standard models to meet your "exact" requirements at the Catalog Pricing.

Visit our web site at **www.ciaowireless.com** for our complete product offering.

Ciao wireless

Ciao Wireless, Inc. 4000 Via Pescador, Camarillo, CA 93012
Tel (805) 389-3224 Fax (805) 389-3629 sales@ciaowireless.com

BOB NELSON

Optimize Signal/Spectrum Analyzer Throughput For High-Volume Manufacturing Test

TO OBTAIN THE HIGHEST THROUGHPUT for the analyzers used in manufacturing test, one should create a test plan that accounts for speed, repeatability, and dynamic range. In this web-exclusive article, Agilent Technologies' Bob Nelson provides you with the blueprint.

To read the article in its entirety, go to http://mwrf.com/contributors/optimize-signalspectrum-analyzer-throughput-high-volume-manufacturing-test.

ALSO, BE SURE CHECK OUT THESE OTHER RECENT ARTICLES IN OUR CONTRIBUTED TECHNICAL EXPERT SERIES.

Visit www.mwrf.com/community/contributors.

KANG CHEN

DAVID A. HALL

MEET THE CHALLENGES OF TESTING EIGHT-ANTENNA LTE

KANG CHEN—
Senior Applications Specialist, Spirent Communications

FIND OUT WHY PXI IS BEING USED FOR RF INSTRUMENTS

DAVID A. HALL—
Senior Product Marketing Manager, RF and Communications, National Instruments

REVISIT IMS2012

The 2012 installment of the RF/microwave industry's flagship event, the *International Microwave Symposium*, has come and gone. Luckily for you, it needn't live on just in memory. Visit *www.mwrf.com* to check out our show coverage, as well as www.engineering tv.com to view exclusive videos from the show floor.

engineering tv

NEWS UPDATES Sent To Your Desktop

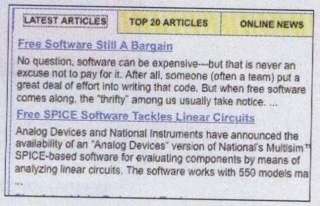
LATEST ARTICLES | TOP 20 ARTICLES | ONLINE NEWS

Free Software Still A Bargain

No question, software can be expensive—but that is never an excuse not to pay for it. After all, someone (often a team) put a great deal of effort into writing that code. But when free software comes along, the "thrifty" among us usually take notice. ...

Free SPICE Software Tackles Linear Circuits

Analog Devices and National Instruments have announced the availability of an "Analog Devices" version of National's Multisim™ SPICE-based software for evaluating components by means of analyzing linear circuits. The software works with 550 models ma ...

Don't believe everything you read, unless it's in the latest issue of *Microwaves & RF UPDATE.* The industry's longest-running weekly e-mail newsletter, it combines insightful commentary with the latest product and industry business news. It is sent directly to your computer desktop each week, and often contains the little things that engineers love, such as links to free white papers and even design software. If you're not already reading it, subscriptions are free, and available from the *Microwaves & RF* website at www.mwrf.com.

MWRF.com has archives of print and online articles dating back to October 2002. Visit mwrf.com today and click the "Back Issues" link. And while you're taking a look around the site, click on "Product Directory" to gain access to our complete directory of products and suppliers.


High pressure,
time sensitive, mission critical.
It's all in a day's work.
Your team depends on you for mission-critical accuracy. And you can depend on the compact Agilent FieldFox spectrum analyzer. At only 6.6 lbs., it ensures peak accuracy without warm-up time and its precise measurements agree with trusted benchtop results. Which means, you'll always be ready to accelerate your team's success.
FieldFox Spectrum Analyzers
Four models up to 26.5 GHz
MIL-PRF-28800F Class 2 rugged
Agrees with benchtop measurements
± 0.5 dB amplitude accuracy (full band)
See how FieldFox measures up—watch the video. Scan the code or visit http://qrs.ly/gb20ppv
Agilent and our Distributor Network
Right Instrument.
Right Expertise.
Delivered Right Now.
metrictest
PART OF THE MICROLEASE GROUP
866-436-0887
www.metrictest.com/agilent
Learn about interference analysis and more with our application note series
www.metrictest.com/agilent/FieldFox.jsp
© Agilent Technologies, Inc. 2012
Anticipate __Accelerate __Achieve
Agilent Technologies

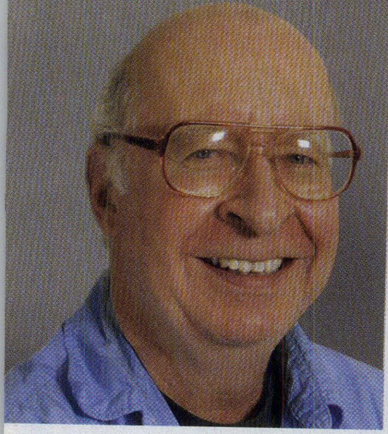

From the
Editor

Searching For That Semi Combo

SEMICONDUCTORS SYMBOLIZE THE state of progress for this industry—arguably, moreso than any other technology or segment. When silicon was the established semiconductor technology and gallium arsenide (GaAs) was just a novelty, foundries were closely held by companies associated with defense applications.

But the industry has changed drastically over the intervening three decades. Open foundries now abound, with services and semiconductor processes available to any customer with sufficient funds. And what processes: These are much more than the silicon bipolar and early GaAs metal-epitaxial-semiconductor field-effect-transistor (MESFET) semiconductor processes that first started replacing vacuum tubes in defense systems. The number of different high-frequency semiconductor processes available today is almost staggering. And newer processes—such as those based on silicon carbide (SiC) and gallium nitride (GaN) substrates—offer the promise of the tube-like power levels often mentioned by the keepers of those earlier captive silicon and GaAs foundries.

From the outset, GaAs substrates offered higher electron mobility than silicon materials; even early developers of discrete and integrated semiconductor devices knew that GaAs could support circuits such as amplifiers and oscillators well into the microwave frequency range. But GaAs had more than a little push from the Defense Advanced Research Projects Agency (DARPA; www.darpa.mil).

DARPA's Microwave/Millimeter-Wave Monolithic Integrated Circuits (MIMIC) program invested about one-half billion dollars of US taxpayers' money over an extended period, beginning in 1986, to nominally develop reliable devices for military applications. Of course, the enormous investment also made it possible for commercial foundries to grow and develop many commercial versions of GaAs MMIC products.

There is no doubt that DARPA has played a significant role in fostering new curiosities (such as GaAs semiconductors) into proven technologies. DARPA and its Microsystems Technology Office (MTO) is now interested in the potential of gallium nitride (GaN) semiconductor technology for defense electronics applications. In some ways, GaAs MMICs met many of the high-frequency needs of the military, but ran out of power. While GaAs devices are usable at millimeter-wave frequencies, they are limited in output power compared to GaN. Not only do military technologists believe that GaN can replace vacuum-tube electronics for high-power applications at microwave frequencies, but they also feel that GaN discrete and integrated devices may be usable into the terahertz frequency range (100 GHz through 10 THz).

DARPA hopes to develop next-generation GaN devices through its Nitride Electronic NeXt-Generation Technology (NEXT) program (http://www.darpa.mil/Our_Work/MTO/Programs/Nitride_Electronic_NeXt-Generation_Technology_(NEXT).aspx). DARPA showed what it could do for GaAs; should anyone doubt that it will make GaN the next big thing in microwave/millimeter-wave active circuits? MWRF

Jack Browne

Technical Contributor

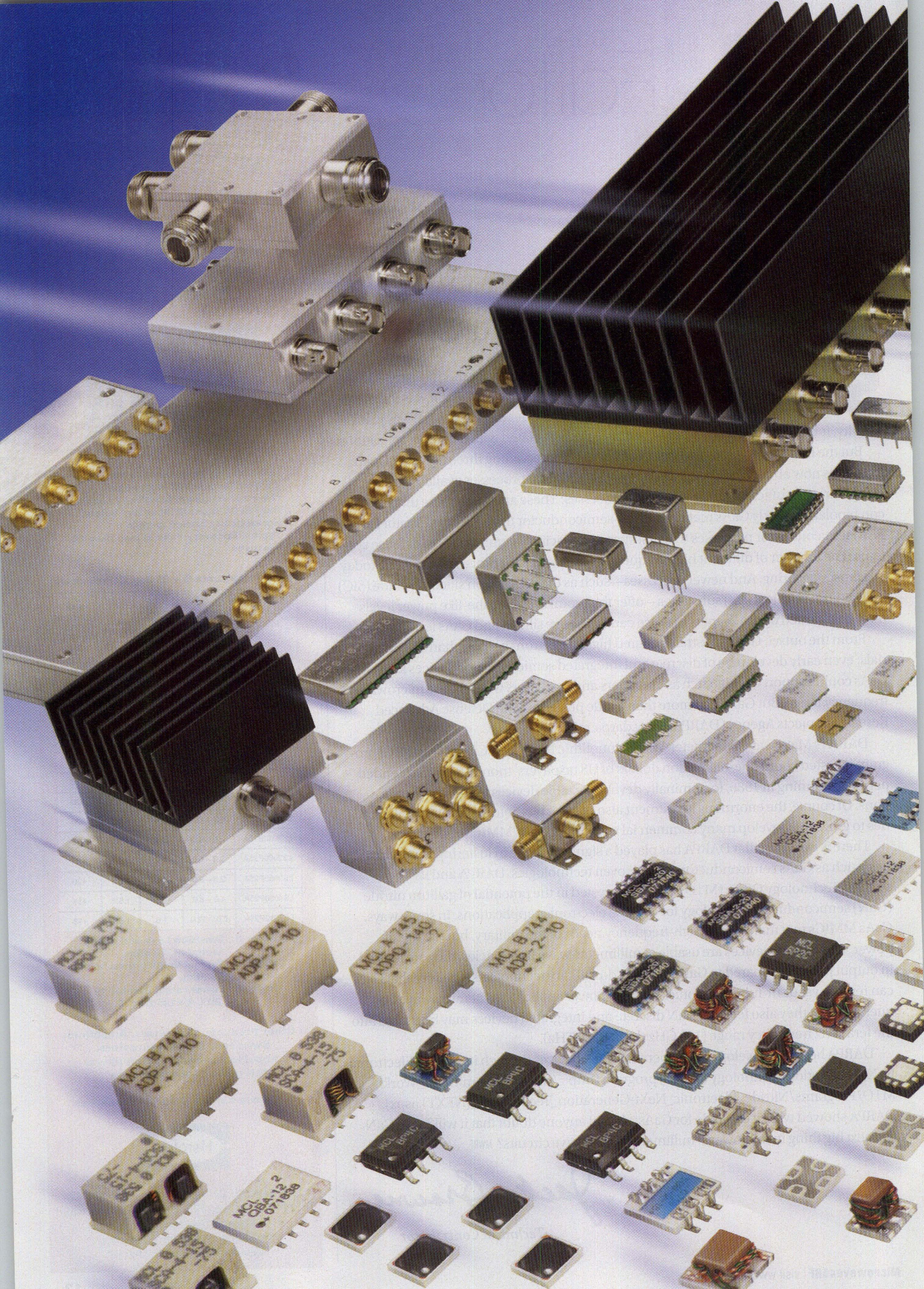
MCL B 744
ADP-2-10
MCL BPNC

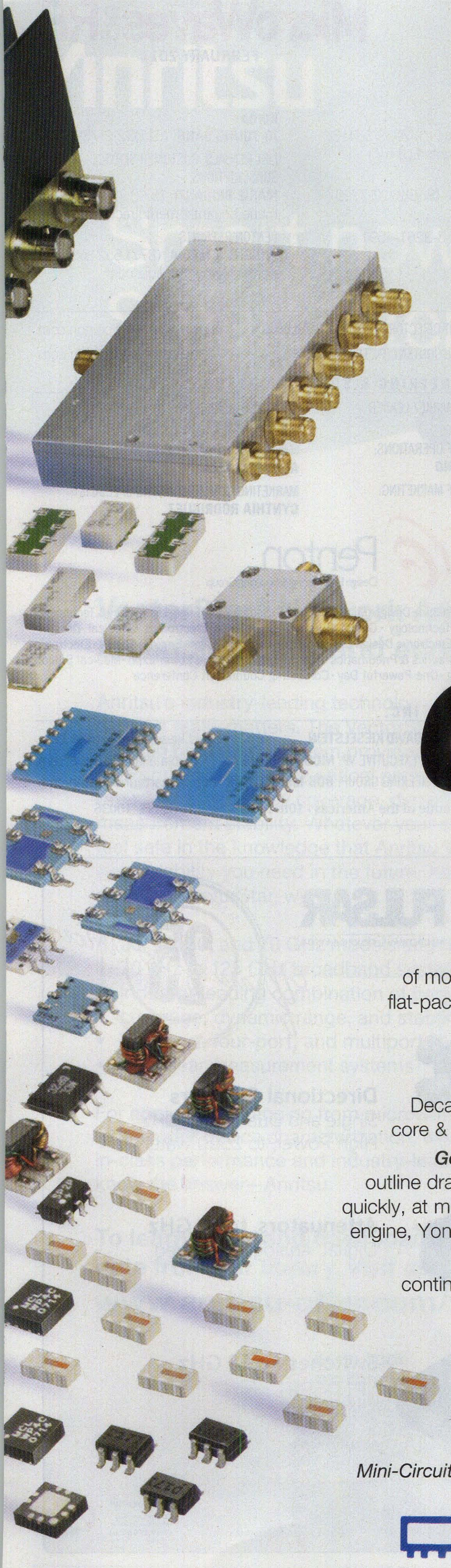

News

AERIAL PLATFORM Buoys UAV Sensor Development

WITH THE INCREASING deployment of unmanned aerial vehicles (UAVs), much research is being devoted to the additional tasks that can be performed by these drones. To allow new airborne payloads to be tested efficiently, a research team at the Georgia Tech Research Institute (GTRI) is developing an airborne testing capability for sensors, communication devices, and other airborne payloads. Dubbed the GTRI Airborne Unmanned Sensor System (GAUSS), this aerial test bed is based on a UAV made by Griffon Aerospace and modified by GTRI **(see photo)**.

The hope is that the airplane itself will simply be a conveyance, eventually allowing any lightweight sensor/communications package to be mounted on it. The GTRI team has developed a modular design that allows the GAUSS platform to be reconfigured for a number of sensor types. Among the possibilities for evaluation are devices that utilize light-detection-and-ranging (LIDAR) and chemical-biological sensing technology.

A project is already underway to develop, install, and test a sensor suite comprised of the following: a camera package; a signal-intelligence (SIGINT) package for detecting and locating ground-based emitters; and a multi-channel, X-band ground-mapping radar. To enable electronic scanning, that radar is being designed using phased-array antenna technology. It also can be programmed to transmit arbitrary waveforms. With such flexibility, the radar will be able to do ground mapping in addition to detecting and tracking objects on the ground.

The combined sensor package is lightweight enough to be carried by the GAUSS UAV. Lightweight sensors allow the use of lighter, smaller UAVs. Such drones can fly lower without being detected.

A variant of the Griffon Outlaw ER aircraft, the GAUSS has a 13.6-foot wingspan and a payload capacity of roughly 40 lbs. The aircraft navigates using a high-precision Global Positioning System (GPS) combined with an inertial navigation system. It can be programmed for autonomous flight or piloted manually. The airborne mission package also includes multi-terabyte onboard data recording and a stabilized gimbal, which isolates the camera from aircraft movement.

This UAV platform will nurture the initial development and testing of new concepts in lightweight airborne sensors.

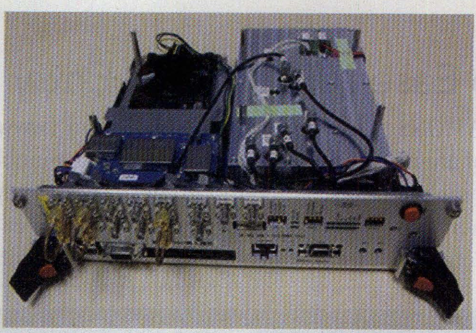

To provide broadband wireless access to unserved and underserved areas, prototypes have been created for the IEEE 802.22 standard. They take advantage of TV White Spaces spectrum.

WHITE SPACE TECHNOLOGY Makes Strides

When the white-space television spectrum opened up worldwide, much hype centered around how it could be reused. For example, that spectrum could bring broadband wireless access (BWA) to underserved areas. Now, that very endeavor can be achieved with the new white-space prototypes from the National Institute of Information and Communications Technology (NICT), Hitachi Kokusai Electric, Inc., and ISB Corp. These prototypes are based on the IEEE 802.22 standard, which was created to bring TV White Spaces (TVWS) BWA to regional areas where it is most needed. In addition to providing BWA to underserved and unserved regions around the world, these prototypes can provide emergency-backup broadband communications.

Specifically, NICT and Hitachi Kokusai Electric have developed the first prototype devices for base-station (BS) and consumer-premise-equipment (CPE) applications that verify the physical layer (PHY) and medium-access-control (MAC) layer design based on IEEE 802.22 **(see photos)**. The PHY part developed by Hitachi Kokusai Electric allows the devices to use vacant TV bands in the TVWS spectrum from 470 to 710 MHz. For its part, the MAC layer part developed by NICT provides a medium-access method based on point-to-multipoint access while supporting different quality-of-service (QoS) levels. It also supports cognitive capabilities of interference estimation, geo-location, and white-space data base (WSDB) access over Internet Protocol (IP).

The prototypes are rounded out by the WSDB from ISB Corp. It avoids interference to incumbent TV broadcasters by automatically selecting a non-interfering TV band. The three firms will continue developing technologies based on the IEEE 802.22 standard. They also will work closely with the WhiteSpace Alliance (WSA; www.whitespacealliance.org) to provide products globally.

Meanwhile, machine-to-machine (M2M) applications also are gaining ground in the white-spaces race. The Weightless Special Interest Group (SIG; www.weightless.org) recently won the Wireless Innovation Forum Technology of the Year 2012 for its global machine communications standard, dubbed Weightless. This award was announced at the Wireless Innovation Forum Conference on Communications Technologies and Software Defined Radio (SDR - WInnComm 2013).

Weightless is a proprietary, royalty-free, open standard for wireless M2M communications using TVWS spectrum. It provides time-division-duplexing (TDD) operation with a wide range of provided data rates and range options. The Weightless standard was designed to minimize cost and power consumption. It features a chipset cost of less than $2.

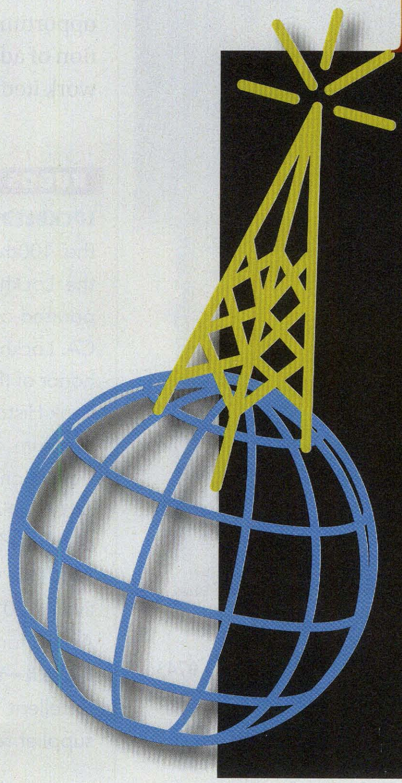

Market QUOTE

According to a report from Visiongain (www.visiongain.com) titled, "Global LTE Base Station Market 2013-2018: The Next Generation Infrastructure for 4G Mobile Telecommunications," the global LTE base-station market will reach

$6.37 billion this year.

Base-station vendors can capture a considerable share of this market by delivering efficiency, reliability, and practicality.

STANDARDS UPDATE

SIGs EMERGE To Ease NFC Market Entry

NEAR-FIELD COMMUNICATIONS (NFC) has garnered a lot of attention for its ability to enable mobile transactions ranging from payments to healthcare monitoring. To promote this technology, the NFC Forum (www.nfc-forum.org) has launched a number of special-interest groups (SIGs). They will bring together leaders in consumer electronics, healthcare, payment, retail, and transportation. Those individuals will collaborate on NFC solution implementation, interoperability, best practices, and future requirements.

The SIGs will educate their respective markets on use cases, implementation issues, and lessons learned. To drive new or modified technical work, they will assemble business requirements. The special-interest groups also will explore ways to speed or smooth the certification of NFC-enabled devices. Each SIG is tasked with establishing and managing liaisons with other groups to further collaborative efforts. They will create regional programs as needed.

By nurturing the interaction of NFC stakeholders in key vertical markets, use cases, and technology segments through these SIGs, the NFC Forum hopes to take a more active role in driving the development, deployment, and adoption of NFC solutions. The five initial SIG Working Groups will report to a new SIG Committee, which reports to the NFC Forum Board. Working through that committee, NFC Forum members will have the opportunity to recommend the formation of additional SIGs and propose new work items.

KUDOS

LOCKHEED MARTIN—Is commemorating the 100th anniversary of its predecessor, the Lockheed Company, which was incorporated on Dec. 19, 1912 in San Francisco, CA. Lockheed Martin is making donations in honor of the company's founders to the Burbank Historical Society's Gordon R. Howard Museum and the Huntington Library, Art Collections and Botanical Gardens. Both organizations work to preserve the history of the early aerospace industry in California.

ANRITSU CO.—Has received Frost & Sullivan's 2012 Global Company of the Year Award for Test & Measurement.

ALTERA—Was awarded ZTE Corp.'s Global Excellent Partnership Award—an annual supplier recognition—for 2012.

CERAMIC FILTERS

LOW PASS BANDPASS HIGH PASS

45 MHz to 15 GHz from 99¢ ea. qty.3000

Over ~~167~~ 185 models...only 0.12 x 0.06" These tiny hermetically sealed filters utilize our advanced Low Temperature Co-fired Ceramic **(LTCC)** technology to offer superior thermal stability, high reliability, and very low cost, making them a must for your system requirements. Visit our website to choose and view comprehensive performance curves, data sheets, pcb layouts, and everything you need to make your choice. You can even order direct from our web store and have units in your hands as early as tomorrow!

Wild Card **KWC-LHP LTCC Filter Kits** *only* $98

Choose any 8 LFCN or HFCN models
Receive 5 of ea. model, for a total of 40 filters
Order your KWC-LHP FILTER KIT TODAY!

RoHS compliant U.S. Patents 7,760,485 and 6,943,646

Now available in small-quantity reels *at no extra charge:*
Standard counts of 20, 50, 100, 200, 500, 1000 or 2000. Save time, money, and inventory space!

Mini-Circuits...we're redefining what VALUE is all about!

Mini-Circuits®
ISO 9001 ISO 14001 AS9100

P.O. Box 350166, Brooklyn, New York 11235-0003 (718) 934-4500 Fax (718) 332-4661

YONI2 U.S. Patents 7739260, 7761442 ***The Design Engineers Search Engine*** *finds the model you need, Instantly* • For detailed performance specs & shopping online see **minicircuits.com**

IF/RF MICROWAVE COMPONENTS

504 Rev B

SUBMARINE-CABLE CAPACITY Has Potential To Double

IN THE RACE to provide increased data capacity for today's consumers, fiber should not be overlooked. Infinera (www.infinera.com) has demonstrated a 100-Gb/s optical signal enhanced with Soft Decision Forward Error Correction (SD-FEC)—a technology that could double the transmission capacity of existing submarine cables. That signal was sent across Telstra Global's (www.telstraglobal.com) dedicated fiber pair within Segment S5 of the AAG cable. Segment S5, which connects San Luis Obispo in California to Hawaii's island of Oahu, spans 4200 km.

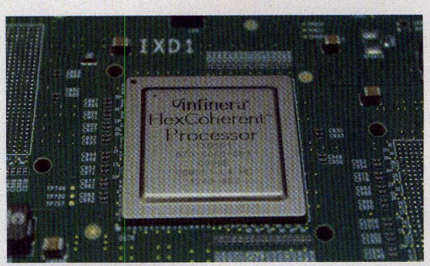

This processor enables real-time SD-FEC processing with 500-Gb/s photonic integrated circuits.

The trial was staged using Infinera's DTN-X platform and a prototype superchannel line card. That line card relies on Infinera's third-generation FlexCoherent processor for real-time SD-FEC processing combined with 500-Gb/s photonic integrated circuits (PICs; **see figure**). With Infinera's FlexCoherent technology, the line card can be configured for a specific modulation format via software controls. By enabling the use of higher-order modulation formats, the SD-FEC allowed Telstra to increase the available capacity on this link. Using the additional error-recovery capability enabled by the SD-FEC, multiple Infinera FlexCoherent modulation formats were able to close the link with no bit errors detected. Such improvements are much needed, as Telstra Global is expecting more than 60% annual growth in its trans-Pacific submarine cable traffic over the next three years.

KUDOS

HUGHES—Has announced shipments of more than 487,000 broadband satellite terminals in 2012, the company's biggest one-year total on record.

INTERCEPT TECHNOLOGY—Is celebrating its 30th anniversary. The company began as a consulting firm performing electrical-engineering-related software and hardware projects.

COAXICOM—Has shipped its 10,000,000th SMA connector. The Florida-based firm says its market share has grown in response to the increased number of counterfeit products being shipped from overseas sources.

Reference Design Features IEEE 802.11ac and 802.11ad

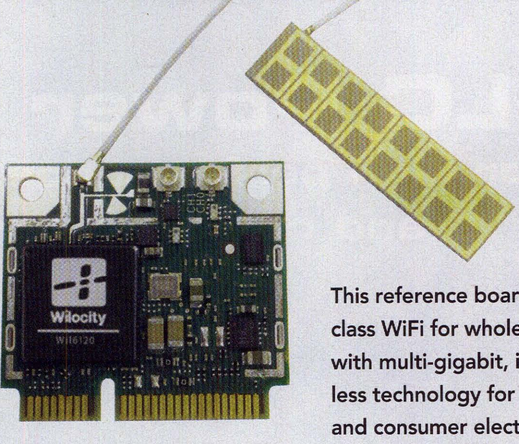

This reference board combines Gigabit-class WiFi for whole-home networking with multi-gigabit, in-room 60-GHz wireless technology for tablets, notebooks, and consumer electronics.

To bring increased capacity, range, and efficiency to wireless-local-area networks (WLANs), the IEEE has created two standards: 802.11ac and 802.11ad. The latter, which was just recently ratified, enables multi-gigabit networking, data syncing, and video and audio streaming while maintaining its wireless bus-extension-docking capabilities. With many firms looking to leverage both of these standards, Qualcomm Atheros, Inc. (www.atheros.com) and Wilocity (www.wilocity.com) have produced a tri-band reference design that combines IEEE 802.11ac and 802.11ad wireless capabilities on one module **(see photo)**.

By merging Qualcomm VIVE 802.11ac WiFi and Wilocity 802.11ad WiGig wireless technologies, the reference design allows consumers to connect to 60-GHz-enabled devices, docks, displays, and storage at multi-gigabit speeds. At the same time, they can maintain their enterprise-wide or whole-home coverage with 2.4/5-GHz WiFi. By integrating a solution that combines whole-home, gigabit-class WiFi with in-room, multi-gigabit connectivity into their devices, equipment manufacturers will benefit from increased speed, reliability, and range.

At the heart of this reference board is a tri-band wireless networking card, which leverages the new Qualcomm VIVE 802.11ac combined with IEEE 802.11ad technology. That card will be available in two options: the QCA9006NFC next-generation form factor (NGFF) and the QCA9006WBD half-mini-card (HMC) specification.

PEOPLE

M/A-COM TECH—John Croteau, the company's President, has been promoted to the position of Chief Executive Officer. Croteau has been named to the company's board of directors as well. He succeeds Charles Bland, who will continue to serve as a member of the board. Bland will remain in an advisory capacity to assist with the transition.

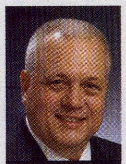
CROTEAU

OPTELIAN—Has appointed Brian Pratt Vice President of Product Marketing. Pratt previously served as Vice President of Business Development for Alcatel-Lucent's Kindsight team.

WILSON ELECTRONICS—Has promoted Broc Jenkins to the position of Business Development Manager, M2M. Since joining Wilson in 2009, Jenkins has worked as a Technical Support Technician and a Technical Support/Customer Service manager.

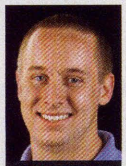
JENKINS

CTIA—THE WIRELESS ASSOCIATION—Has announced several new staff positions. Athena Polydorou has been appointed Executive Director of the Wireless Foundation educational outreach program. In addition, Jackie McCarthy has been named Wireless Internet Development Director. Finally, Matthew Gerst has been promoted from Counsel to Director in the External and State Affairs Department.

MICRON TECHNOLOGY—Richard M. Beyer has been appointed to the company's board of directors. Beyer previously served as Chairman and Chief Executive Officer of Freescale Semiconductor.

SAN-TRON—Bob Carbonell has joined the company as Eastern Regional Sales Manager. An active reservist in the US Air National Guard, he boasts more than 24 years of military and RF/microwave-industry experience.


CARBONELL

IEEE INDUSTRY STANDARDS AND TECHNOLOGY ORGANIZATION (IEEE-ISTO)—Has announced two appointments to its board of directors. Allan Foster is currently Vice President, Community at ForgeRock. Michael Violette serves as President of Washington Laboratories and Director of American Certification Body.

NXP SEMICONDUCTORS—Hans Rijns and Dave French have been assigned joint responsibility for the company's R&D activities. Rijns, who has been appointed Chief Technology Officer, will combine this role with his current position as Senior Vice President & Head of Research. French, now Executive Vice President of R&D, will combine this responsibility with his position as General Manager of BU Portable & Computing.

EAST COAST MICROWAVE—James Doyle has joined the company as President and Chief Executive Officer. He succeeds Bruce Cooper, who is stepping down after 24 years to assume a non-Executive Chairman position. Doyle previously served as President and Chief Executive Officer of XMA Corp.

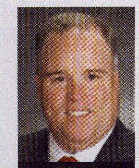
DOYLE

RFMD—Kevin W. Kobayashi, an RFMD Fellow, has been named a Fellow of the Institute of Electrical and Electronics Engineers (IEEE). Kobayashi was recognized for his contributions to monolithic microwave integrated circuits (MMICs). He is the principal author of 130 technical publications and the holder of 48 US patents.


KOBAYASHI

BOEING—Michael Kurth has been named Vice President and General Manager, Unmanned Airborne Systems Programs. Kurth previously served as Managing Director of Boeing Defence UK Ltd. (BDUK).

LORAL—Avi Katz has been appointed President. Katz previously served as the company's Senior Vice President, General Counsel, and Corporate Secretary. He will continue in the latter two roles.

GSMA—Ahmad Abdulkarim Julfar, Chief Executive Officer of Etisalat Group, has been elected to the organization's board of directors. Julfar will serve on the GSMA board for a two-year term through December 2014.

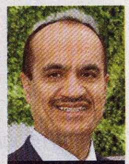
JULFAR

CONTRACTS

TeleCommunication Systems (TCS)—Has received an order from the Australian Defence Science and Technology Organisation (DSTO) for its very-small-aperture-terminal (VSAT) satellite systems.

General Dynamics C4 Systems—The US Army has ordered an upgrade for 100 AN/PRC-155 manpack radios. This upgrade will enable the radios to communicate with the military's Mobile-User-Objective-System (MUOS) satellite-communications system. The order is valued at $5 million.

GENERAL DYNAMICS Receives Army radio upgrade order

HARRIS CORP. Wins $31-million Trinidad and Tobago contract

Altair Semiconductor—The company's FourGee Long-Term-Evolution (LTE) chipset has been selected by Franklin Wireless. The Verizon Wireless-certified chipset will be used to power Franklin's line of single-mode, LTE-enabled products for the US market.

Wavestream—Has been awarded a contract by Honeywell to supply Ka-band transceivers. The transceivers will be integrated into airborne antenna systems, providing in-flight connectivity to the Inmarsat Global Xpress (GX) network. Scaled production is expected to begin in 2014.

Harris Corp.—Has been awarded a $31-million contract by the Republic of Trinidad and Tobago. Harris will provide a public-safety access point (PSAP) and 800-MHz Project 25 (P25) trunked radio system for the Trinidad and Tobago Police Service.

FRESH STARTS

AT4 wireless and Anritsu—Anritsu test equipment for third-generation (3G) and Long-Term-Evolution (LTE) conformance and carrier testing will now be used in AT4 wireless' testing laboratories. The agreement includes RF, RRM, and protocol testing equipment, which will be used in AT4 wireless locations ranging from Spain to the US, Taiwan, and Japan. In addition, Anritsu's Canadian subsidiary, Anritsu Electronics, has established a partnership with Wavefront, a Canadian non-profit organization supporting wireless commercialization and research. Per the arrangement, Anritsu and Wavefront are establishing an LTE Layer 1, 2, and 3 pre-screen testing facility.

Raytheon Co.—Will be awarding grants to K-12 teachers nationwide in support of science, technology, engineering, and math (STEM) education. Raytheon's MathMovesU program will honor 32 math professionals with awards of $2500 each along with a matching grant of $2500 to each of their schools. This annual award's call for nominations is open through May 15.

Passive Plus—Is offering vertical tape-and-reel orientation for its line of traditional high-Q, low-ESR capacitors. These capacitors are RoHS-compliant and offered in both magnetic and non-magnetic terminations.

Mouser Electronics—Has expanded its RF Wireless Technology site on Mouser.com. The updated site features an enhanced Solutions spotlight feature, enabling design engineers to easily find newly released RF modules as well as design resources and industry news. In addition, Mouser has signed a distribution agreement with ams, an Austrian manufacturer of analog integrated circuits (ICs) and sensors.

u-blox—Has received approval for its LISA-U110 UMTS/HSPA wireless module from SK Telecom, a Korean mobile operator. The certification allows the LISA modem to be used in consumer and machine-to-machine (M2M) applications operating over SK Telecom's 3G network.

Sonnet Software—Has announced a new sales and customer technical support representative for Germany, the Netherlands, Austria, and France. advICo microelectronics GmbH is now providing exclusive sales distribution and technical support for Sonnet Suites high-frequency 3D planar electromagnetic (EM) software products in these countries.

Gogo—Has been selected to outfit more than 400 aircraft—spanning several major airlines operating in the US and internationally—with its Ku-band satellite connectivity services.

Anite—Has validated the first Global Certification Forum (GCF) TD-LTE/TD-SCDMA Inter-Radio Access Technology (Inter-RAT) test cases. Anite now supports all of the GCF LTE protocol test requirements for TD-LTE mobile operators ahead of their network launches.

Anaren—Has established an online resource for users of its Xinger-brand subminiature passive RF components. Branded Submini Central and located on Anaren's website, the new resource offers application notes, de-embed files, and informational videos.

TeleCommunication Systems (TCS)—Has been issued nine US patents—all in the fourth quarter of 2012—related to mobile location, secure communications, public safety, wireless data, and messaging.

Navman Wireless—Has been acquired by Danaher Corp., a Fortune 250 science and technology company. Navman Wireless will function as a standalone Danaher operating company, retaining its brand, personnel, and locations.

RF Europe —Has signed a European distribution agreement with Eastern Optx. Based in New Jersey, Eastern OptX's product line includes radar target simulation systems, radio altimeter test sets, and channel replicators.

Plextek—Has announced a corporate restructuring, which is intended to separate its design consultancy (rebranded as Plextek Consulting) from its other business units. Plextek Radar Group has been rebranded as Blighter Surveillance Systems. In addition, Plextek's RF IC design business has been separated out in the form of Plextek RF Integration.

Agilent Technologies—The company's new poster, "Understanding the Intricacies of LTE and LTE-Advanced," is available. To obtain a copy, go to www.agilent.com/find/LTE-Forward.

Women in Wireless—Has launched a new chapter in Boston, MA. The nonprofit organization promotes female leaders within mobile and digital media.

Inside Track with David J. Aldrich,

PRESIDENT AND CHIEF EXECUTIVE OFFICER, SKYWORKS SOLUTIONS

Interview by NANCY FRIEDRICH

NF: I understand that Skyworks is doing an increasing amount of business in the tablet or e-reader segment. Can you share any numbers with us? And how does this growing business compare with some of your legacy markets in wireless, such as cellular handsets?

DA: According to Morgan Stanley, tablet shipments could reach more than 350 million units by 2015. Much like smartphones, this market segment is performance-driven. It is serving as a gateway for e-commerce, on-demand content, location-based advertising, cloud-based services, and social networking. With an increasing number of tablets becoming cellular-enabled—particularly at fourth-generation (4G) data rates—IEEE 802.11ac connectivity will be prevalent. What's interesting is that this product category did not exist just a few short years ago. Today, because the RF semiconductor requirements are similar to those of smartphones, it is complementary to our cellular handset business and generates substantial incremental revenue for Skyworks.

NF: How do you expect those numbers to grow?

DA: With the recent introduction of various screen sizes and lower price points, we expect tablet adoption rates to dramatically increase over the course of 2013 and beyond—clearly at the expense of traditional personal computers (PCs). Consumer appetite is for portable form factors that deliver fast web access and entertainment (video, audio, location-based services, etc.). These requirements bode well for tablets.

NF: What unique needs do tablets have in terms of design? And what challenges?

DA: There are numerous similarities between smartphones and tablets in terms of functionality. As a result, many of the analog-processing and power-management requirements are comparable. For high-end devices, it always comes down to performance and battery life.

NF: How has Skyworks overcome those challenges?

DA: We have extensive experience in RF and analog system design and a deep understanding of silicon-on-insulator (SOI), complementary-metal-oxide-semiconductor (CMOS), gallium-arsenide (GaAs), bipolar-field-effect-transistor (BiFET), and silicon-germanium (SiGe) process technologies. In addition, we have developed a library of nearly 1000 patents and supporting intellectual property (IP) and possess leading capabilities in advanced integration—including proprietary shielding, three-dimensional (3D) die stacking, and flip-chip technologies. With a long history of innovation, we have become accustomed to delivering increasingly smaller form factors and providing our customers with breakthrough system solutions. We partner with our customers to meet their need for analog and RF solutions that can solve the inherent problems in compact, mobile, high-performance devices, such as battery life, size, signal interference, and cost.

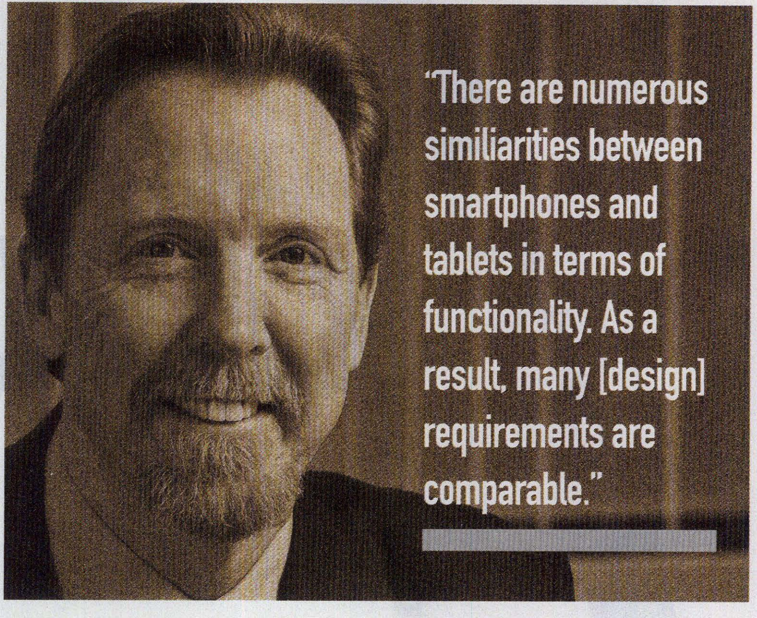

NF: I understand that the company has made some changes recently in hopes of more closely aligning its front-end and analog businesses.

DA: The changes are all designed to more closely align our sales, product, technology, and marketing teams with the end markets we serve. For example, it is the role of our marketing organization to ensure alignment between our technology roadmap and evolving systems requirements and standards. We are attempting to offer more complete system solutions that leverage our uniquely broad portfolio.

NF: How will this change affect the way that Skyworks operates this year?

DA: We are already seeing increased collaboration between our front-end solutions and high-performance analog teams as well as the benefits associated with a more streamlined organization.

NF: Will the firm be better prepared to pursue new opportunities in emerging markets, such as the medical field?

DA: Skyworks currently offers a broad portfolio of RF/microwave products for a diverse set of vertical markets including medical, automotive, smart energy, home automation, and wireless infrastructure. We will be looking to increase our dollar content per platform across these and other markets—particularly as we become better equipped to offer our customers complete system solutions.

NF: Are you considering new opportunities in some of the industrial markets?

DA: With wireless connectivity becoming pervasive across a growing number of consumer electronics, machine-to-machine applications, and home-automation systems—among others—we expect there to be an increasing number of opportunities in adjacent markets, such as industrial. As a result, we are effectively doubling down on several opportunities—not only to further diversify, but to enhance overall profitability.

NF: What applications is Skyworks currently targeting?

DA: There are several important technology trends to follow—all driven by our customers' needs. Some of these include achieving higher levels of integration, envelope tracking, and carrier aggregation for mobile-device manufacturers. As always, original equipment manufacturers (OEMs) are seeking ways to incorporate all popular second- (2G), third- (3G), and 4G bands—as well as switches and filters—into a single module for an unprecedented level of integration and carrier coverage. This integrated approach will significantly reduce the amount of required design resources. Eventually, manufacturers will be able to utilize a single core design team to simultaneously release platforms for multiple markets.

NF: Does the company have any advice on restructuring?

DA: Under any circumstance, we believe it is important to always maintain focus on your customers. They are the single most important reason for your existence and what should be driving all of your business decisions and actions. MWRF


40 GHz
Low Loss and
Phase Stable
Quick Lock
Precision
Armored

INTEGRATED BiCMOS CHIP SET Covers 400 GHz

MOST OF TODAY'S CMOS/BiCMOS designs for terahertz applications target the circuit blocks. Recently, however, substrate-integrated-waveguide (SIW) antennas have been integrated with active terahertz circuits in CMOS/BiCMOS by researchers at Singapore's Institute of Microelectronics, A*STAR. The team includes Sanming Hu; Yong-Zhong Xiong (now with MicroArray Technologies); Bo Zhang (now with Xi'an University of Posts and Telecommunciations); Lei Wang (now with the University of Electronic Science and Technology of China); Teck-Guan Lim (now with JDS Uniphase Corp.); Minkyu Je; and Mohammad Madihian.

The researchers' terahertz transmitter (Tx) and receiver (Rx) chipset operates at roughly 400 GHz in 0.13-μm silicon-germanium (SiGe) BiCMOS technology. In the transmit chip, the SIW antenna also works as a high-pass filter. In doing so, it keeps the unwanted harmonics from being radiated out of the chip. The key is the SIW antenna's high-pass filtering characteristic, which enables it to suppress the unwanted fundamental and second harmonic signals by 50 and 30 dB, respectively. In addition to the SIW antenna, the transmit chip houses a voltage-controlled oscillator (VCO), buffer, modulator, power amplifier (PA), and frequency tripler.

The receive chip contains an SIW antenna with a tunable bandwidth. It is integrated with a two-mode subharmonic mixer, which achieves conversion loss that is ~5 dB lower than loss suffered by conventional designs. This chip consumes 50 nA from a 1.2-V supply.

To improve performance, the researchers created some novel function blocks. They found that the transmitter's output power could be raised to ~0 dBm or higher by using a high-power VCO and their redesigned amplifier, which provided gain of ~20 dB at 140 GHz. See "A Si-Ge BiCMOS Transmitter/Receiver Chipset with On-Chip SIW Antennas for Terahertz Applications," *IEEE Journal of Solid-State Circuits*, Nov. 2012, p. 2654.

Crystal-Less WBAN Receiver Consumes Just 0.24 nJ/b

CARDIOVASCULAR DISEASE and diabetes are now affecting a larger number of people. Because of the asymptomatic or intermittent properties of these diseases, long-term continuous and ubiquitous real-time health monitoring are critical to their detection and treatment. At the Korea Advanced Institute of Science and Technology (KAIST), an energy-efficient, crystal-less, double-frequency-shift-keying (double-FSK) transceiver for wireless-body-area-network (WBAN) sensor nodes has been designed by Joonsung Bae, Kiseok Song, Hyungwoo Lee, Hyunwoo Cho, and Hoi-Jun Yoo.

In a WBAN, body-worn sensor nodes periodically send physiological or multimedia data to a central hub node. According to the IEEE 802.15.6 standard, energy efficiency is a top priority for WBAN sensor nodes. The lifetime of sensor nodes is expected to extend to five years for implants and one week for a wearable device using limited energy resources, such as coin batteries. Among other design challenges is the need for a low-power transceiver with fast turn-on time with tight duty-cycle control between sleep and active modes.

To lower the cost of their device and its energy consumption, the researchers replaced the crystal oscillator with an injection-locking digitally controlled oscillator (DCO). By choosing a calibration method that uses an injection-locking detector, they found that the frequency drift of that DCO could be calibrated within 100-kHz accuracy over a 100-deg. temperature variation. To satisfy WBAN requirements like quality of service (QoS), they adopted the double-FSK modulation scheme with a divider-based transmitter by a power-efficient switching modulator. Upon its fabrication, the crystal-less, double-FSK, WBAN-compatible sensor-node transceiver consumed 1 and 2 mW in calibrating and transmitting modes, respectively, at a data rate to 10 Mb/s. It provided an 80-MHz reference source with 100-kHz accuracy by auto-calibrated digitally controlled oscillator. See "A Low-Energy Crystal-Less Double-FSK Sensor Node Transceiver for Wireless Body-Area Network," *IEEE Journal Of Solid-State Circuits*, Nov. 2012, p. 2678.

Inkjet-Printed Antennas Reach Beyond 10 GHz

USING AN INKJET printing process, it is possible to fabricate low-cost organic substrates that will serve devices requiring smaller and lighter-weight components. The inkjet printing of metallic nanoparticles also has allowed the production of flexible devices. Although antennas have been printed, they have been both low gain and narrow band. At Saudi Arabia's King Abdullah University of Science and Technology, Benjamin S. Cook and Atif Shamim have conjured a fully characterized inkjet printing process that can be used to fabricate low-cost, paper-based, high-gain, and ultrawideband (UWB) antennas.

The partners characterized the inkjet printing process using metallic nanoparticle inks on a paper substrate for frequencies to 12.5 GHz. By comparing laser versus heat sintering of the metallic nanoparticles, they demonstrated the cost and time benefits of laser sintering. It allows for quicker sintering with little to no substrate heating and lower energy requirements.

Among the antennas fabricated using the inkjet-printing process were a UWB Vivaldi antenna with 8 dBi gain. In addition, a slow-wave log-periodic dipole array leveraged a new miniaturization technique to show 20% width reduction. See "Inkjet Printing of Novel Wideband and High Gain Antennas on Low-Cost Paper Substrate," *IEEE Transactions On Antennas And Propagation*, Sept. 2012, p. 4148.

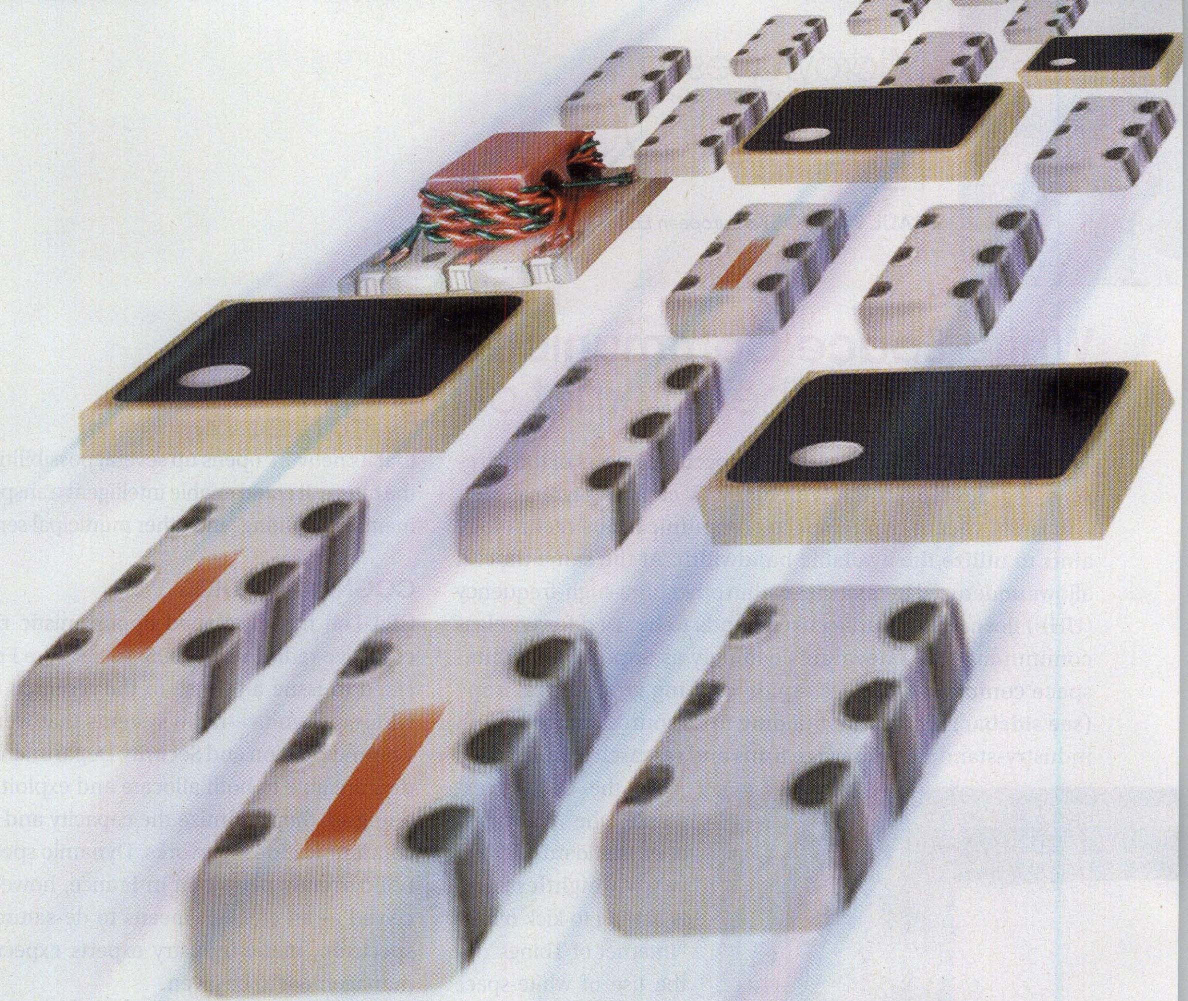

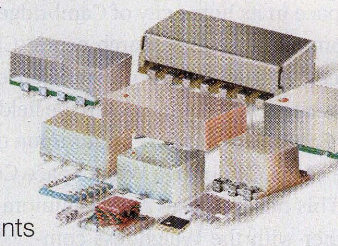

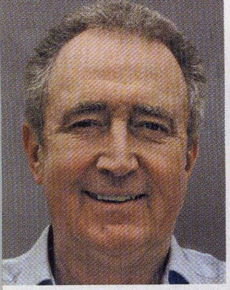

PAUL WHYTOCK, *European Editor*

White-Space Communications Will Kickstart The "Internet of Things"

WHITE SPACE refers to unoccupied parts of the wireless spectrum. With many TV channels typically left vacant, white-space communications technology aims to utilize the available bandwidth. At the same time, it allows underused frequencies within other ultra-high-frequency (UHF) licensed and unlicensed bands to be used for wireless communication. Known misleadingly as Super WiFi, white-space communications is rapidly gaining ground in Europe **(see sidebar)**. Efforts are building from sources ranging from industry-standards groups to firms and research centers.

In the UK, for example, the Weightless open-standards group (www.weightless.org) is aiming to kick off the "Internet of Things" via the use of white-space communications. The group plans to deliver its first complete specification this quarter. Meanwhile, mobile wireless-data service provider Neul (www.neul.com) has issued version 0.9 of the Weightless Specification. The company also has deployed a city-wide, fully functional wireless network in white space in its home city of Cambridge, England. In nearby France, communications research center CEA-Leti (www.leti.fr/en) has been granted a government license to experiment with television white-space equipment in the field.

Neul's Cambridge network builds upon the completion of the first phase of the Cambridge White Space Consortium's wireless network. This network uses Neul's equipment and cloud interface together with the Weightless communications standard. In doing so, it proves that its white-space network coexists with televisions and wireless microphones without causing interference or disruption.

Of course, city space does create a challenging propagation environment. There is more than 120-dB link loss through buildings, foliage, walls, furniture, and human beings. Neul believes that its network opens up several possibilities for the Smart City of the future. It could enable intelligent transport and traffic management, city lighting, and other municipal services.

COGNITIVE RADIOS

CEA-Leti has developed opportunistic radio technologies (or cognitive radio) since 2005. In fact, the French government decided to issue a license to the research center because of the wireless cognitive-radio systems that were developed by Leti's Communication and Security Department (STCS). Cognitive radios are able to both allocate and exploit spectral resources. In doing so, they optimize the capacity and capability of wireless-communications networks. Dynamic spectrum management is not currently permitted in France, however. Because it is perceived as an efficient means to de-saturate the crowded radio spectrum, many industry experts expect permission for such management to be given.

It's a different matter in the US, where unlicensed opportunistic spectrum usage has been authorized in the free channels of the television spectrum or television white space. Studies have been evaluating whether a similar paradigm could be applied in Europe—for instance, in the framework of the European Conference of Postal and Telecommunications Administrations. The technology developed by Leti can be applied in both Europe and the US. The STCS's cognitive-radio research focuses on two fundamental issues related to dynamic spectrum access: free-channel detection and flexible, high-spectrum-efficiency communication systems with low power leakage in the adjacent channels (known as adjacent-channel leakage ratio).

The licensing of spectrum space is always a key issue in wireless communication. Here in the UK, however, national communications regulator Ofcom (www.ofcom.org.uk) has said that it would not seek to license access to the spectrum relative to white-space communications. Ofcom expects the first examples of white-space technology to come online this year.

WHAT'S NOT IN A NAME?

THE NAME "SUPER WiFi" is misleading because white-space communications is not based on WiFi technology. Instead of using the 2.4-GHz frequency, white-space communications employ the lower-frequency white spaces between television channel frequencies. These allow signals to travel further and penetrate walls better than technologies based on the higher frequencies.

The term "white spaces" refers to the frequencies allocated to a broadcasting service. This allocation process creates a bandplan that assigns white space.

GSMA MOBILE.™ WORLD CONGRESS

Barcelona | 25 – 28 February 2013

THE NEW MOBILE HORIZON

The mobile ecosystem continues to expand at lightning speed, with endless innovation and new applications of connected technology. Similarly, the industry's premier event is expanding in 2013. Mobile World Congress is relocating to a new world-class venue, Fira Gran Via, in the heart of the Mobile World Capital. With this convergence, the possibilities for global impact are endless.

Join us in Barcelona as together we explore the **New Mobile Horizon**

An Event of:

MOBILE WORLD CAPITAL™ BARCELONA

www.MobileWorldCongress.com

Scan to Learn More

NANCY FRIEDRICH | Editor-in-Chief
JACK BROWNE | Technical Contributor

DEVICE DIVERSITY Drives Industry Forward

AS APPLICATIONS FOR RF/MICROWAVE TECHNOLOGIES HAVE EXPANDED, SEMICONDUCTOR TECHNOLOGIES HAVE GROWN IN NUMBER, PROVIDING DESIGNERS WITH HEALTHY CHOICES.

SEMICONDUCTOR TECHNOLOGIES are now more diverse than at any time in the history of the RF/microwave industry. At one time, they were entirely based on silicon. Then, with more than a little push from military funding, gallium arsenide (GaAs) became the "darling" semiconductor technology of the high-frequency industry. GaAs was projected in various 1980s studies to be the ultimate RF/microwave semiconductor material, and GaAs monolithic microwave integrated circuits (MMICs) would eventually replace silicon and provide all transistors, diodes, and integrated circuits (ICs) needed for any electronic market. Today, producers and providers of gallium nitride (GaN) say that it is the semiconductor material to beat, and they are predicting the kind of dominance for GaN that was once projected for GaAs.

Admittedly, GaN is an impressive semiconductor substrate material, especially for high-frequency applications. It can support operating frequencies well into the millimeter-wave range, at very high output-power levels, and with high gain. GaN may lack the excellent noise characteristics of GaAs that enable high-performance low-noise amplifiers (LNAs) at microwave and millimeter-wave frequencies, but it has clearly become the device material of choice for high-power microwave semiconductors.

GaN devices work well with very high supply voltages, such as +48 and +50 VDC. For example, NXP Semiconductors (www.nxp.com) has developed a number of +50-VDC discrete power transistors based on its GaN high-electron-mobility-transistor (HEMT) process technology, with provides generous output-power levels with high efficiency. The firm's model CLF1G0035-50 is usable from DC to 3.5 GHz with better than 50 W output power and 43% power-added efficiency at test points of 1 and 2 GHz. It is suitable for a number of different applications, including in jammers, radar transmitters, commercial cellular systems, and public mobile radios.

For even higher power levels, the company's model CLF1G0035-100 is a high-power 100-W transistor that is usable from DC to 3.5 GHz. It provides 11.2-dB gain at 1 GHz and 11.7-dB gain at 2 GHz, with continuous-wave (CW) PAE of 47.9% at 1 GHz and better than 53% at 2 GHz. Both GaN HEMT transistors are supplied in flange-type packages with or without mounting holes (**Fig. 1**). But while GaN performance is impressive, the technology must overcome some hurdles for broader customer acceptance. "GaN's

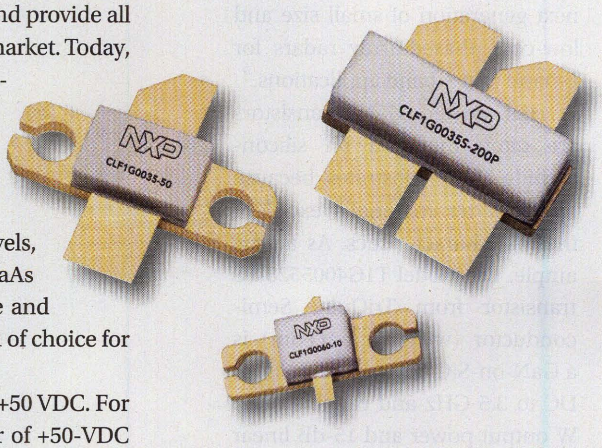

1. GaN devices such as these are capable of high output levels, and packaging is critical to provide effective thermal management. [Photo courtesy of NXP Semiconductor (www.nxpsemiconductor.com).]

current biggest challenge is that it is expensive," admits Mark Murphy, NXP's Marketing Director for RF Power. "The challenge is to find a better cost structure that will allow it to be used in more commercial applications."

In an attempt to address the cost issues, M/A-COM Technology Solutions (www.macomtech.com) recently introduced a line of GaN wideband power transistors in plastic packages. Although data is not yet available for these devices, they are supplied in 3 x 6 mm plastic packages and designed for low-cost L- and S-band radar and satellite-communications (satcom) applications. As Damian McCann, M/A-COM's Director of New Technology Initiatives, explains: "We have created a range of rugged and reliable high voltage, unmatched transistors with exceptional electrical and thermal performance...these products will enable our customers to create the next generation of small size and low-cost phased-array radars for L-band and S-band applications."

High-power GaN transistors are often mounted on silicon-carbide (SiC) substrates because of the latter material's excellent thermal characteristics. As an example, the model T1G4005528-FS transistor from TriQuint Semiconductor (www.triquint.com) is a GaN-on-SiC device usable from DC to 3.5 GHz and capable of 55 W output power and 15-dB linear gain at 3.5 GHz. It is supplied in a metal-ceramic flange package and operates from a +28-VDC supply. The company offers GaN-on-SiC devices at power levels as high as 100 W from DC to 18 GHz (model TGF2023-20).

SiC is also a starting material for many current high-power transistor products. Like GaN, SiC received a big push from military funding, and some of the results showed the promise of SiC devices at high power levels. Unfortunately, the technology has so far been limited to RF and lower microwave frequencies, and is actually gaining many followers for power supplies and power-switching applications.

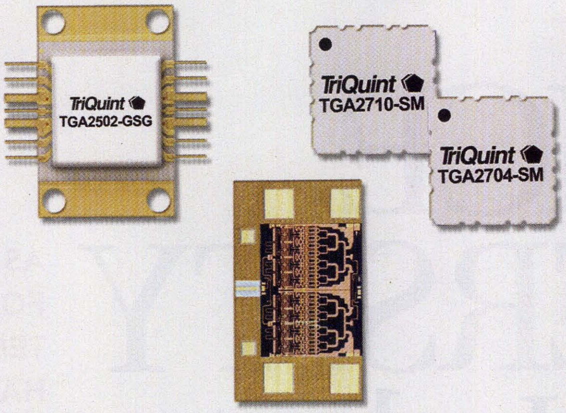

2. These GaAs PA modules are mounted in novel ground-signal-ground (GSG) packages that allow flexible mounting on a PCB. [Photo courtesy of TriQuint Semiconductor (www.triquint.com).]

Nevertheless, Cree (www.cree.com) has developed some higher-frequency devices based on SiC substrates—including the model CRF-22010 transistor, a SiC MESFET with 10 W output power and 12-dB gain at 2.2 GHz. The firm, which is also active in GaN technology, has also developed lower-frequency SiC devices operating at much higher voltages: model CMF10120D is a high-power transistor that draws 24 A at +1200 VDC and is suitable for both motor drives and switched-mode power supplies.

Microsemi (www.microsemi.com) has likewise applied SiC transistor technology to motor-drive and power-supply activities. But this is also a company that has developed a number of different technologies to cover a broad range of markets, including automotive, industrial, medical, commercial, and military applications. The firm recently announced availability of a complete medical network radio link for implantable medical devices such as pacemakers and cardiac defibrillators. The new radio link is comprised of the company's ZL70321 implantable radio module and its ZL70120 base station radio module, both of which are based on the firm's low-power model ZL70102 medical implantable communications service (MICS) band radio transceiver chip. Martin McHugh, Microsemi's Product Line Manager, notes: "With Microsemi's two-module radio link, companies can now focus research dollars and development efforts on new therapies that enable a better quality of life."

Also at lower frequencies, silicon laterally diffused metal oxide semiconductor (LDMOS) technology has been a dominant device material for cellular base stations and RF/microwave radios for some time (although proponents of GaN feel that the newer technology may one day replace LDMOS as the technology of choice in high-power wireless base stations). Like GaN, silicon LDMOS transistors can work at high voltages, such as +50 VDC, making the two device technologies almost interchangeable for broadcast and commercial communications applications.

Although LDMOS devices are more typically designed for pulsed and CW applications at frequencies below about 1500 MHz, they are capable of impressive output levels. Drawing from the legacy of Motorola Semiconductor's LDMOS technology, the model MRF6VP41KH is a +50-VDC LDMOS transistor in an air-cavity ceramic package with 1000 W output power from 10 to 500 MHz. Suitable for commercial aerospace and industrial-scientific-medical (ISM) band applications, it has excellent thermal performance and can achieve high drain efficiency.

While GaN is now being touted as the successor to GaAs, the latter is hardly finished as a viable high-frequency semiconductor technology. The technology and its suppliers have received generous support

over the years from government agencies such as the Defense Advanced Research Projects Agency (DARPA). As a result, GaAs in its many forms—in low-noise and higher-power circuits—is well entrenched throughout the RF/microwave industry. Major GaN suppliers such as TriQuint Semiconductor (www.triquint.com), continue to support GaAs foundry services. In fact, TriQuint's GaAs foundry, which was established in 1985, is one of the world's large GaAs foundry facilities and works with both 100- and 150-mm wafers. TriQuint recently announced a low-cost PA module for cellular GSM and EDGE applications in smartphones, computer tablets, and other wireless consumer products. The PA measures just 5.0 x 3.5 mm and is based on the firm's GaAs heterojunction-bipolar-transistor (HBT)/CuFlip™ technology. In addition to GaAs and GaN, the foundry also provides indium-gallium-phosphide (InGaP) HBT processing services.

SiC is now utilized as a starting material for many current high-power transistor products.

TriQuint recently added to its GaAs product portfolio with a number of packaged GaAs pseudomorphic-high-electron-mobility-transistor (pHEMT) PA modules for applications from 6 to 38 GHz. Suitable for commercial satcom systems, point-to-point radios, and military radar and electronic-warfare (EW) systems, they are supplied in packaging that supports multilayer printed-circuit-board (PCB) layouts.

The PAs use the company's Die-on-Tab packaging approach to simplify handing. The amplifiers benefit from vacuum reflow process which creates nearly void-free bonds between dies and bases with excellent thermal stability. One of the packaging approaches **(Fig. 2)** is a ground-signal-ground (GSG) package configuration that allows users to mount the amplifiers "right-side up" or "upside down" on a PCB. Examples of the new PA line are models TGA2502-GSG with 3.6 W output power from 13 to 16 GHz and model TGA2575-TS with 3 W output power from 32 to 38 GHz.

GaAs technology is also well supported by commercial foundry and device supplier United Monolithic Semiconductors (www.ums-gaas.com). UMS touts GaAs-based solutions through 100 GHz, and recently took the "plastic-package" approach to create a low-cost GaAs MMIC circuit for W-band applications from 76 to 77 GHz, including in automotive commercial radar systems and industrial sensors. Model CMH1270a98F is a dual-channel transmitter/receiver that works with intermediate-frequency (IF) signals from DC to 100 MHz. It is also available in chip form, measuring just 2.95 x 2.00 x 0.10 mm.

Hittite Microwave Corp. (www.hittite.com) is another company well known for its lower-cost GaAs-based MMIC solutions, with GaAs products available through 100 GHz. A recent example is the model HMC3653LP3BE, a GaAs HBT amplifier supplied in a 3 x 3 mm plastic QFN package. It delivers 15 dB gain from 7 to 15 GHz and as much as +15 dBm output power at 1-dB compression with +28 dBm output power at the third-order intercept point. The plastic-packaged MMIC amplifier, which boasts a noise figure of only 4 dB, is ideal for point-to-point and point-to-multipoint radios, VSAT, broadcast relay links, and X-band communications systems. It is designed for +5-VDC supplies and draws about 44 mA current over a wide operating temperature range (–40 to +85°C).

Using a slightly different process, ANADIGICS (www.anadigics.com) recently introduced its model AWB7129 power amplifier (PA) for small cellular-communications infrastructure stations, such as picocells and customer premises equipment (CPE). It is based on the company's patented InGaP-Plus™ HBT MMIC technology to deliver a combination of high efficiency, linearity, and effective thermal management.

At lower power levels, GaAs is facing some competition from semiconductor processes that have moved higher in frequency in recent years. Silicon complementary-metal-oxide-semiconductor (CMOS) processes have gained ground on GaAs. Some firms, such as TowerJazz (www.jazzsemi.com), now offer devices and processing based on RF CMOS and other lower-power technologies such as silicon-germanium (SiGe) BiCMOS well into the microwave frequency range.

Marco Racanelli, TowerJazz Senior Vice President, sees the firm's SiGe products as legitimate threats to the market share long help by GaAs in lower-noise applications: "We also see the highest performance SiGe technologies now reaching noise-figures that can compete head to head with GaAs for applications such as Global-Positioning-System (GPS) low-noise amplifiers (LNAs) and so believe some of these applications will move away from GaAs in the future." Racanelli adds that "GaAs will retain some market share of high-end Wi-Fi PAs. In cellular communications, GaAs PAs will continue to dominate, but inroads on the low end of the market are being made by CMOS."

Dr. Keith Strickland, Chief Technical Officer at Plessey Semiconductors Ltd. (www.plesseysemiconductors.com), says it may be a bit premature to cast off GaAs and start awarding prizes to GaN devices. He notes that GaN is still limited in terms of suitable substrates, and each substrate poses problems. "Sapphire, for example, has a relatively poor thermal conductivity which spoils the advantage of GaN, and the GaN may need to be transferred to another substrate, such as SiC."

Strickland adds that the excellent high-frequency characteristics of GaAs devices still make them valuable: "GaAs as a current state of the art through about 100 GHz. It has an advantage of being relatively well understood, with substrates that are native to the technology and will keep it cost-effective for very high frequency front end and microwave applications... but because GaAs does not have the thermal performance of GaN, Si, or SiC, it may lose out to GaN or SiC in the future for high-power applications." MWRF

WIDEBAND PLL + VCOs

4 GHz with 4 Outputs Ideal for Next Generation MIMO Applications

Analog, Digital & Mixed-Signal
ICs, Modules, Subsystems & Instrumentation

Wideband PLL & VCO, 33 - 4100 MHz, 4 Outputs

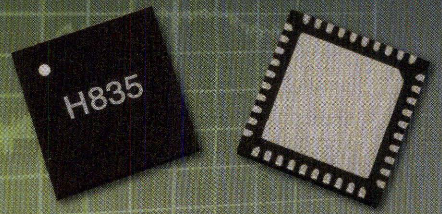

- Maximum Phase Detector Rate: 100 MHz
- PLL FOM:
  -230 dBc/Hz Integer Mode
  -227 dBc/Hz Fractional Mode
- <160 fs Integrated RMS Jitter (1 kHz - 100 MHz)
- Low Noise Floor: -165 dBc/Hz
- 4 Single-Ended or 2 Differential Outputs

Closed Loop Fractional Phase Noise at 3600 MHz, Divided by 1 to 62

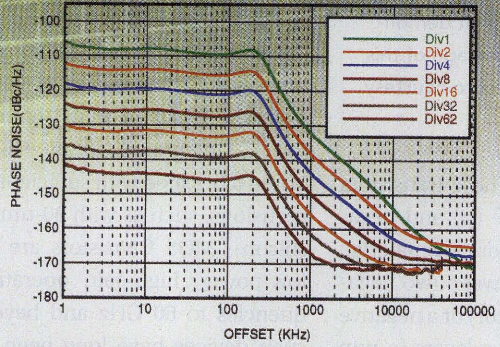

Fractional Spurious Performance at 2646.96 MHz, with Exact Frequency Mode ON or OFF

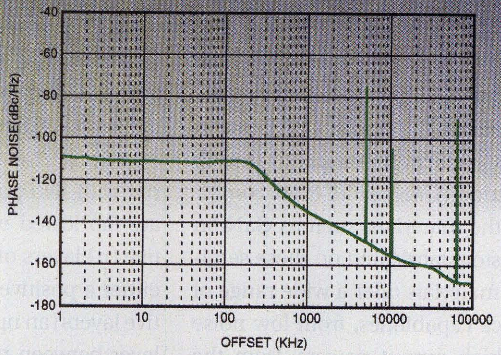

	Part Number	Frequency (MHz)	Function	Closed Loop SSB Phase Noise @ 10 kHz Offset	Open Loop VCO Phase Noise @ 1 MHz Offset	Pout (dBm)	RMS Jitter Fractional Mode (fs)	Integrated PN Fractional Mode (deg rms)
	HMC829LP6GE	45 - 1050 1400 - 2100 2800 - 4200 Fo	Wideband PLL+VCO	-108 dBc/Hz @ 4 GHz	-134 dBc/Hz @ 4 GHz	4	159	0.229 @ 4 GHz
	HMC830LP6GE	25 - 3000	Wideband PLL+VCO	-114 dBc/Hz @ 2 GHz	-141 dBc/Hz @ 2 GHz	6	159	0.114 @ 2 GHz
	HMC832LP6GE	25 - 3000	Wideband RF VCO (+3.3V)	-114 dBc/Hz @ 2 GHz	-139 dBc/Hz @ 2 GHz	7	159	0.114 @ 2 GHz
	HMC833LP6GE	25 - 6000	Wideband PLL+VCO	-114 dBc/Hz @ 2 GHz	-141 dBc/Hz @ 2 GHz	-4	159	0.11 @ 2 GHz
	HMC834LP6GE	45 - 1050 1400 - 2100 2800 - 4200 Fo 5600 - 8400	Wideband PLL+VCO	-108 dBc/Hz @ 4 GHz	-134 dBc/Hz @ 4 GHz	5 2 2 -10	159	0.23 @ 4 GHz
NEW!	HMC835LP6GE	33 - 4100	Wideband PLL+VCO	-105 dBc/Hz @ 4 GHz	-133 dBc/Hz @ 4 GHz	7	160	0.23 @ 4 GHz

@HittiteMWCorp

Hittite
MICROWAVE CORPORATION

2 Elizabeth Drive • Chelmsford, MA 01824
978-250-3343 tel • 978-250-3373 fax

Visit Us: www.hittite.com
Contact Us: pll@hittite.com

Receive the latest product releases - click on "My Subscription"

JACK BROWNE | Technical Contributor

Performance Guides Transistor Selection

With such a large number of RF/microwave transistor technologies currently available, basic requirements like output power at a given frequency can speed the selection process.

TRANSISTORS FOR RF/MICROWAVE applications are based on several different elements and compounds, with each substrate material bringing its own strengths and weaknesses. Not long ago, the choice for a microwave transistor was essentially between silicon and gallium arsenide (GaAs). But the last few decades have seen the emergence and growth of additional high-frequency semiconductor substrates, including indium phosphide (InP); silicon carbide (SiC); silicon germanium (SiGe); gallium nitride (GaN); and even combinations of the materials, such as GaN on SiC. Transistors fabricated on these semiconductor materials offer a wide range of performance capabilities, from low noise figures to high output powers, from the high-frequency (HF) range through millimeter-wave frequencies.

The comparison of silicon bipolar-junction-transistor (BJT) devices to GaAs transistors, such as metal-epitaxial-semiconductor field-effect transistors (MESFETs), has long been simply the differentiation of the two technologies' operating frequency ranges. In addition to using different substrate materials, silicon bipolar transistors and GaAs MESFETs differ in structure, although both are three-terminal semiconductor devices. The terminals in a silicon bipolar transistor are the base, collector, and emitter; a small current at the base terminal can switch or control a much larger current between the collector and emitter terminals.

Bipolar transistors are formed of two junction diodes on semiconductor material with two polarities. These transistors are fabricated on positive (p) and negative (n) layers of semiconductor material: either a positive layer between two negative layers (an npn transistor) or a negative layer between two positive layers (a pnp transistor). Bipolar transistors conduct both majority and minority carriers.

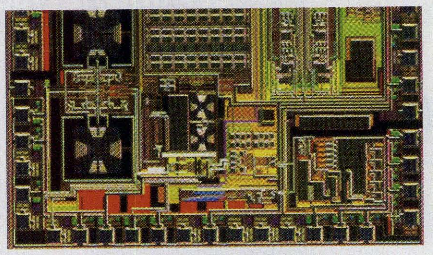

1. This highly integrated circuit demonstrates the silicon CMOS heritage of this SiGe device technology. [Photo courtesy of IBM (www.ibm.com).]

In contrast, an FET's terminals are the gate, source, and drain—a voltage at the gate can control a current between source and drain. A FET is also known as a unipolar transistor because it uses only one form of conductor, electrons, or holes. Current flows from the drain to the source, with the conductivity varied by the electric field that is produced when a voltage is applied between the gate and source terminals. The current that flows between the drain and the source is controlled by the voltage between the gate and the source. FETs, in both silicon and GaAs forms, can be used as switches or as amplifiers.

Silicon metal-oxide-semiconductor FETs (MOSFETs) are capable of high power-handling capabilities at lower frequencies and in switching power supplies. GaAs FETs—although not capable of the high power levels of silicon MOSFETs—can operate through microwave and millimeter-wave frequencies, typically in solid-state low-noise or power amplifiers. FETs can provide current and/or voltage gain.

In addition to serving for many years as the substrate of choice for many high-power silicon bipolar transistors at sub-microwave frequencies, silicon has also been the basis for many high-frequency CMOS integrated-circuit (IC) devices. When fabricated with sufficiently small dimensions, such as with 90-nm processes, silicon CMOS transistors are capable of low-power, high-gain operation at frequencies to 60 GHz and beyond. While such devices have long been associated with digital and computer applications, their low cost and capabilities for millimeter-wave operation make them attractive candidates for use in higher-frequency consumer applications. These include point-to-point backhaul radios at 60 GHz and automotive radar systems at 77 GHz.

As part of efforts to develop higher-frequency, higher-power transistors, silicon has also worked with other elements as part of compound materials substrates, including silicon germanium (SiGe) and silicon carbide (SiC). SiGe substrates have held great promise for higher-frequency applications while silicon-carbide (SiC) materials offer much potential for higher power levels.

IBM (www.ibm.com) has done a great deal of work on high-frequency SiGe BiCMOS devices, offering foundry services

for customers needing high-frequency analog and mixed-signal ICs. IBM's SiGe technology is based on 130-nm silicon CMOS foundations, and is suitable for applications at 60 GHz and higher frequencies **(Fig. 1)**. The firm offers "multi-project wafers," with a number of different customers having their designs fabricated on the same wafer so that one customer is not required to field the expenses for an entire process run (for more, see p. 46).

Last year, Renesas Electronics (www.renesas.com) announced its work using a blend of SiGe and carbon, resulting in its model NESG7030M04 SiGe:C heterojunction bipolar transistor (HBT) for low-noise applications. Developed for 5-GHz wireless-local-area-network (WLAN) applications, this transistor features a noise figure of only 0.75 dB with about 14-dB gain in the 5.8-GHz band. This performance represents a significant improvement in noise-figure performance over the company's earlier SiGe HBT devices. The firm explains that the addition of carbon has made it possible to optimize the device's collector-base profile, increasing the range of supply voltages that can be used.

In terms of SiC, these discrete devices and modules are capable of high-voltage, high-power operation through lower microwave frequencies. An early developer of the technology, Cree (www.cree.com), offers SiC MOSFET die and packaged devices at voltages to 1200 V, such as the low-frequency model CMF10120D. Suitable for motor drives and switched-mode power supplies, it draws 24 A at +1200 VDC.

Over a decade ago, the firm introduced its model CRF-22010, a SiC MESFET capable of 10 W output power and 12-dB gain at 2.2 GHz. The Class A linear transistor is designed for a +48-VDC supply. But the company is also heavily involved in GaN device development, recently introducing 50-V GaN HEMTs for commercial cellular communications applications, including model CGHV22100 with 100 W output power from 1800 to 2200 MHz for Long-Term-Evolution (LTE) cellular base stations. The GaN HEMT **(Fig. 2)** features 20-dB gain with as much as 35% power-added efficiency across its frequency range.

Many companies are finding the elec-

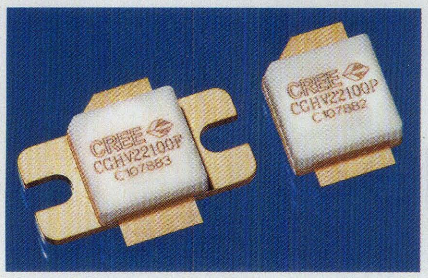

2. These packaged 50-V GaN HEMTs are capable of 100 W output power from 1800 to 2200 MHz for use in cellular communications networks. [Photo courtesy of Cree (www.cree.com).]

trical capabilities of GaN and the thermal capabilities of SiC to be a powerful combination, fabricating GaN-on-SiC transistors with excellent high-power, high-frequency capabilities. The model T1G4005528-FS transistor from TriQuint Semiconductor (www.triquint.com) is a discrete GaN-on-SiC HEMT that is usable from DC to 3.5 GHz. It provides 15-dB linear gain at 3.5 GHz with 55-W output power at that frequency when operating from a +28-VDC supply. It is built with the firm's 0.25-μm production GaN process and supplied in a metal-ceramic flange package. It is suitable for commercial and military applications in radios, radar, and avionics systems. The company's highest-power discrete GaN-on-SiC HEMT is model TGF2023-20, with 100 W output power from DC to 18 GHz. It offers maximum power-added efficiency of 52%, with 17.5-dB power gain at 3 GHz.

Just what kind of output-power levels are in store for GaN devices? Military organizations such as DARPA (www.darpa.mil) foresee GaN amplifiers as compact solid-state replacements for vacuum-tube electronics in radar systems. As an example, the Beverly Microwave Division of Communications and Power Industries (www.cpii.com) developed its model VSS3607 GaN amplifier for S-band radar transmitters. It yields 1.3 W saturated output power from 2.7 to 2.9 GHz when operating with pulse widths from 1 to 100 μs at 10% duty cycle. The GaN amplifier draws 13 A at +30.5 VDC and provides 62-dB small-signal gain. It measures 9.5 x 15.5 x 1.75 in. and weighs 11 lbs. When 12 of these units are power combined as the model VSS3605 amplifier, however, they achieve 13 kW output power from 2.7 to 2.9 GHz with 71-dB small-signal gain. Of course, with so many amplifiers, the package size is somewhat larger, at 19.0 x 25.5 x 23.5 in. and 230 lbs.

Researchers pursuing higher-frequency uses for semiconductor devices have considered the various types of transistors and semiconductor devices used for microwave and millimeter-wave applications; they have generally compared GaAs versus GaN devices, or even InP devices. [Last year, NASA's Jet Propulsion Laboratory (JPL; www.jpl.nasa.gov) reported InP ICs operating to frequencies as high as 670 GHz.] For example, emerging applications in the terahertz (THz) region, which typically includes frequencies just below the infrared region, from 100 GHz to 10 THz, show much promise for imaging radar, and broadband communications systems.

The thermal conductivity of GaN is much higher than that of GaAs, about 170 W/m-K for GaN versus about 50 W/m-K for GaAs, which allows for much higher power levels for GaN devices compared to GaAs transistors. GaN also offers more than twice the bandgap energy of InP and GaAs. Quite simply, GaAs and InP transistors are limited in output power at higher frequencies, especially compared to GaN, making GaN an attractive semiconductor material for potential THz applications.

In addition, DARPA has invested in InP device technology for higher frequencies as part of its THz Electronics program. The organization's efforts have resulted in improvements in InP HBTs and HEMTs, making possible a 670-GHz LNA based on InP active devices, as compact, lower-power replacements for vacuum-electronics devices. Major defense contractors, such as Northrop Grumman (www.northropgrumman.com), have long applied InP HEMT MMIC technology for fabrication of amplifiers and other components operating in the millimeter-wave range, at frequencies past 200 GHz, for passive imaging and other satellite-communications (satcom) applications. MWRF

JACK BROWNE | Technical Contributor

Foundries Offer Large Process Menus

High-frequency chip and device designers can draw on a wide range of process technologies from the large number of semiconductor foundries serving this industry.

HIGH-FREQUENCY DESIGN ENGINEERS currently enjoy access to an unprecedented variety of semiconductor foundries and semiconductor processes. Most commercial foundries provide at least two wafer runs per year for their major processes and, in addition, often offer opportunities to experiment by sharing space on a multiple project wafer with other customers. The electrical functions offered by these many processes range from low-noise and high-power analog circuits to dense, high-speed digital circuits and wafers with combinations of analog and digital circuits. Some of the latter extend well beyond 100 GHz.

Many semiconductor suppliers, notably those without their own foundries, rely on foundry services to create their semiconductor-based products. Not having a foundry on premises has advantages, since it shifts the responsibilities for the care and maintenance of the foundry and its associated test equipment to the vendor. But this also sacrifices total control over the process and the vast opportunities for experimentation. Still, semiconductor foundries that sell their services generally pride themselves on their capabilities. They typically offer customers many levels of service, with as little or as much help as needed.

Most semiconductor foundry services start with a process design kit (PDK). This is a software-based tool built around the latest computer-aided-engineering (CAE) software, such as Microwave Office® from AWR Corp. (www.awrcorp.com), the Advanced Design System (ADS) from Agilent Technologies (www.agilent.com), and Ansoft Designer with Nexxim from Ansoft (www.ansoft.com). When contracting with a gallium-arsenide (GaAs) foundry such as United Monolithic Semiconductors (www.ums-gaas.com), a customer receives a PDK that is designed for a suitable semiconductor process (such as a low-noise or power process), and compliant with the customer's computer operating system and other simulation tools.

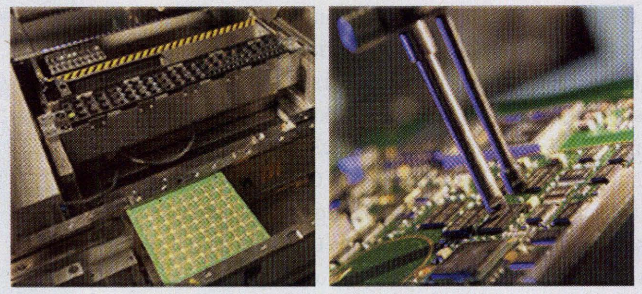

RFMD, an open foundry offering services based on III-V semiconductor materials such as GaAs and GaN, promises wafer turnaround in just six weeks. [Photos courtesy of RFMD (www.rfmd.com).]

The PDK incorporates active and passive device models developed (and known to be effective) by the foundry, and essential to creating GaAs monolithic-microwave-integrated-circuit (MMIC) active and passive circuits with the foundry's various semiconductor processes. Such software design tools are vital for creating a MMIC layout that the foundry can translate into a real wafer, using its own design-rule-check (DRC) process to verify the accuracy and validity of the layout.

Following a successful DRC process, the foundry will create a wafer mask that aids in fabricating the many physical levels of a GaAs semiconductor. Then, depending upon the foundry arrangement, the mask is used to produce two or more wafers filled with the customer's design. In the case of the UMS foundry, production wafers are inspected visually, as well as via RF and direct-current (DC) process-control-monitoring (PCM) measurements that help determine final wafer quality and acceptance. UMS provides delivery of wafers by means of a GelPak® box or in diced form on UV film. Of special benefit to many customers, UMS offers two-day training courses that help to convey the foundry's GaAs MMIC design methodology. Topics covered include process, modeling, CAE tools, reliability, electrical measurement, picking, packaging, and industrialization.

Semiconductor foundries share special relationships with CAE software developers because of the strict requirements for PDKs. In many cases, a foundry will support multiple technology processes—each with its own set of PDKs, and each designed for use with a specific commercial electronic-design-automation (EDA) software tool. For example, one of the largest silicon semiconductor foundries, IBM Microelectronics (www.03.ibm.com/technology/), offers RF CMOS, RF silicon-on-

insulator (SOI), and silicon-germanium (SiGe) BiCMOS technologies at different locations, using 8-in. wafers for most of the semiconductor processes and 12-in. wafers for its standard silicon CMOS process in its Fishkill, NY facility.

As different as the capabilities of each process are, they all depend on their own PDKs developed for use with the ADS software from Agilent Technologies. In order for the combination to be effective, the performance capabilities of each semiconductor process must be accurately reflected by the simulation capabilities of the EDA software. Any update in the process technology must trigger an update with the EDA tools for this combination of process and software to provide optimum results.

For many years, the choice of foundry for an RF/microwave customer was between high-frequency silicon or GaAs process. But even one of the most successful GaAs foundries, TriQuint Semiconductor (www.triquint.com), now offers a number of different process technologies. TriQuint, which is one of the world's largest commercial GaAs foundries, offers GaAs pseudomorphic high-electron-mobility-transistor (pHEMT) and metal-epitaxial-semiconductor field-effect-transistor (MESFET) semiconductor technologies. Using 100- and 150-mm wafers, the foundry can deliver both low-noise and high-power GaAs MMIC circuits at frequencies beyond 100 GHz with a 0.6-μm MESFET process and with pHEMT processes supporting device features as small as 0.13 μm. The foundry has combined complementary technologies such as GaAs MESFET and/or pHEMT circuits with indium-gallium-phosphide (InGaP) heterojunction-bipolar-transistors (HBTs) on a single InGaP/GaAs wafer to provide tremendous flexibility for customers. Along with many foundries that started with GaAs, TriQuint now also supports GaN foundry services. For its highest-power devices, TriQuint employs GaN-on-SiC technology to combine the excellent high-frequency, high-power capabilities of GaN material with the excellent thermal conductivity of SiC. GaN is an attractive building material for both high-frequency and high-power use, and a growing number of foundries offer GaN-based foundry services. For example, RFMD (www.rfmd.com) is another example of a foundry that started with GaAs and has branched into GaN foundry services **(see figure)**. Such is also the case with Global Communication Semiconductors (GCS; www.gcsincorp.com), which has long supported GaAs foundry services only to add GaN to its lineup.

One of its customers, Nitronex (www.nitronex.com), recently completed qualification of GCS's GaN-on-silicon foundry process in support of Nitronex's discrete and MMIC GaN devices. The qualification process included extensive DC, RF, thermal, reliability, and other parametric testing to ensure that devices fabricated at GCS are every way equal to devices made at Nitronex's Durham, NC facility. Having the GaN foundry's output in addition to its own capabilities has Nitronex well positioned for sharp growth in power GaN devices. According to Charlie Shalvoy, the company's Chief Executive Officer, "The combination of our proprietary 100-mm GaN-on-Si process, and the full suite of production and new process development capabilities at GCS, gives us the ability to be a leader in the rapidly emerging market of GaN RF power devices."

In many cases, a foundry **will support multiple technology processes,** each with its own set of PDKs.

Silicon-carbide (SiC) substrates were once considered a leading candidate for high-power applications, and a number of foundries provide a full range of services based on SiC wafers, including GSC, Ascatron (www.ascatron.com), Cree (www.cree.com), Raytheon UK (www.raytheon.co.uk), and United Silicon Carbide (www.unitedsic.com). But many of these foundries have worked with higher-frequency GaAs substrates, including GSC and Raytheon, and the relatively low electron mobility of SiC materials relative to some of the other semiconductor substrates results in relatively low cutoff frequencies for SiC devices. Still, for power switching applications and motor drives, or any low-frequency application that requires high power density, SiC represents an attractive starting point.

But even foundries that started with SiC, such as Cree, have considered the benefits of higher-frequency materials like GaN, and have consequently expanded their foundry operations to include services based on GaN wafers. Although CREE is well established as a providing of lighting solutions with its light-emitting-diode (LED) devices and modules, the company also supports foundries for high-power SiC processes suitable for lower-frequency power switching and control and a 50-V GaN HEMT process that has resulted in 100-W GaN HEMT devices for LTE cellular communications applications from 1800 to 2200 MHz.

For lower-power, higher-frequency operation, InP-based HEMTs still show the highest cutoff frequencies and lowest noise of all three-terminal devices, and silicon-germanium (SiGe) transistors and diodes have routinely been fabricated for applications well into the millimeter-wave range—including for integrated-circuit (IC) transceivers at 160 and 165 GHz. But silicon CMOS has also shown a great deal of life at higher frequencies, with 90-nm silicon CMOS capable of fabricating ICs with +1-VDC transistors operating at 60 and 77 GHz, and more expensive 65-nm silicon CMOS processes typically delivering transistors operating beyond 100 GHz. However, for the higher-power levels sought for many microwave and millimeter-wave transmit applications, GaN and the foundries that support it have caught the attention of more than a few customers in both commercial and military applications. MWRF

WIDEBAND
TRANSFORMERS & COUPLERS

Transformers

Model Number	Frequency (MHz)	Impedance Ratio	Schematic
TM4-0	0.2 - 350	4:1	
TM1-0	0.3 - 1000	1:1	
TM1-1	0.4 - 500	1:1	
TM1.5-2	0.5 - 550	1.5:1	
TM2-1	1 - 600	2:1	
TM1-6	5 - 3000	1:1	
TM2-GT	5 - 1500	2:1	
TM4-GT	5 - 1000	4:1	
TM8-GT	5 - 1000	8:1	
TM4-1	10 - 1000	1:4	
TM4-4	10 - 2500	1:4	
TM1-2	20 - 1200	1:1	
TM1-9	100 - 5000	1:1	
TM1-8	800 - 4000	1:1	

Couplers

Model Number	Frequency (MHz)	Coupling	Coupling Flatness
GC6-2	1 - 700	6 dB ±0.5 dB (Nom.)	±1.0 dB
GC6-1	10 - 500	6 dB ±0.5 dB (Nom.)	±1.0 dB

Features

> Low Cost
> Wide Bandwidth
> Good Amplitude / Phase Unbalance
> Rugged Welded Construction
> RoHS Compliant
> Patented REL-PRO® Technology

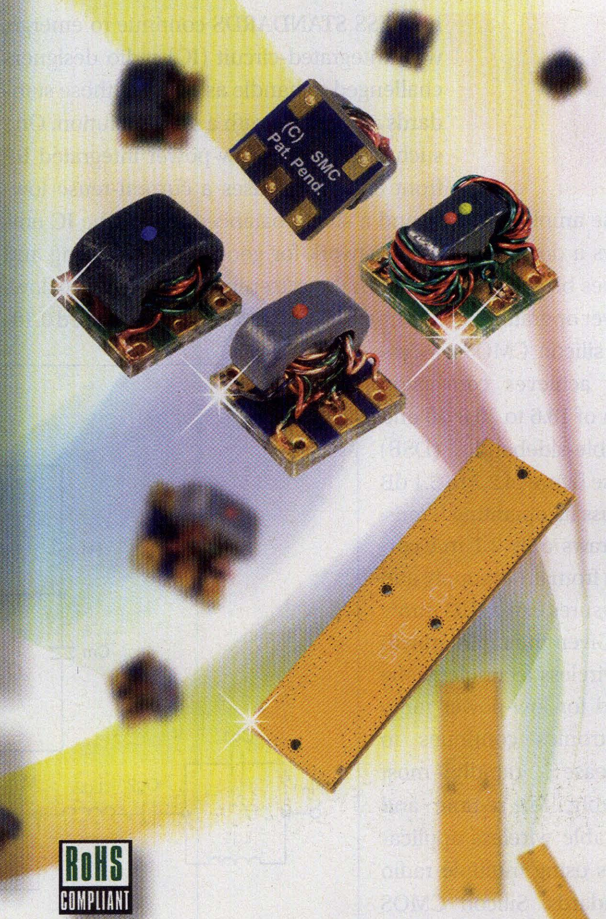

RoHS COMPLIANT

SYNERGY®
MICROWAVE CORPORATION

Phone: (973) 881-8800 | Fax: (973) 881-8361
E-mail: sales@synergymwave.com
Web: WWW.SYNERGYMWAVE.COM
Mail: 201 McLean Boulevard, Paterson, NJ 07504

KUI FU
Masters Degree Candidate

XIAORONG GUO
Professor

CHUNHUA WANG
Professor and Doctoral Supervisor

YUXIANG TU
Doctorate Degree Candidate

CHISHI LIU
Masters Degree Candidate

College of Information Science and Engineering, Hunan University, Changsha 410082, People's Republic of China; e-mail: fukuihsy@163.com.

JOE P. MCGEEHAN
Professor
Center for Communication Research, University of Bristol, Bristol, BS8 1UB, United Kingdom; www.bris.ac.uk.

Low-Power Receiver
Serves Multiple Wireless Standards

This extremely low-power front-end receiver design employs a current-reuse low-noise amplifier and switch-based single-balanced frequency mixer, achieving high conversion gain across its broad operating frequency range.

WIRELESS STANDARDS continue to emerge, with integrated-circuit (IC) radio designers challenged to handle as many of those standards as possible with a single solution. One such solution is a low-power integrated RF front end which uses a current-reuse low-noise amplifier (LNA) and a single-balanced mixer. The IC employs a double-resonant network for good input matching and reuses bleeding current from the mixer in the LNA for true low-power operation. The front-end IC is fabricated in a standard 0.18-μm silicon CMOS process and achieves conversion gain of 18.6 to 20.8 dB and double-sideband (DSB) noise figure of 2.3 to 5.1 dB across its operating bands. It draws only 2.1 mA current from a 1-V supply and measures 0.61 x 0.53 mm^2.

Given the rapid growth of wireless technology, the need for low-power radio electronics continues to increase rapidly—most notably, for remote and portable wireless applications using multiple radio standards. Silicon CMOS has been used in a number of low-power radio-frequency integrated circuits (RFICs) for wireless applications,[1-3] but often

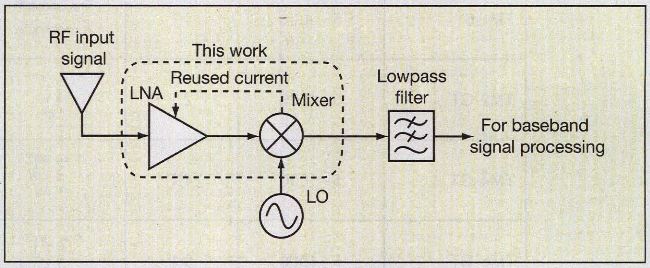

1. This block diagram shows how the low-power receiver might be used in a communications system.

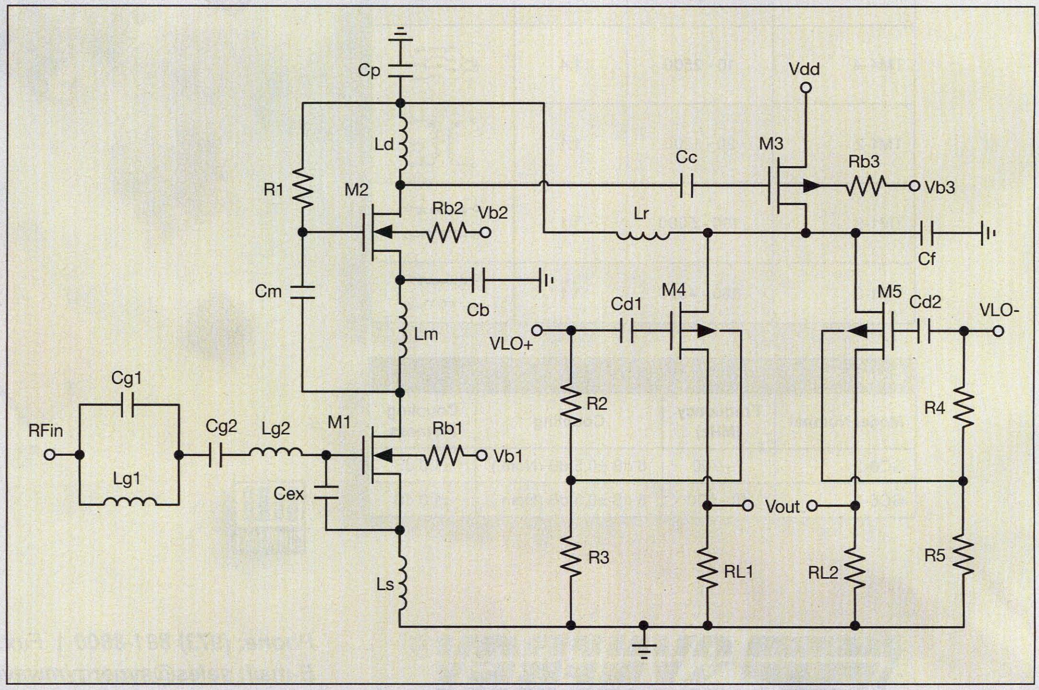

2. This is a more-detailed block diagram of the low-power receiver front end showing its circuit elements.

IMS 2013

International Microwave Symposium
IEEE 2-7 June 2013, Seattle, WA MTT-S

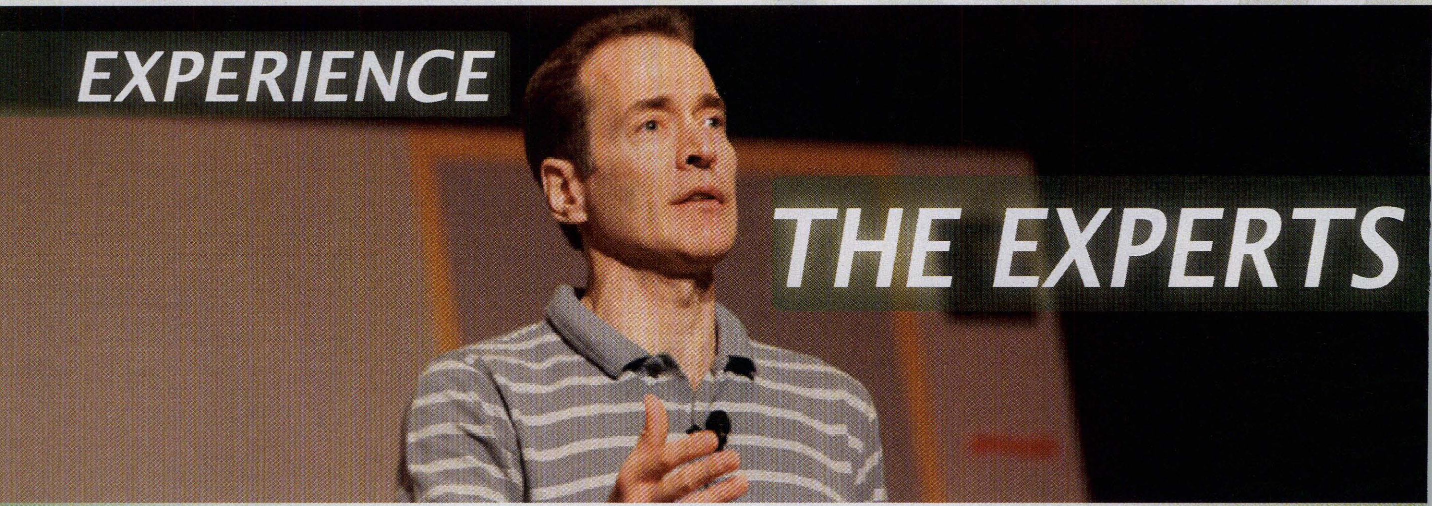

INTELLECTUAL PROPERTY, PATENTS AND COMMERCIALIZATION: OPTIMIZING YOUR SUCCESS!

Join IMS2013 for what is sure to be an exciting and fervent Plenary talk led by Dr. Patrick Ennis, Global Head of Technology, Intellectual Ventures.

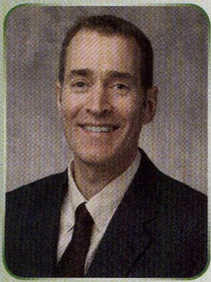

Invention Capital: Why the World Needs More of it
Monday, 3 June 2013

"It is an exciting time to be a technologist. Every day, breakthroughs in research laboratories offer the promise of products and solutions to meet a range of global challenges and opportunities. However, it is very difficult to successfully commercialize technology; and unfortunately most efforts fail. We need to improve the success rate, otherwise billions of dollars of R&D funding will be wasted, and innovation-driven economies will stall. Invention Capital is a missing link in the value-creation chain."

Dr. Patrick Ennis will talk about how researchers from a variety of scientific and technical fields can optimize the value- creation chain. He will be sharing new models such as Open Innovation and Invention Capital that are necessary to successfully commercialize technology, in today's challenging environment where the speed of technology development and adoption has so accelerated that even leading technology companies find it hard to just keep up. This is an opportunity for leading researchers to understand the latest trends in managing valuable IP and bringing it closer to commercialization.

IMS IS WHERE...

- state-of-the-art materials, devices, components, subsystems, design and test equipment are showcased by over 550 companies.
- researchers choose to present their work. The future of RF & Microwave debuts here first!
- new products are unveiled and new partnerships formed.
- your current and future customers go for product evaluation.
- your competitors know they need to be.

FOR EVENT DETAILS VISIT
HTTP://IMS2013.MTT.ORG

IEEE MTT-S

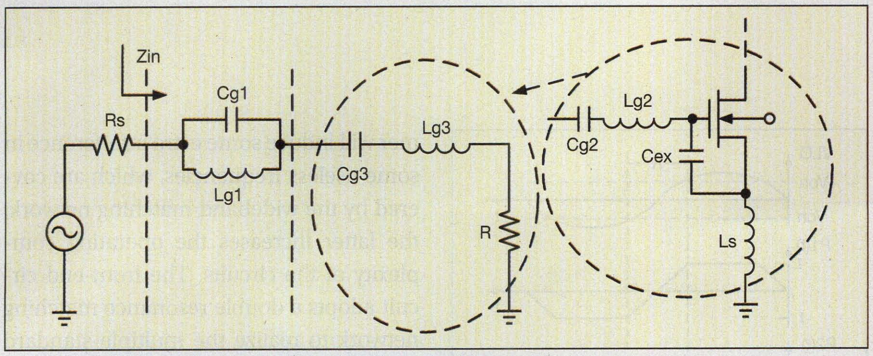

3. This is an equivalent-circuit diagram of the receiver's input circuitry and its double-resonator matching network.

in narrowband designs that are not suited for multiple-standard applications. In addition, many of these wireless CMOS RFICs are guilty of high power consumption, limiting their value for multiple-standard wireless applications.[4-9]

Minimizing power consumption usually involved reducing the supply voltage and current of a circuit. In the past, a conventional cascade structure (CS)[10] has been used in LNAs to optimize different performance parameters, including gain and reverse isolation. Nevertheless, this structure is not suitable for low-voltage applications since the supply voltage should be twice as large as the threshold voltage (V_{th}) of the LNA's transistors. A folded cascade CS topology proposed in ref. 11 operated at a supply voltage of only 0.7 V, but it induced more branch current and went against the ultra-low-power front-end design. A conventional cascade CS topology capable of reducing the supply voltage down to 0.6 V was unveiled in ref. 12, with good gain performance. However, the transistors in that configuration were working in a weak inversion region, which induced degradation of gain and noise-figure (NF) performance.[13]

Current-reuse topologies and forward-body-bias techniques have been used more recently to achieve low power consumption in RFICs.[1,13,14] But these efforts

Table 1: Comparing communications bands.

Wireless standard	Frequency spectrum (MHz)	Centralized frequency spectrum (MHz)
GSM-900	935 ~ 960	935 ~ 960
DCS-1800	1805 ~ 1850	1805 ~ 2483
DECT	1881 ~ 1897	
PCS-1900	1930 ~ 1960	
TDS-CDMA	2010 ~ 2025	
WCDMA	2100 ~ 2170	
802.11b/g	2400 ~ 2483	
Bluetooth	2400 ~ 2483	

always focused on low-power LNA circuits—without inclusion of a low-power mixer—and often to the detriment of amplifier performance, such as linearity or NF. This current report applies current reuse and forward-body-bias techniques to the combination of an LNA and a mixer, improving the performance of both.

As **Table 1** shows, the frequency range of personal wireless communications standards is extensive. As a result, a double-resonant input matching network for the LNA/mixer was designed to resonate at center frequencies within 935 to 960 MHz and 1805 to 2483 MHz, respectively. The input architecture helps to achieve good impedance matching within these bands and to suppress noise between these two spans without an additional notch filter. The front-end circuit incorporates both current-reuse and forward-body-bias techniques to minimize current consumption at low supply voltages. The circuit reuses bleed current from the mixer to energize the LNA[15] and a local-oscillator (LO) signal forward-body-bias technique to minimize current draw.

Figure 1 shows the block diagram of an ultra-low-power RF receiver. RF input signals enter the LNA from the antenna. The LNA amplifies these voltage input signals by reusing bleed current from the mixer. Amplified signals from the LNA enter the single-balanced mixer and are mixed with the LO signals. The intermediate-frequency (IF) output signals from the mixer are processed by the lowpass filter. Finally, the filtered signals enter the baseband signal system for further processing.

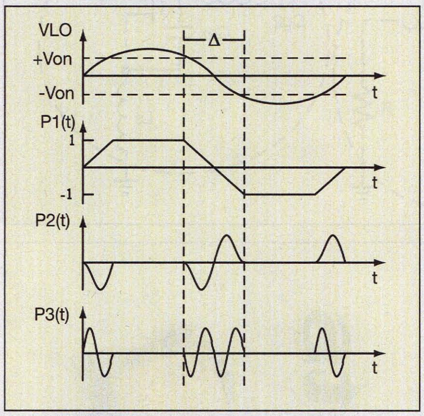

4. These plots show the resulting waveforms for P1(t), P2(t), and P3(t) for an applied LO voltage.

Figure 2 shows the proposed multiple-standard low-power CMOS RF receiver front-end circuit. It contains a stacked NMOS LNA and a single-balanced PMOS mixer. To minimize power consumption, the front-end employs current-reuse and forward-body-bias techniques, although these techniques will not degrade noise figure or linearity. Traditional multiple-standard receivers usually gained good input impedance matching by means of a wideband matching network[5] or tunable frequency matching network.[16] The former will induce some extra interference in some useless frequencies, which are covered by the wideband matching network; the latter increases the operating complexity of the circuits. The front-end circuit adopts a double resonance matching network to realize the multiple-standard input impedance matching.

As shown in **Fig. 2**, the parallel $L_{g1} - C_{g1}$ and series $L_{g2} - C_{g2}$ resonances are series connected. For design flexibility, a source degeneration inductor, L_S, is placed in series with the source. a capacitor, C_{ex}, is added in parallel with the gate-source of the amplifying transitor, M1.

In **Fig. 3**, the source degenerate topology is replaced by its equivalent circuit. The input impedance can be expressed as:

(See Eq. 1, this page.)

where:

g_{m1} = the transconductance of M1 and

C_{gs1} = the gate-source capacitance of M1.

The values of capacitor C_{g3} and inductor L_{g3} can be calculated by Eqs. 2 and 3:

$$C_{g3} = \frac{C_{g2} \cdot (C_{gs1} + C_{ex})}{C_{g2} + (C_{gs1} + C_{ex})} \quad (2)$$

$$L_{g3} = L_{g2} + L_s \quad (3)$$

Parameter Z_{in} synthesizes an input impedance with a real part equal to $g_{m1}L_S/C_n$ where capacitance $C_n = C_{ex} + C_{gs}$, to be matched with source resistance, $R_S = 50\ \Omega$.

$$Z_{in} = S\left(\frac{L_{g1}}{C_{g1} \cdot L_{g1} + 1}\right) + \frac{1}{SC_{g3}} + SL_{g3} + \frac{g_{m1}L_s}{(C_{gs1} + C_{ex})} \quad (1)$$

$$A_1 = \frac{v_{d1}}{v_{in}} = \frac{g_{m1}}{\omega_0 \cdot SC_{gs1}} \cdot \frac{1}{R_{in}} \cdot \left(SL_m // R_1 // \frac{1}{SC_{out1}}\right) \quad (4)$$

To achieve the required input impedance matching at the desired frequency bands, resonances $L_{g1} - C_{g1}$ and $L_{g3} - C_{g3}$ are designed to resonate at center frequencies within 935 to 960 MHz and 1805 to 2483 MHz,

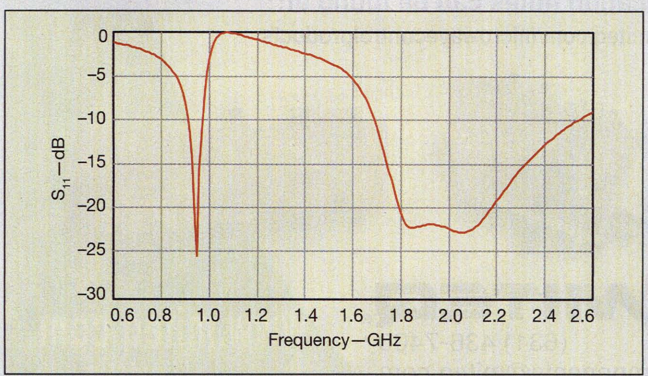

5. The front-end receiver's S_{11} input-reflection-coefficient response was simulated from 0.6 to 2.6 GHz.

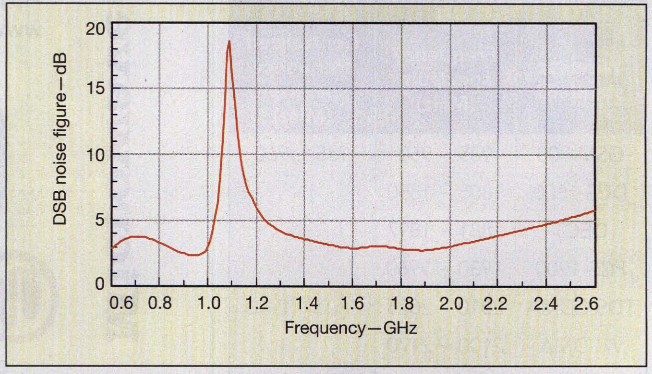

6. The front-end receiver's double-sideband (DSB) noise figure was simulated from 0.6 to 2.6 GHz.

respectively. In this way, the input circuit not only accomplishes better impedance matching in both bands of 935 to 960 MHz and 1805 to 2483 MHz, but also suppresses interference within the middle band from 960 to 1805 MHz without using an additional notch filter. The values of the resonating inductors and capacitors can easily be calculated by using the equation $\omega = 1/2\pi(LC)^{0.5}$.

To achieve a low-power design, the current-reuse technique was used twice in the front-end circuit. In one instance, it was applied to the two-stage cascade common-source LNA. As was shown in **Fig. 2**, the signal amplified by device M1 is coupled to the gate of device M2 by capacitor C_m while the source of M2 is bypassed by capacitor C_b. The inductive load L_m and L_D of the first and second amplifier stages can help to achieve high power gain; the supply voltage will not be influenced, as the voltage drop across them is negligible. Resistor R1 is added to supply a DC bias for device M2. By applying M1 and M2 to share the same bias current, the power consumption of the LNA is minimized. Body effects and parasitic capacitances are not considered. The voltage-transfer function of the first and second stages can be expressed by Eqs. 4 and 5:

(See Eq. 4, p. 54.)

$$A_2 = \frac{v_{d2}}{v_{d1}} = g_{m2}(r_{o2} // SL_d // \frac{1}{SC_{out2}}) \quad (5)$$

where:

C_{outn} = the output capacitors (where n = 1, 2) for M1 and M1;

r_{on} = the output resistance for M1 and M2; and

ω_0 = the working frequency.

The supply current of the LNA is obtained from the bleed current of the mixer, rather than from the DC source. By doubling the instance of current reuse, current consumption is minimized while bleeding current from the mixer helps to improve the conversion gain of the mixer. Device M3 is the transconductance transistor, while C_p and C_c are bypass and coupling capacitors, respectively. Inductor L_r and parasitic capacitance C_f at the common source node of the mixer's switching transistors, M4 and M5, are chosen for values to improve interstage impedance matching between the LNA and mixer. The $L_r - C_f$ resonance also helps to suppress 1/f noise at the mixer's output. Resistors R_{L1} and R_{L2} are load resistors. The conversion voltage gain of the mixer can be found from Eq. 6:

$$A_3 = (2/\pi)g_{m3}R_L \quad (6)$$

Therefore, the overall voltage conversion gain of the RF front end can be calculated from Eq. 7:

$$A = A_1 \cdot A_2 \cdot A_3 \quad (7)$$

To achieve further savings in power consumption and ensure the feasibility

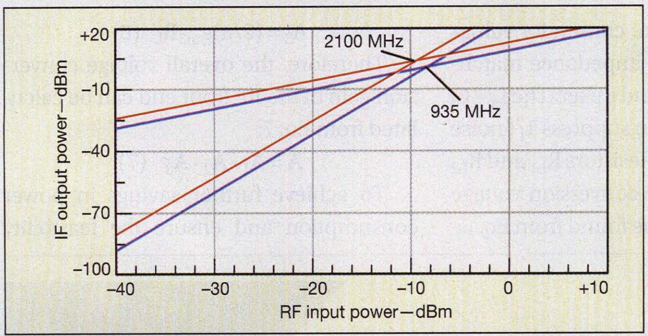

7. The conversion gain of the front-end receiver was simulated from 0.6 to 2.6 GHz.

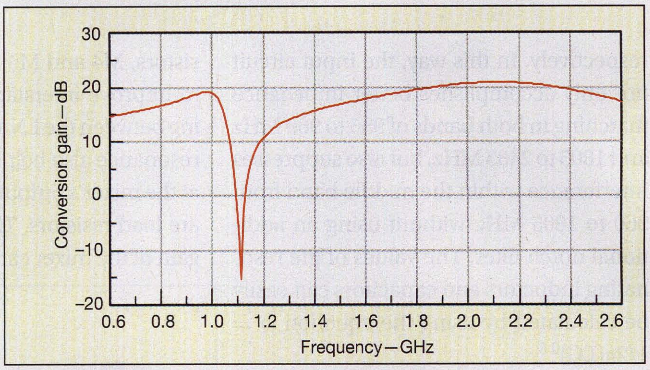

8. The input third-order-intercept (IIP3) response of the front-end receiver was simulated at 935 and 2100 MHz.

of current reuse between the LNA and the mixer, the supply voltage of the LNA and mixer should be decreased. Usually, the conventional method for accomplishing this is by making the transistors work in their weak inversion regions, although this can degenerate noise figure and gain performance levels. Thus, the forward-body-bias technique is applied to solve this weak point. Typically, the threshold voltage (V_{th}) equations for both NMOS and PMOS transistors are given as[13]:

$$V_{thn} = V_{th0} + \gamma(\sqrt{2\varphi_f - V_{bs}} - \sqrt{2\varphi_f}) \quad (8)$$

$$V_{thp} = V_{th0} - \gamma(\sqrt{2\varphi_f + V_{bs}} - \sqrt{2\varphi_f}) \quad (9)$$

where:
V_{th0} = the threshold voltage when $V_{bs} = 0$;
γ = the body-effect coefficient;
ϕ_f = the bulk Fermi potential; and
V_{bs} = voltage between the body and source.

From Eqs. 8 and 9, V_{th} can be modified by changing V_{bs}. Thus, the MOS transistors can achieve a dynamic threshold voltage. Since a forward body bias effectively lowers the threshold voltage, the MOS transistors can operate at a reduced bias voltage while maintaining equivalent device characteristics in terms of gain, noise figure, and linearity. However, as the forward body bias turns on the source-to-body junction of the MOS transistors, a DC current flows across the junction with an exponential dependence on the body voltage, leading to additional power consumption and possible latch-up failure. To prevent excessive junction conduction, a current-limiting resistor should be included at the body terminal.

By adding suitable positive voltages (V_{b1} and V_{b2}) and current-limiting resistors (R_{b1}, R_{b2}) to the body terminals of devices M1 and M2, a forward-body-bias architecture is formed in the front end. From Eq. 8, with the increase of V_{bs} and the decrease of V_{thn}, the NMOS transistors can work in a strong inversion region under low-bias-voltage conditions. The stacked NMOS LNA can operate at reduced supply voltages as low as 0.6 V, which is convenient to reuse the bleeding current when the supply voltage is equal to the drain voltage of transconductance transistor M3.

A positive voltage (V_{b3}) and a current-limiting resistor (R_{b3}) are added to the body terminal of PMOS transistor M3. As Eq. 9 shows, V_{bs} is then increased and V_{thp} is decreased, so that the PMOS transistors also work in a strong inversion region under low-supply-voltage conditions.

The mixer employs a novel forward-body-bias method for the switching transistors. The mixer is heavily dependent on the ideal characteristics of the switching transistors, so a local-oscillator (LO) signal forward-body-bias technique is adopted to improve the switching characteristics of devices M4 and M5. The LO voltage is connected to the body terminals of transistors M4 and M5, which can maintain the same waveform and phase, and reduce the voltage amplitude by divider resistors R2/R3 and R4/R5. The body voltage is then cyclical changed with the LO signal, which can be determined by means of Eq. 10:

$$V_{LO+} = V_{LO-} = V_{bs}\cos(\omega_{LO}t) \quad (10)$$

From Eq. 9, when $V_{LO+} > 0$ and $V_{LO-} < 0$, the value of V_G for device M4 increases, and $|V_{GS}|$ declines and $|V_{thp}|$ increases, accelerating the PMOS transistor to satisfy

Table 2: Reviewing recently reported multiple-standard receivers.

Reference	5	6	7	8	9	This work
Contents	LNA	LNA + mixer	LNA + mixer	LNA	LNA	LNA + mixer
Bandwidth (GHz)	0.2 ~ 3.8	2 ~ 6	0.8 ~ 2.5	3 ~ 6.5	3 ~ 10	0.93 ~ 0.96/ 1.8 ~ 2.5
Noise figure (dB)	2.8 ~ 3.4	3.18 ~ 5.47	< 6	1.9 ~ 3.4	3 ~ 7	2.3 ~ 2.4/ 2.7 ~ 5.1
S_{11} (dB)	< −9	< −10		< −12	< −9	< −14/< −11
Gain (dB)	19	35	20 ~ 21.5	16	12.5	18.6 ~ 19.0/ 18.7 ~ 20.8
IIP3 (dBm)	−4.2	−17.4 ~ −11.3	−20			−8.2/−9.8
Supply (V)	1	1.8	1.8	1.06	1.2	1
Power (mW)	5.7	56	18	4.5	7.2	2.1
Technology	0.13 µm	0.18 µm	0.18 µm	0.18 µm	90 nm	0.18 µm

the cutoff condition that $|V_{GS}| < |V_{thp}|$. Device M4 enters the cutoff state quickly.

At the same time, the value of V_G for device M5 declines, $|V_{GS}|$ increases and $|V_{thp}|$ declines, accelerating the PMOS transistor to satisfy the turn-on condition, $|V_{GS}| > |V_{thp}|$ and device M5 enters the turn-on state quickly. The LO signal is coupled to the body terminal and enables the threshold voltage to change in a cyclical manner. This not only helps the mixer to work at low power consumption, but also raises the switching speeds of the transistors. The switching characteristics of the active devices is nearly ideal, and the noise figure and linearity are improved considerably.

The thermal noise is greatly generated when switching transistors turn-on simultaneously. The average noise current within one LO period can be expressed by means of Eq. 11:

$$i_{o,n} = 4I[V_n/(S \times T)] \quad (11)$$

where:

V_n = the 1/f noise of the MOS transistor;

T = the cycle time of the LO;

I = the DC current of the switching transistor; and

S = the LO signal slope at point zero.

Parameter S is critical to noise performance: a larger value of S means smaller noise current. Parameter S can be increased to improve the switching characteristic, so it is propitious to reduce noise current. Linearity is an important performance of RF front-end, especially for the last stage of the whole circuit. Thus, the linearity of this front-end circuit is greatly influenced by the switching transistors M4 and M5. Their output current, i_o, has a nonlinear relationship with input voltage v_s, which can use the Taylor series to expand as shown in Eq. 12:

$$i_o = p_1(t) \cdot v_s + p_2(t) \cdot v_s^2 + p_3(t) \cdot v_s^3 + \cdots \quad (12)$$

From Eq. 12, where p_n is the derivative of $i_0 \sim V_s$, the typical waveform is shown in **Fig. 4**. When the switching transistor is on, $p_1(t) = 1$, $p_2(t) = p_3(t) = 0$, while in the switching time period Δ, $p_1(t)$, $p_2(t)$, $p_3(t)$ are unequal to zero. The voltage mode for the input third-order intercept point, V_{IIP3}, can be analyzed by means of Eq. 13:

$$V_{IIP3} = 10\log[4|p_1|/3|p_3|] \quad (13)$$

From Eq. 13, it can be concluded that smaller values of $|p_3|$ mean higher IIP3 and better linearity. With the aid of the LO signal forward-body-bias technique, the switching time, Δt, is reduced, implying that the time for $|p_3| \neq 0$ is reduced and the IIP3 performance has been enhanced.

The RF receiver front-end design was implemented in the 0.18-µm silicon CMOS process at the foundry of the Taiwan Semiconductor Manufacturing Company (TSMC; www.tsmc.com). By using the forward-body-bias technique, the receiver's supply voltage drops to 1 V when

(continued on p. 77)

JOHN E. PENN
Adjunct Professor
Johns Hopkins University, Engineering for Professionals (EP),
6810 Deerpath Rd., Ste. 100, Elkridge, MD 21075; www.ep.jhu.edu

Design Distributed MMIC Amplifiers

Distributed amplifiers can provide outstanding performance across extremely broad bandwidths—provided that attention is paid to the choice of circuit elements and their positioning in the layout.

DISTRIBUTED AMPLIFIERS are notable for providing very broadband gain. The concept of connecting parallel gain stages with transmission lines harkens back to 1948; Bill Packard, the co-founder of Hewlett-Packard Co., used vacuum tubes for the gain stages.[1] The broadband gain possible with such amplifiers still has a place. Even though many modern monolithic-microwave-integrated-circuit (MMIC) amplifiers are optimized for specific bands, many applications require broadband gain through high microwave frequencies.

Since 1989, Johns Hopkins University (JHU; www.jhu.edu) has offered a MMIC design course. As part of the course, a student has the opportunity to design a MMIC, have the design fabricated by a commercial semiconductor foundry (TriQuint Semiconductor; www.triquint.com), and later have it tested. Professor Craig Moore, who co-taught the class from 1989 to 2003, used a distributed amplifier that he designed around 1988 as a design example for the course.

An updated distributed-amplifier design using TriQuint's TQPED 0.5-µm GaAs pseudomorphic high-electron-mobility transistors (pHEMTs) was designed and fabricated along with the student designs for the 2006 JHU MMIC design course. The pHEMTs have higher gain and lower noise than the 0.5-µm GaAs metal-epitaxial-semiconductor field effect transistors (MESFETs) used for the 1988 design. The updated 0.5-µm pHEMT design worked well and was documented in the technical literature.[2]

The distributed-amplifier design was revisited in the Fall 2011 JHU MMIC design course using a high-frequency TriQuint TQP13 0.13-µm pHEMT process. Those updated designs are documented in this article. It should be noted that one of the students in the 2011 class, Andrew King, completed an effective distributed-amplifier design with gain that rolled off gradually from 14 dB at 2.5 GHz to 5 dB at 36 GHz. Depending on the operating frequency, available space, and other factors, the "transmission-line" feeds of the distributed amplifier can be either truly distributed (such as the microstrip in King's design) or lumped-element, transmission-line equivalent circuits.[3] The distributed amplifier described here uses the lumped-element approach.

The drain (output) and gate (input) feed lines of the distributed amplifier design are terminated in a 50-Ω resistor. As in the design of ref. 2, a spiral inductor was connected in parallel

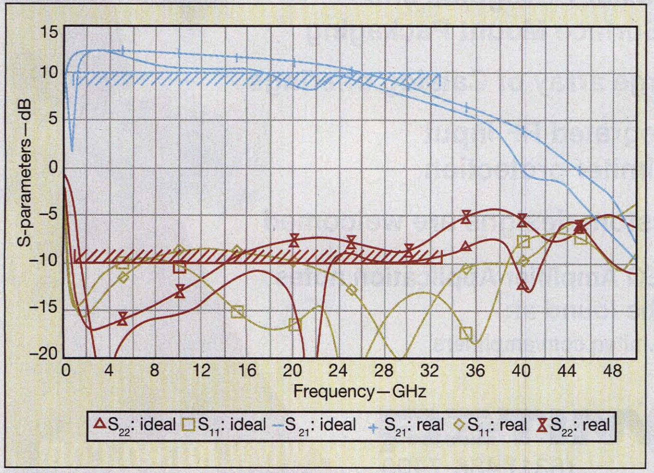

1. The S-parameter performance of an ideal distributed amplifier design (thin lines) is compared to a distributed amplifier with real (lossy) TriQuint elements (thick lines).

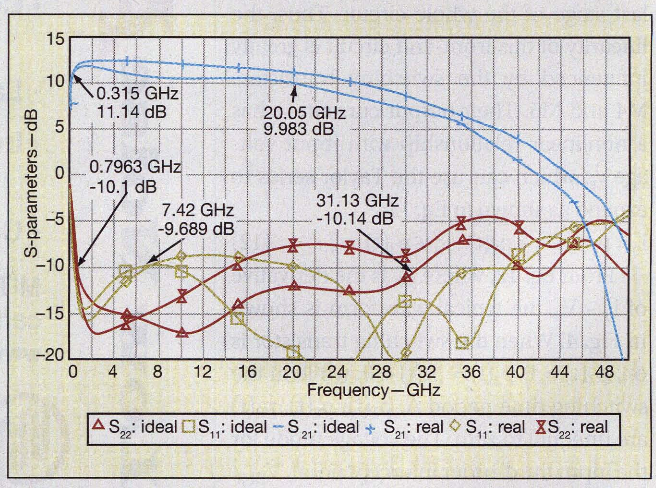

2. The S-parameter performance of a distributed amplifier design with ideal elements (thin lines) is compared to a DC-to-30-GHz amplifier with real elements (thick lines) from the TriQuint process.

to the 50-Ω drain termination to reduce DC power consumption. This limits the low-end frequency response to about 1 GHz and, as the design has two decades of bandwidth, the resonance of this inductor causes a slight ripple in the gain (at about 20 GHz) as shown in the preliminary S-parameter simulation **(Fig. 1)**. The simulation compares the amplifier design based on TriQuint's TQP13 passive elements (real or "lossy" elements), without interconnections, versus ideal lumped-element components (ideal).

Originally, an external DC gate bias was to be supplied, but it can be difficult to make a broadband DC supply for a distributed amplifier with two decades of gain. Following a suggestion from Craig Moore, the gate DC supply was simplified by terminating the 50-Ω load resistor to a substrate viahole ground connection

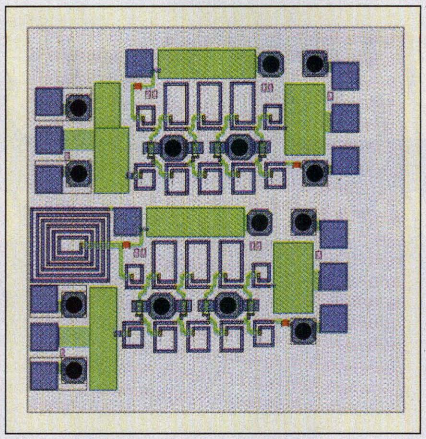

3. This layout shows distributed amplifier designs for the TriQuint foundry on a 54 x 54 mil die.

to provide a 0-V gate-source voltage (V_{gs}). This eliminated the flexibility of controlling the drain current, but removed the additional DC bias pad and any resonances that might be created in the gate DC bias supply. For the TQP13 PHEMT process, the 0-V V_{gs} bias provides good gain, with low noise figure at moderate DC power consumption.

A second, nearly identical distributed-amplifier design was fabricated—one lacking the power-saving spiral inductor on the drain bias. This inductor limits low-end gain to 1 GHz while its resonance causes a midband gain ripple. The resulting DC-to-30-GHz amplifier is less power efficient than the earlier design, since one-third of the 4-V supply is dissipated in the 50-Ω drain termination, but it eliminates the gain ripple of the inductor resonance. **Figure 2** offers a comparison of the S-parameters for the original ideal-element amplifier versus the modified DC-to-30-GHz design with real (TriQuint) elements. **Figure 3** shows the layouts of both distributed amplifiers on a 54 x 54-mil die. At the top of the die is the DC-to-30-GHz distributed amplifier, with the 1-to-30-GHz version on the bottom.

Both designs are essentially the same except for the spiral inductor in the drain bias. Electromagnetic (EM) simulation software from Sonnet Software (www.sonnetsoftware.com) was used to simulate the layout, revealing a potential instability at higher frequencies (about 30 GHz)—see **Figs. 4 and 5**. The chief concern is the relatively large decoupling capacitor on the drain DC bias and its relatively close spacing to the spiral inductors of the drain feed line.

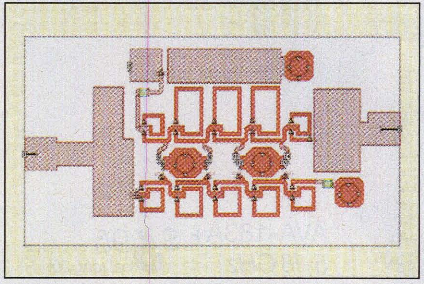

4. This layout plot of the DC-to-30-GHz distributed amplifier was created with EM simulation software from Sonnet Software.

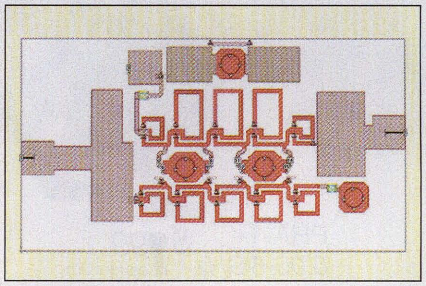

6. This is a modified layout plot of the DC-to-30-GHz distributed amplifier, using EM simulation software from Sonnet Software.

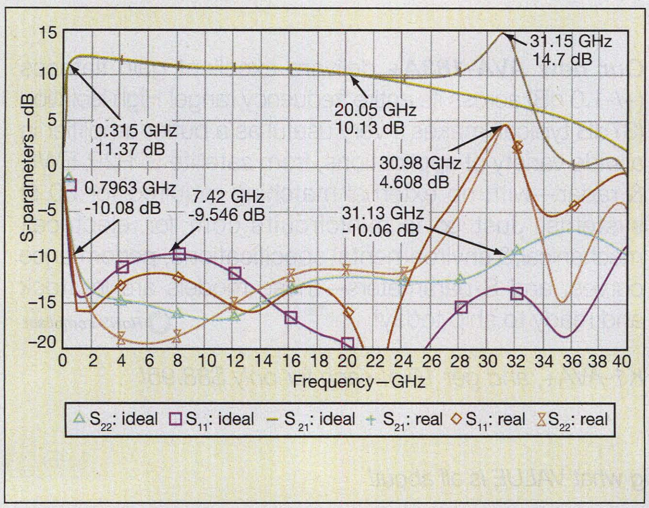

5. This Sonnet Software EM simulation shows the DC-to-30-GHz distributed amplifier with a 31-GHz stability problem.

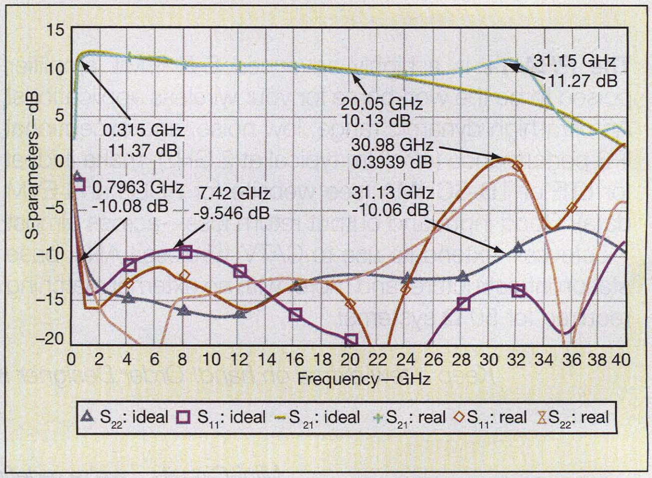

7. The simulated performance of the modified DC-to-30-GHz distributed amplifier was generated with simulation software from Sonnet Software.

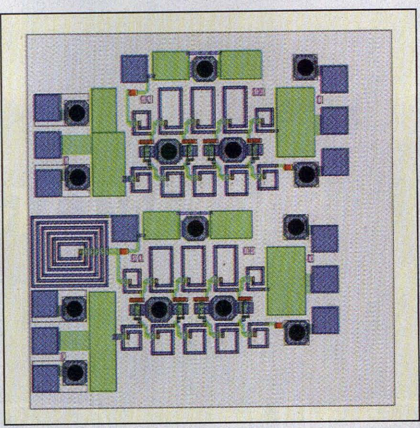

8. This is a layout plot of the modified distributed amplifier designs based on TriQuint elements on a 54 x 54 mil die.

To improve the design, the large 12-pF capacitor was split into two 6-pF capacitors to allow a shorter path to ground for higher-frequency operation, at the same time maintaining the 12-pF total capacitance to benefit lower-frequency operation. Also, the capacitor was moved further from the spiral inductors of the drain feed to reduce parasitic coupling. Finally, ideal 5-Ω resistors on the drain were added in the simulation, mitigating the previous instability problem (at around 30 GHz)—see **Figs. 6 and 7**. **Figure 8** shows a modified layout with the modified capacitor and stabilizing resistors on the same 54 x 54-mil die.

When the student designs were returned from the foundry, it appeared that the original distributed amplifier designs were inadvertently submitted, rather than the modified designs with improved stability. During testing, both distributed amplifiers showed promise at lower bias voltages, as well as at their nominal design voltages, but appeared only conditionally stable at certain intermediate voltages. These oscillations appeared to be well above 45 GHz, but would disappear near the nominal design voltages of 3 V (1 to 30 GHz) and 4 V (DC to 30 GHz) or higher. **Figure 9** shows a plot of measured performance for the two designs which differ only by the DC supply bypass inductor. The noise figure and gain were measured at 4-V bias for the DC-to-30-GHz version, showing slightly higher noise figure than expected—but still respectable—at 3 dB from 15 to 26 GHz (the highest frequency measured), as shown in **Fig. 10**. **Figure 11** shows efficiency and output power versus input power for the more-efficient 1-to-30-GHz amplifier at 10 GHz, with 20% power-added efficiency (PAE) at 2-dB gain compression.

Both versions of the distributed amplifier worked well: the 1-to-30-GHz version providing higher output power and efficiency, while the DC-to-30-GHz version had gain below 1 GHz and avoided the gain ripple from the resonance of the DC bypass inductor. There did, however, appear to be some conditional stability concerns. If there is room on a future class fabrication, perhaps the modifications to the layouts that were intended to improve stability can be tested. MWRF

ACKNOWLEDGEMENTS

The author would like to thank TriQuint Semiconductor for their support of the MMIC fabrication for the JHU MMIC design class. Additional thanks are due to Applied Wave Research (AWR; www.awrcorp.com), Agilent Technologies (www.agilent.com), and Sonnet Software for providing design software support for both students and instructors. Also, thanks to the author's former co-educator, Craig Moore, for his design suggestions. Additional thanks go to Dr. M.L. Edwards for creating the MMIC design course at Johns Hopkins University in 1989.

REFERENCES

1. E.L. Ginzton, W.R. Hewlett, J.H. Jasberg, and J.D. Noe, "Distributed Amplification, Proceedings of the IRE, Vol. 69, 1948, p. 956.
2. John E. Penn, "Designing MMIC Distributed Amplifiers," Microwaves & RF, November 2007, http://mwrf.com/semiconductor/designing-mmic-distributed-amplifiers.
3. John E. Penn, "Convert Distributed MICs to MMICs, Microwaves & RF, July 2003, http://mwrf.com/components/convert-distributed-mics-mmics.

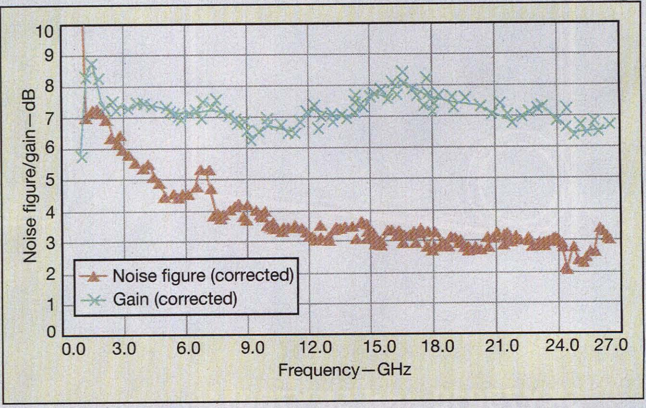

10. These data show the noise figure and gain of the DC-to-30-GHz distributed-amplifier design.

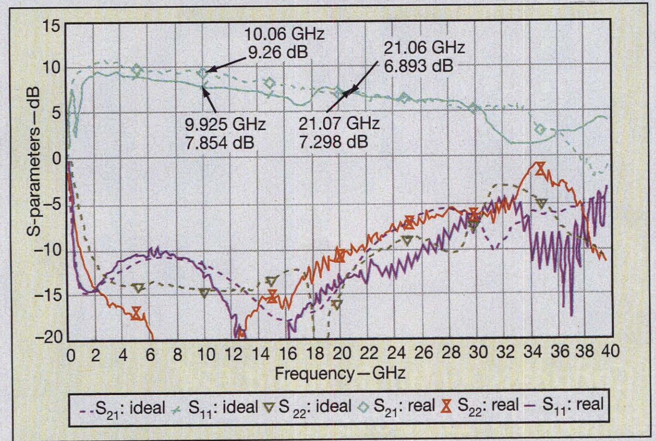

9. These S-parameter curves plot the performance of the two different distributed-amplifier designs.

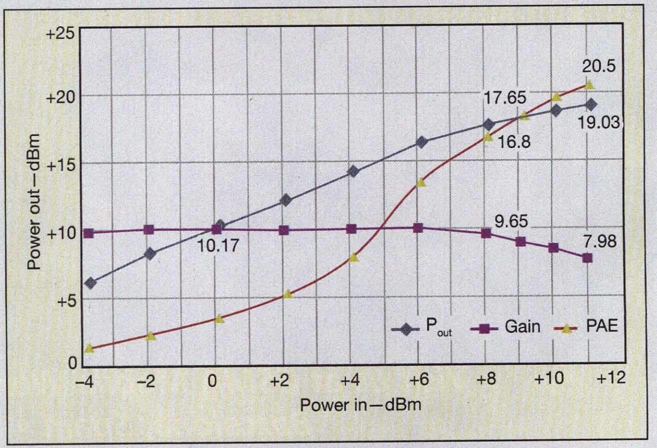

11. These curves show the output power, gain, and PAE of the 1-to-30-GHz distributed-amplifier design at 10 GHz.

HIGH POWER

5 - 500 WATTS PRODUCTS

POWER DIVIDERS

RoHS

Model #	Frequency (MHz)	Insertion Loss (dB) [Typ./Max.] ◊	Amplitude Unbalance (dB) [Typ./Max.]	Phase Unbalance (Deg.) [Typ./Max.]	Isolation (dB). [Typ./Min.]	VSWR (Typ)	Input Power (Watts) [Max.] ▫	Package
2-WAY								
CSBK260S	20 - 600	0.28 / 0.4	0.05 / 0.4	0.8 / 3	25 / 20	1.15:1	50	377
DSK-729S	800 - 2200	0.5 / 0.8	0.05 / 0.4	1 / 2	25 / 20	1.3:1	10	215
DSK-H3N	800 - 2400	0.5 / 0.8	0.25 / 0.5	1 / 4	23 / 18	1.5:1	30	220
P2D100800	1000 - 8000	0.6 / 1.1	0.05 / 0.2	1 / 2	28 / 22	1.2:1	5	329
DSK100800	1000 - 8000	0.6 / 1.1	0.05 / 0.2	1 / 2	28 / 22	1.2:1	20	330
DHK-H1N	1700 - 2200	0.3 / 0.4	0.1 / 0.3	1 / 3	20 / 18	1.3:1	100	220
P2D180900L	1800 - 9000	0.4 / 0.8	0.05 / 0.2	1 / 2	27 / 23	1.2:1	5	331
DSK180900	1800 - 9000	0.4 / 0.8	0.05 / 0.2	1 / 2	27 / 23	1.2:1	20	330
3-WAY								
S3D1723	1700 - 2300	0.2 / 0.35	0.3 / 0.6	2 / 3	22 / 16	1.3:1	5	316

◊ In excess of theoretical split loss of 3.0 dB
▫ With matched operating conditions

HYBRIDS

RoHS

Model #	Frequency (MHz)	Insertion Loss (dB) [Typ./Max.] ◊	Amplitude Unbalance (dB) [Typ./Max.]	Phase Unbalance (Deg.) [Typ./Max.]	Isolation (dB) [Typ./Min.]	VSWR (Typ)	Input Power (Watts) [Max.]	Package
90º								
DQS-30-90	30 - 90	0.3 / 0.6	0.8 / 1.2	1 / 3	23 / 18	1.35:1	25	102SLF
DQS-3-11-10	30 - 110	0.5 / 0.8	0.6 / 0.9	1 / 3	30 / 20	1.30:1	10	102SLF
DQS-30-450	30 - 450	1.2 / 1.7	1 / 1.5	4 / 6	23 / 18	1.40:1	5	102SLF
CSDK3100S	30 - 1000	0.8 / 1.2	0.05 / 0.2	0.2 / 3	25 / 18	1.15:1	50	378
DQS-118-174	118 - 174	0.3 / 0.6	0.4 / 1	1 / 3	23 / 18	1.35:1	25	102SLF
DQK80300	800 - 3000	0.2 / 0.4	0.5 / 0.8	2 / 5	20 / 18	1.30:1	40	113LF
MSQ80300	800 - 3000	0.2 / 0.4	0.5 / 0.8	2 / 5	20 / 18	1.30:1	40	325
DQK100800	1000 - 8000	0.8 / 1.6	1 / 1.6	1 / 4	22 / 20	1.20:1	40	326
MSQ100800	1000 - 8000	0.8 / 1.6	1 / 1.6	1 / 4	22 / 20	1.20:1	40	346
MSQ-8012	800 - 1200	0.2 / 0.3	0.2 / 0.4	2 / 3	22 / 18	1.20:1	50	226
180º (4-PORTS)								
DJS-345	30 - 450	0.75 / 1.2	0.3 / 0.8	2.5 / 4	23 / 18	1.25:1	5	301LF-1

◊ In excess of theoretical coupling loss of 3.0 dB

COUPLERS

RoHS

Model #	Frequency (MHz)	Coupling (dB) [Nom]	Coupling Flatness (dB)	Mainline Loss (dB) [Typ./Max.]	Directivity (dB) [Typ./Min.]	Input Power (Watts) [Max.] ▫	Package
KDS-30-30	30 - 512	27.5 ±0.8	±0.75	0.2 / 0.28	23 / 15	50	255 *
KFK-10-1200	10 - 1200	40 ±0.75	±1.0	0.4 / 0.5	22 / 15	150	376
KBS-10-225	225 - 400	10.5 ±1.0	±0.5	0.6 / 0.7	25 / 18	50	255 *
KDS-20-225	225 - 400	20 ±1.0	±0.5	0.2 / 0.4	25 / 18	50	255 *
KBK-10-225N	225 - 400	10.5 ±1.0	±0.5	0.6 / 0.7	25 / 18	50	110N *
KDK-20-225N	225 - 400	20 ±1.0	±0.5	0.2 / 0.4	25 / 18	50	110N *
KEK-704H	850 - 960	30 ±0.75	±0.25	0.08 / 0.2	38 / 30	500	207
SCS100800-10	1000 - 8000	10.5 ±1.5	±2.0	1.2 / 1.8	8 / 5	25	361
KBK100800-10	1000 - 8000	10.5 ±1.5	±2.0	1.2 / 1.8	8 / 5	25	322
SCS100800-16	1000 - 7800	16.8 ±1.5	±2.8	0.7 / 1	14 / 5	25	321
KDK100800-16	1000 - 7800	16.8 ±1.5	±2.8	0.7 / 1	14 / 5	25	322
SCS100800-20	1000 - 7800	20.5 ±2.0	±2.0	0.45 / 0.75	12 / 5	25	321
KDK100800-20	1000 - 7800	20.5 ±2.0	±2.0	0.45 / 0.75	14 / 5	25	322

* Add suffix - LF to the part number for RoHS compliant version.
▫ With matched operating conditions

Unless noted, products are RoHS compliant.

SYNERGY®
MICROWAVE CORPORATION

Phone: (973) 881-8800 | Fax: (973) 881-8361
E-mail: sales@synergymwave.com | Web: www.synergymwave.com
Mail: 201 McLean Boulevard, Paterson, NJ 07504

The Signal Source Noise Control & Signal Processing Experts.

N. BENMOSTEFA Doctor
M. MELIANI Professor
M. FEHAM Professor
STIC Laboratory, Department of Electrical Engineering, Faculty of Technology, University Abou Bekr Belkaid-Tlemcen, Post Box 230, Pole Chetouane, 13000 Tlemcen, Algeria; www.univ-tlemcen.dz.

H. OUSLIMANI Professor
University of Paris Quest Nanterre la Defense, Paris, France; www.u-paris10.fr.

Metamaterials Form Miniature Bandstop Filters

Through the use of metamaterial complementary split ring resonators (CSRRs), it is possible to fabricate high-performance microwave bandstop filters without adding lumped elements.

METAMATERIALS, WHICH exhibit simultaneous negative permittivity and permeability, offer many intriguing possibilities for high-frequency circuits such as filters. Through the use of such left-handed materials (LHMs) as they are known, and subwavelength split-ring resonators (SRRs) and complementary split ring resonators (CSRRs), it may be possible to build compact microstrip bandstop filters for use at microwave frequencies. The use of SRRs and CSRRs for miniature microwave filters will be investigated in this article, with the aid of analysis performed by means of finite-element-method (FEM) software.

The usefulness of metamaterials have been reported often, with the electromagnetic (EM) properties of these materials first predicted by Veselago.[1] The properties of these materials are based on negative values of the dielectric constant, ε, and the permittivity, μ, with LHMs exhibiting negative refractive indices resulting in antiparallel phase and group velocities.[2,3] For a LHM, the wave vector forms a left-handed triplet with vectors and wave fronts, with propagating EM waves traveling toward the source—i.e., opposite the direction of energy flow through the medium.

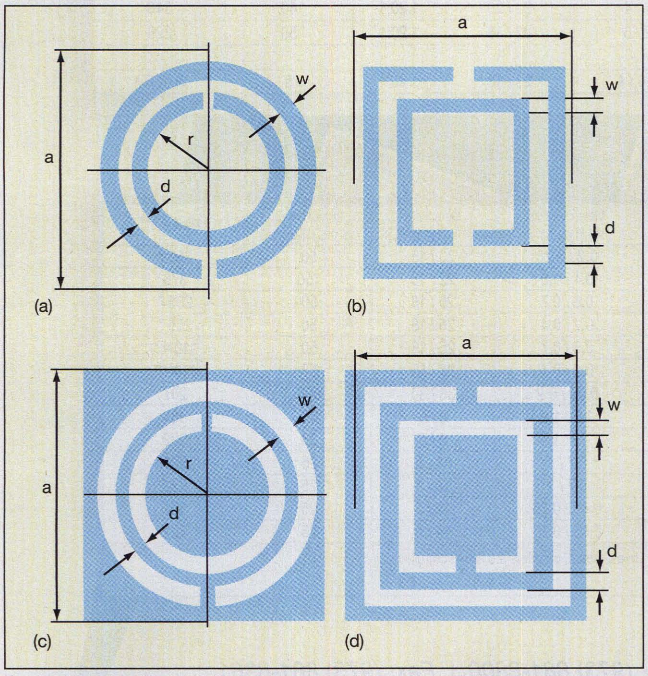

1. These layouts show (a) circular and (b) square split-ring resonators, and (c) circular and (d) square complementary split-ring resonators.

The first artificial LHM operating in the microwave region was reported by Smith, et al.[4] Pendry, et al.[5] proposed to combine a periodic array of metallic posts with a periodic structure consisting of SRRs. The SRR is one of the essential structures of metamaterials. It produces a negative effective μ near the resonant frequency while the metallic wires of a SRR behave like a two-dimensional plasma, with negative ε to the plasma frequency. Left-handed wave propagation has also been demonstrated in one-dimensional configurations consisting of a metallic rectangular waveguide operating below cutoff and periodically loaded with SRRs.[6]

Previous structures that had exhibited left-handed propagation effects were not considered as potential component candidates in microwave and wireless systems, where compatibility with planar circuit technology is desirable. LHMs based on planar transmission lines have been reported by Grbic, et al.,[7] demonstrating the existence of backward-wave radiation in a host coplanar waveguide loaded with series capacitors and shunt connected inductors. With the aid of the EM duality theorem, it follows that negative μ can be obtained from a complementary SRR etched in the ground plane of a microstrip line.

The present authors have taken advantage of the small electrical sizes of SRRs at their resonant frequencies (typically one-tenth or less the value of the free space wavelength) to design planar compact microstrip bandstop and ultrawideband (UWB) filters using two techniques. One of these involves microstrip line loaded with SRRs, while the other uses a microstrip circuit with CSRRs etched in the ground plane of the printed-circuit board (PCB), beneath the microstrip line. The authors have designed metamaterial CSRR filters, with the CSRRs

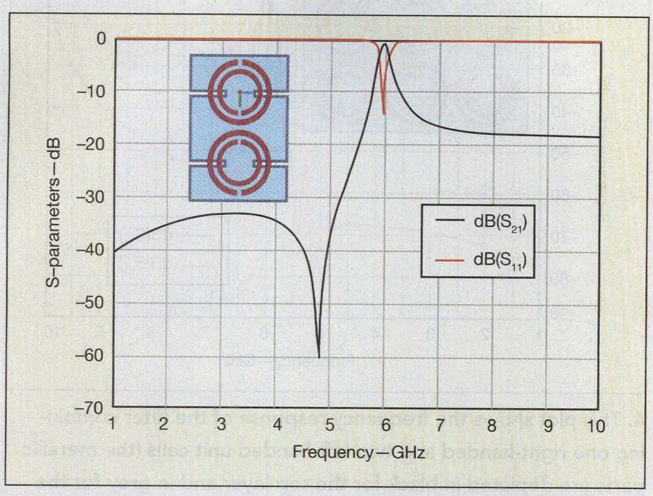

2. This plot shows the frequency response of an SRR-based coplanar-waveguide (CPW) left-handed line from 1 to 10 GHz.

integrated into the active regions of the filters.

As **Fig. 1** shows, a CSRR is the dual counterpart of an SRR, which is a constitutive element for the synthesis of negative permittivity media. CSRRs are mainly driven by an axial time-varying electric field, rather than an axial magnetic field (as in the case of SRRs). The rationale behind using metamaterial CSRRs was to promote the miniaturization of bandstop and UWB filters as viable alternatives to existing designs,[2-6] without compromises in performance or size.

The frequency selectivity of CSRRs suggests their suitability for use in filters, since they are ideal for fabrication in planar constructions when they are mainly excited by an axial time-varying electric field.[11] CSRRs are formed by parallel combinations of inductors (L's) and capacitors (C's), with the LC resonant tank electromagnetically coupled to the host line. The equivalent-circuit model for CSRRs, loaded transmission line, and its relevant values of the inductors and capacitors can be calculated using methods described in ref. 8.

Figures 1(c) and 1(d) present the conventional layout of a CSRR microstrip structure where the CSRRs are etched into the ground plane beneath the microstrip. The possibility of obtaining such broad frequency response by means of balanced lines opens the door to the application of these structures in the design of broadband filters. In addition, the position of the transmission zeroes can be adjusted to eliminate spurious bands and to control out-of-band rejection, which can also be improved by increasing the number of resonator/filter stages. These properties have been exploited and applied to the design of several kinds of filters.

In exploring the possibilities of filters based on CSRRs, the first step involved combining different cells with right-handed and left-handed behaviors to obtain bandpass response.[9,10] These two kinds of lines present a transmission zero above and below the first transmission band, making it possible to achieve high-frequency bandpass filter behavior with sharp cutoffs on both sides of the passband **(Figs. 2-4)**. Poor rejection was the consequence of only using one kind of cell.

Alternate right/left-handed cells with circular CSRRs were fabricated using a number of different commercial circuit-board materials, including RO3010™ high-frequency laminates from Rogers Corp. (www.rogerscorp.com). The RO3010 circuit material is a ceramic-filled polytetrafluoroethylene (PTFE) composite with a relative dielectric constant, ε_r, of 10.2 at 10 GHz in the z axis (thickness) of the material. It has coefficient of thermal expansion (CTE) of 17 ppm/°C which is comparable to that of copper for good mechanical stability over a wide temperature range. For fabricating the CSRRs, a substrate with thickness, h, of 0.49 mm was used. The radius of the smaller SRRs was r = 1.39 mm, with the width and distance between the rings, d, equal to 0.2 mm and the same in all of the SRRs. The radius of the bigger SRRs was r = 1.52 mm. The wire width, w_w, was 2.16 mm, while the gap length, l_g, was 1.6 mm and the total length of the filter was 1.5 cm.

A second type of filters that was designed and analyzed were based on alternate right-/left-handed cells with square CSRRs.

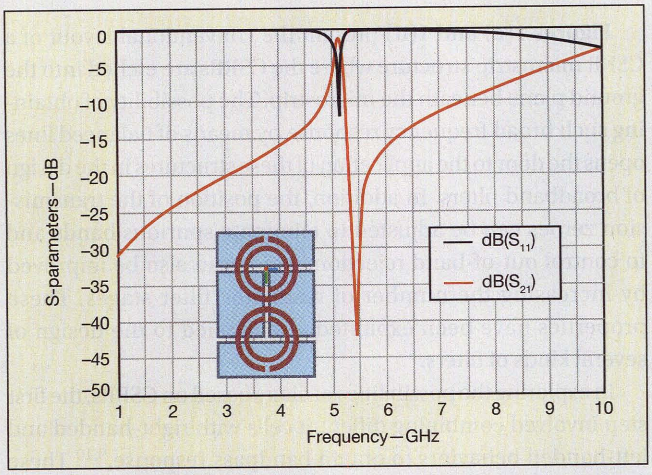

3. This plot shows the frequency response of an SRR-based (CPW) right-handed line from 1 to 10 GHz.

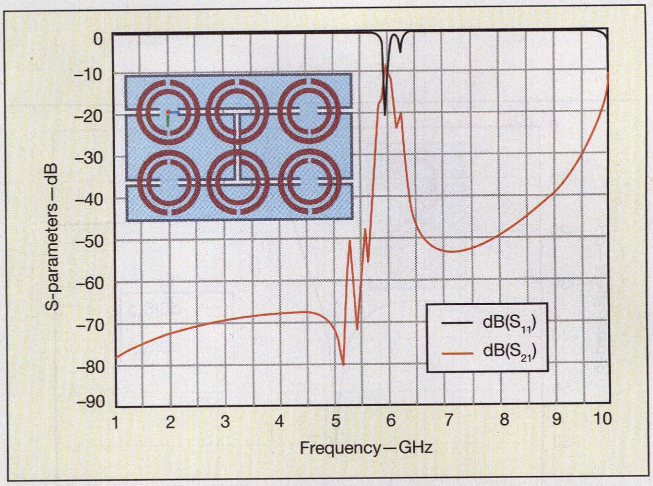

4. This plot shows the frequency response of the filter combining one right-handed and two left-handed unit cells (the metallic parts are depicted in black for the top layer and in grey for the bottom layer of the substrate).

With the help of HFSS three-dimensional (3D) EM simulation software from Ansys (www.ansys.com), a CSRR filter was designed based on the RO3010 circuit material. The dimensions of each square consisted of external edges of 4.86 x 4.86 mm and thickness, h, of 0.49 mm. The smaller SRR is 2.78 x 2.78 mm, with the width and distance between the rings equal to c = d = 0.2 mm and the same in all SRRs. The bigger SRRs measure 3.04 x 3.04 mm, with wire width of w = 2.16 mm, gap length, l_g = 1.6 mm, and the total length of the filter at 1.5 cm.

Figures 5-7 show the influence of the form of SRR on the response of the filter. SRRs and CSRRs can be used to design filters with bandwidths employing either SRR-based coplanar-waveguide (CPW) transmission lines[9,12] or CSRR-based microstrip structures.[10,13,14] In coplanar technology, the right-handed lines involve the combination of SRRs etched on the bottom side of the line and capacitive gaps etched on the coplanar waveguide (see **Figs. 3 and 6**). CSRR-based microstrip right-handed structures combine shunt inductances with CSRRs etched on the ground plane to obtain the desired response.

As can be seen in **Figs. 4 and 7**, as well as being very compact (the length of the active part is 1.5 cm), a filter with CSRRs exhibits a very selective and symmetric narrow-band response thanks to the combination of the two types of coplanar metamaterial unit cells. If compared with a conventional coupled-line filter with similar characteristics, the total length of the metamaterial filter is roughly three times shorter than the conventional filter.

To demonstrate the use of CSRRs, a standard third-order maximally flat bandpass filter with quarter-wavelength short-circuit resonators was first designed based on the formulas in ref. 15. The simulation results of the structure are shown in **Fig. 8**. Two CSRRs with a separation distance of 20 mm were used. The dimension of each ring is as follows: r = 1.4 mm, c = 0.25 mm, d = 0.4, and g = 0.3. The circuit board material was 0.787-mm-thick RT/duroid® 5870 laminate from Rogers Corp., which exhibits a relative dielectric constant of

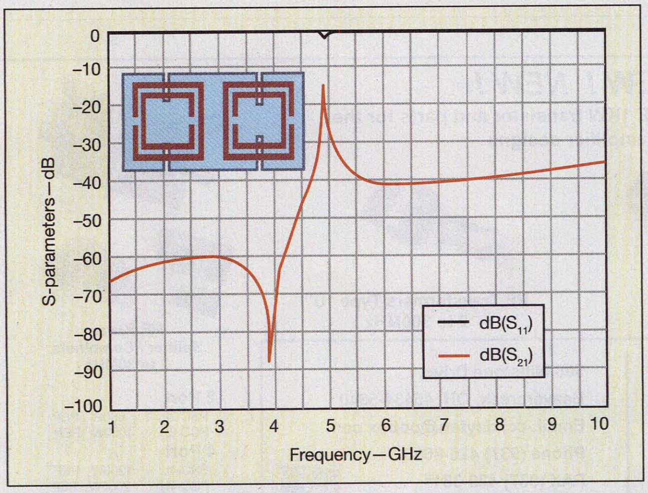

5. The S-parameters reveal the frequency response of an SRR-based CPW left-handed line.

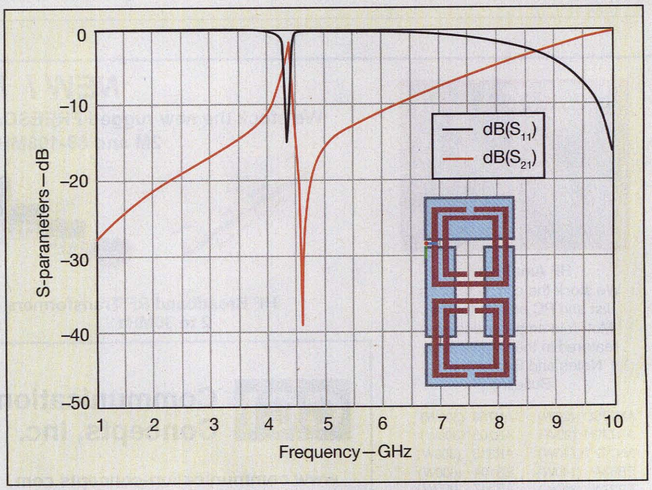

6. The S-parameters show the frequency response of an SRR-based CPW right-handed line.

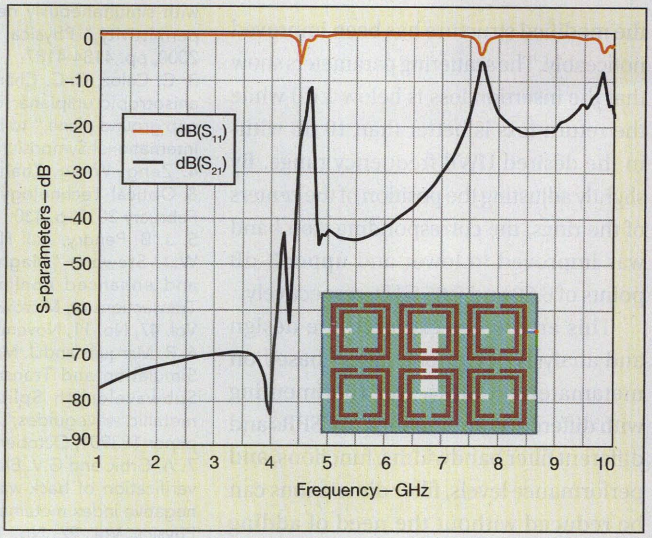

7. The S-parameters reveal the frequency response of the filter combining one right-handed and two left-handed unit cells.

2.33 at 10 GHz in the z-axis (thickness) of the material. The scattering parameters illustrate that the rings resonate at 5.60 GHz, where the insertion loss reaches more than 10 dB.

Figure 9 shows that there are problems associated with this structure. The stopband rolloff is very gradual, especially following the resonance.[15] To integrate this structure into the UWB filter design, its insertion-loss and return-loss characteristics must be improved. Analysis of the structure has revealed that the poor performance is due to the impedance mismatches between the CSRRs and their host transmission line. Etching away parts of the ground plane has resulted in an increase in inductance. To compensate for this, a capacitive load in the form of an open-circuited stub with length L and width W was introduced to counter the increase in inductance **[Fig. 8(b)]**. The positions of the CSRRs (as they alter the field distribution) will also impact the impedance matching with the transmission line and the shape of the stopband. The improved performance in **Fig. 8(b)** compared to **Fig. 8(a)** is the result of displacing the centers of the CSRRs by 1.85 mm from the center of the microstrip.

Figure 9 also shows the simulation results of (a) the conventional CSRR-microstrip structure and (b) the modified CSRR-microstrip structure. The open circuited-stub has a length L of 5 mm and width W of 1.3 mm. The performance of

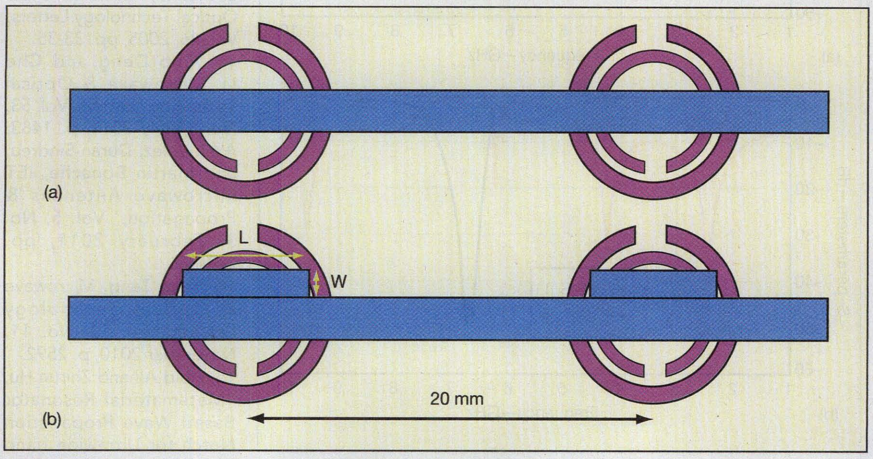

8. The two layouts compare (a) a conventional CSRR-microstrip structure and (b) a modified CSRR-microstrip structure. The dark and gray regions represent the microstrip line and CSRRs etched in the ground plane, respectively.

the modified structure has been improved noticeably. The scattering parameters show that the insertion loss is below 1 dB while the return loss is better than 10 dB within the desired UWB frequency range. By slightly adjusting the position of the centers of the rings, the corresponding stop band was improved to lower and upper 3-dB points of 6.50 and 7.85 GHz, respectively.

This article has explored the design and analysis of compact filters based on metamaterial CSRRs. By experimenting with different combinations of CSRRs and different filter bandwidths, functions, and performance levels, filter dimensions can be reduced without the need of adding lumped elements. When size and planar structures are important, such metamaterial filters offer an attractive alternative to traditional LC filters. MWRF

REFERENCES

1. V.G. Veselago, "The electrodynamics of substances with simultaneously negative values of ε and μ," Soviet Physics Uspekhi, Vol. 10, 1968, p. 509.
2. D.R. Smith, W.J. Padilla, D.C. Vier, S.C. Nemat-Nasser, and S. Schultz, "Composite medium with simultaneously negative permeability and permittivity," Physical Review Letters, Vol. 84, 2000, pp. 4184-4187.
3. C. Caloz, C.-C. Chang, and T. Itoh, "A novel anisotropic uniplanar compact photonic band-gap ground plane," to be presented in IEEE AP-S International Symposium, Boston, MA, July 2001.
4. Zeng, Wang, Zhang, and Zhu, Microwave & Optical Technology Letters, Vol. 52, No. 2, February 2010, p. 430.
5. J. B. Pendry, A.J. Holden, D.J. Robbins, and W.J. Stewart, "Magnetism from conductors and enhanced nonlinear phenomena," IEEE Transactions on Microwave Theory & Techniques, Vol. 47, No. 11, November 1999, pp. 2075-2084.
6. R. Marqués and J. Martel, "Left–handed media Simulation and Transmission of EM Waves in Subwavelength Split-ring resonator-loaded metallic waveguides," Physical Review Letters, paper 183901, October 2002.
7. A. Grbic and G.V. Eleftheriades, "Experimental verification of back-ward-wave radiation from a negative index metamaterial," Journal of Applied Physics, Vol. 92, No. 10, November 2002, pp. 5930-5934.
8. M. Gil, J. Bonache, and F. Martín, "Metamaterial Filters: A Review," Science Direct, August 2008, pp. 186-197.
9. Gil, Morata, Fernandez, Rottenberg, and De Raedt, Microelectronic Engineering, Vol. 88, 2011, pp. 1-5.
10. J. Bonache, F. Martín, F. Falcone, J. García, I. Gil, T. Lopetegi, M.A.G. Laso, R. Marqués, F. Medina, and M. Sorolla, "Super compact split ring resonators CPW band pass filters," Proceedings of the IEEE-MTT International Microwave Symposium Digest, Fort Worth, TX, June 2004, pp. 1483–1486.
11. P. Mondal, M.K. Mandal, A. Chaktabarty, and S. Sanyal, "Compact bandpass filters with wide controllable fractional bandwidth,"IEEE Microwave & Wireless Components Letters, Vol. 16, 2006, pp. 540-542.
12. J. Bonache, F. Martín, F. Falcone, J. García-García, I. Gil, T. Lopetegi, M.A.G. Laso, R. Marqués, F. Medina, and M. Sorolla, "Compact coplanar waveguide band pass filter at S-band," Microwave and Optical Technology Letters, Vol. 46, 2005, pp. 33-35.
13. Guo Deng and Che Li, Microwave & Optical Technology Letters, Vol. 53, No. 7, July 2011, p. 1483; Azna Velez, Duran-Sindreu, and Martin Bonache, IET Microwave Antennas & Propagation, Vol. 5, No. 3, February 2011, pp. 277-281.
14. Yang Tang, Microwave & Optical Technology Letters, Vol. 52, No. 11, November 2010, p. 2592.
15. Abid Ali and Zhirun Hu, "Metamaterial Resonator Based Wave Propagation Notch for Ultrawide band Filter applications," IEEE Antennas & Wireless Propagation Letters, Vol. 7, 2008, pp. 210-212.

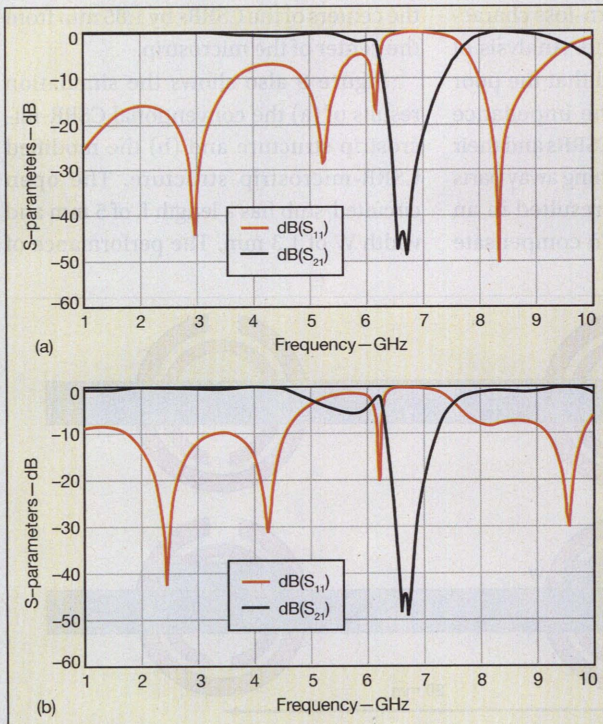

9. These simulation results show (a) the conventional CSRR-microstrip structure and (b) the modified CSRR-microstrip structure.

JOY WEISS
President
Dust Networks Product Group

ROSS YU
Product Marketing
Manager

JONATHAN SIMON
Systems Engineering
Director

Linear Technology Corp., 1630 McCarthy Blvd., Milpitas, CA 95053;
(408) 432-1900, www.linear.com.

Minimize Power In Wireless Sensing

Wireless sensor networks (WSNs) are helping to extend the usefulness of the modern Internet, especially when those wireless networks can be powered by ambient energy sources.

WIRELESS SENSING systems can provide information about the physical world that enable new levels of efficiency, safety, and security, especially when those systems can be implemented with the lowest power consumption possible. Wireless sensing networks offer the flexibility of sensor placement that is simply not possible with wired systems. And by minimizing power consumption, wireless sensing systems can be deployed with dramatic cost reductions compared to traditional wired sensing systems.

Low power wireless sensor networking (WSN) standards, particularly mesh architectures that utilize time-synchronized channel hopping (TSCH), enable every node in the network to run on batteries or harvested energy without sacrificing reliability or data throughput. This frees application developers to put sensors anywhere—not just where power is available, but wherever the application requires sensor data. Linear Technology (www.linear.com), in particular the firm's Dust Networks product group, has been pursuing advances in the areas of highly reliable, low power TSCH-based WSN and energy harvesting technologies. Such technologies go hand in hand to increase opportunities for application developers to deploy systems that require few (if any) battery changes, further reducing the lifetime cost of deploying wireless sensors and spurring the progress of the Internet of Things (IoT).

A 2012 study by ON World (www.onworld.com) shows that the two attributes of a WSN that matter most to industrial customers are reliability and low power consumption **(Fig. 1)**. Third on the list is cost: Without solving the reliability and power issues, cost is not yet a customer priority. Based on Dust Networks' years of research and development of TSCH-based products and deployment of thousands of commercial products, it is clear that the combination of precisely synchronized time slotting, channel hopping, and an ultralow power radio enables the lowest power, most reliable WSNs.

Introduction of the IEEE 802.15.4 standard created an excellent radio platform for WSNs. The IEEE 802.15.4 standard defines a 2.4-GHz, 16-channel spread-spectrum low-power physical (PHY) layer upon which many IoT technologies have been built, including ZigBee and WirelessHART. It also defines a medium-access-control (MAC) layer, which has been the foundation of ZigBee. Unfortunately, the single-channel nature of this MAC makes its reliability unpredictable. For improved reliability, the WirelessHART protocol, also known as IEC62591, defines a multichannel link layer based on the 15.4 MAC layer, which helps achieve the high reliability (better than 99.9%) needed for industrial WSN applications.

In early 2012, a new version of the IEEE 802.15.4 MAC, called IEEE 802.15.4e, was ratified; it embodies multichannel mesh and time slotting. The typical power output for IEEE 802.15.4-compliant radios is around 0 dBm. These radios operate with transmit and receive current in the 15-30-mA range. The best-in-class operating conditions include transmit current of only 5.4 mA for transmit power of 0 dBm and receive current of only 4.5 mA (based on an LTC5800 device operating from 2400.0 to 2483.5 MHz).

The original IEEE 802.15.4 MAC necessitates that the nodes in the mesh network that route information from neighboring nodes are always on, while nodes that only send/receive their own data, often called "reduced function devices," can sleep between transmissions. In order for every node in the network to be low power, communications between nodes must be scheduled, and it is necessary to have a shared sense of time in the network. The tighter the synchronization, the less time the routing node radios must be in an "on" state, which minimizes power consumption.

Best-in-class TSCH systems synchronize all nodes in a multi-

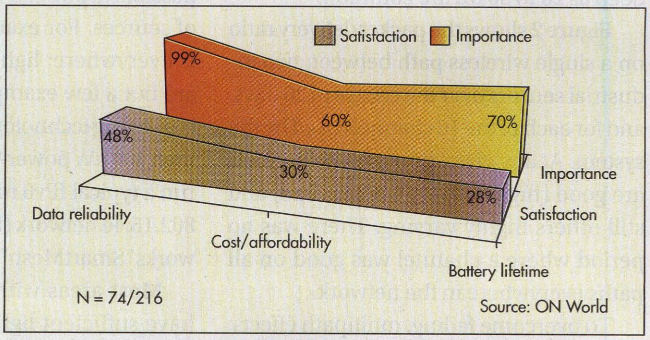

1. This diagram [from ON World (www.onworld.com)] shows the perceived importance of different WSN attributes.

hop mesh network to within a few tens of microseconds. Once there is a shared sense of accurate time in the network—and a schedule of time slots for pairwise transmission between nodes in the network—channel assignment can be incorporated in the schedule, enabling channel hopping.

Wireless channels are not perfect or ideal, of course, and numerous conditions can prevent a transmitted signal from being fully recovered by a receiver. As radio power decreases, wireless reception can become even more difficult. For example, interference can occur when multiple transmitters send signals simultaneously over the same frequency. This is particularly problematic if the different systems cannot hear each other, but the intended receiver can hear all of the transmitted signals (the "hidden terminal problem"). Backoff, retransmission, and acknowledgment mechanisms are required to resolve collisions from multiple transmitted signals within the same frequency band. Interference can come from within the network, from another similar network operating in the same radio space, or from a different radio technology operating within the same frequency band. The latter is a common occurrence in the 2.4-GHz band shared by Wi-Fi, Bluetooth, and IEEE 802.15.4.

A second, unpredictable phenomenon called multipath fading can prevent successful transmission even when the line-of-sight link margin is sufficient. This occurs when multiple copies of the transmission bounce off objects in the environment (ceilings, doors, people, etc.), with each reflected copy traveling a different distance. When interfering destructively, fades as deep as 20 to 30 dB are common.

Figure 2 shows the packet delivery ratio on a single wireless path between two industrial sensors over the course of 26 days, and for each of the 16 channels used by the system. At any given time, some channels are good (high delivery), others bad, and still others highly varying. There was no period where a channel was good on all paths everywhere in the network.

To overcome fading, multipath effects, and other conditions that can degrade radio performance, it is critical that WSNs employ multiple channels. By time-synchronizing and scheduling the network into slots, transmissions can be precisely scheduled on specific known channels, and the choice of channel can change with every transmission. Scheduling network transmissions can solve the hidden terminal problem and virtually eliminate in-network collisions. Such a mechanism has been proven successful in more than 10,000 WirelessHART networks in the field, which routinely achieve multiyear battery life and greater than 99.9% reliability.

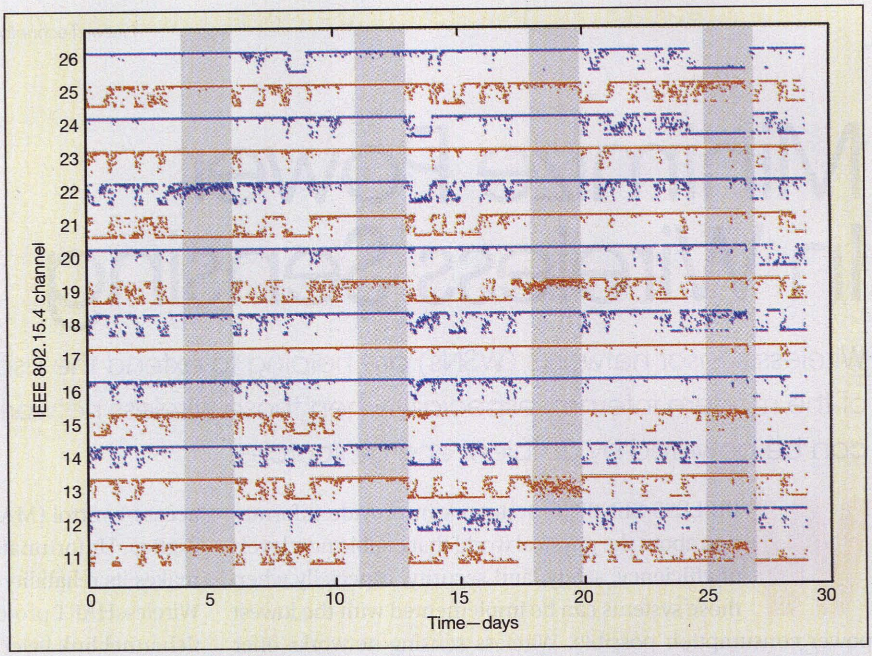

2. Data over time shows the breakdown of packet delivery across a WSN's 16 channels.

In laying out a WSN node, once its power requirements have been minimized, greater flexibility is possible when choosing a power source for the node. If the power requirements are sufficiently low, it may be possible to power a WSN from any number of sources. For example, ambient energy is everywhere: light, vibration, and heat are but a few examples. Practical energy-harvesting technologies can generate more than 150 µW power—more than enough to run a typical IPv6 routing node in an IEEE 802.15.4e network (for example, Dust Networks' SmartMesh™ IP product).

Most areas within an office building have sufficient light to run a low-power TSCH WSN. According to the United States General Services Administration, which sets the guidelines for US public buildings, the more brightly lit areas, such as workstation areas, enjoy 500 lux of lighting. Given 200 to 300 lux light, a number of small photovoltaic cells are available for indoor applications. These include the model 4100 photovoltaic power module from G24i (www.g24i.com) and the AM-1815 indoor cell from Sanyo (www.sanyo.com), both of which are capable of supplying sufficient power to operate an IPv6 router in an IEEE 802.15.4e TSCH network.

Many energy harvesting transducers produce only a few hundred millivolts of output, so step-up voltage DC/DC converters are often required to convert these outputs to a usable supply voltage range. Integrated circuits (ICs) such as the model LTC3105 from Linear Technology combine maximum power point control, so that the transducers operate at peak efficiency. The LTC3105 also enables the addition of a battery backup to the circuit.

The IoT is being given a healthy boost through the availability of wireless sensors. Time synchronized, slotted multichannel systems confer customer-critical benefits to WSNs: reliability and network-wide low power operation. The WirelessHART and IEEE 802.15.4e standards are excellent embodiments of this approach. MWRF

JOLIE R.
Design Engineer for Data
Transmitting Systems for IRS Satellites

DR. D. VENKATA RAMANA
Head, Ka-Band Data Transmitter
Development Team

Communication Systems Group, ISRO Satellite Centre, Old Airport Road, Bangalore-560017, India, e-mail: dvramana@isac.gov.in, jolier@isac.gov.in.

QPSK Modulator Transmits Satcom Data

This unique modulator provides both spectral and power efficiency when transmitting unequal data rates from two different satellite payloads.

DIGITAL MODULATION is often a means of transmitting payload data from orbiting satellites to ground stations. Such is the case for satellites in the Indian Remote Sensing (IRS) satellite system. In one such approach, quadrature phase-shift-keying (QPSK) modulation provides both spectral and power efficiency. In a QPSK modulator, two data streams simultaneously modulate a carrier signal. For optimum use of available satellite power, an unbalanced QPSK (UQPSK) modulator is often used. The design and simulation for such a modulator will be shown here, along with methods for demodulating such signals.

Communications channels in satellite-communications (satcom) systems, as well as communications systems in general, can be categorized as being power- or bandwidth-limited. For power-limited communications channels, coding schemes are typically applied to save power at the expense of bandwidth. In bandwidth-limited channels, spectrally efficient modulation schemes are often used to conserve bandwidth. The prime goal of spectrally efficient modulation is to optimize bandwidth efficiency, which is defined as the ratio of the data rate to the channel bandwidth (in b/s/Hz). A secondary goal of such a modulation scheme is to achieve high bandwidth efficiency with minimum signal power.

QPSK modulation results in optimum use of both spectrum and power when the data rates for the two channels—or the in-phase (I) and quadrature (Q) signal components—are the same. But when two data streams at different bit rates from two independent payloads must be transmitted, the normal procedure of formatting the data for modulation onto the carrier becomes very complicated. The easiest way is to transmit the two different data streams on the two QPSK channels by direct modulation, which results in the two channels of the modulator having different data rates. The higher of the data rates determines the bandwidth required for the modulated carrier and the transmitter output power will be equally shared by the two different data streams.

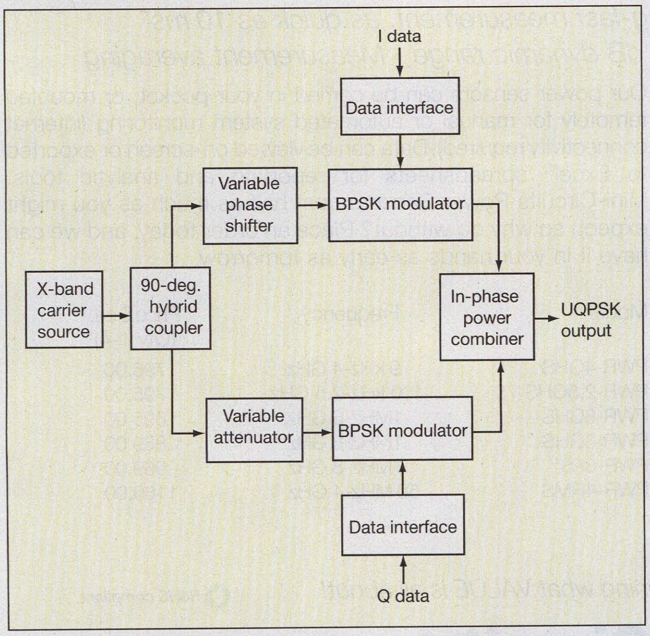

1. This block diagram represents the proposed UQPSK modulator for satcom applications.

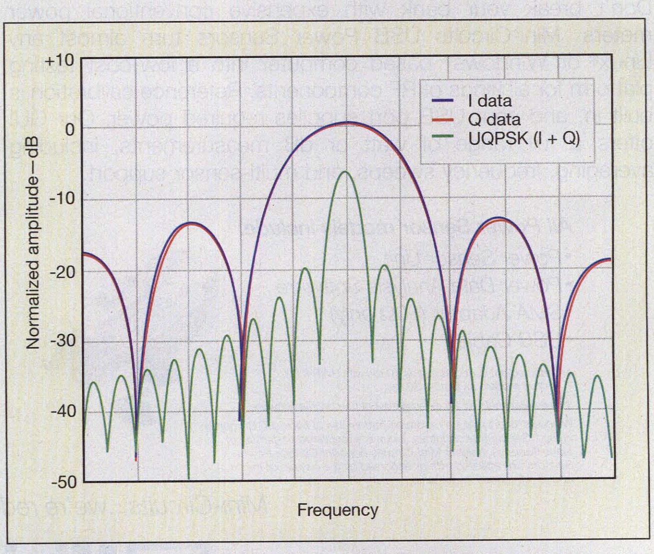

2. This figure shows the I and Q data along with the simulated UQPSK spectrum for the satcom modulator.

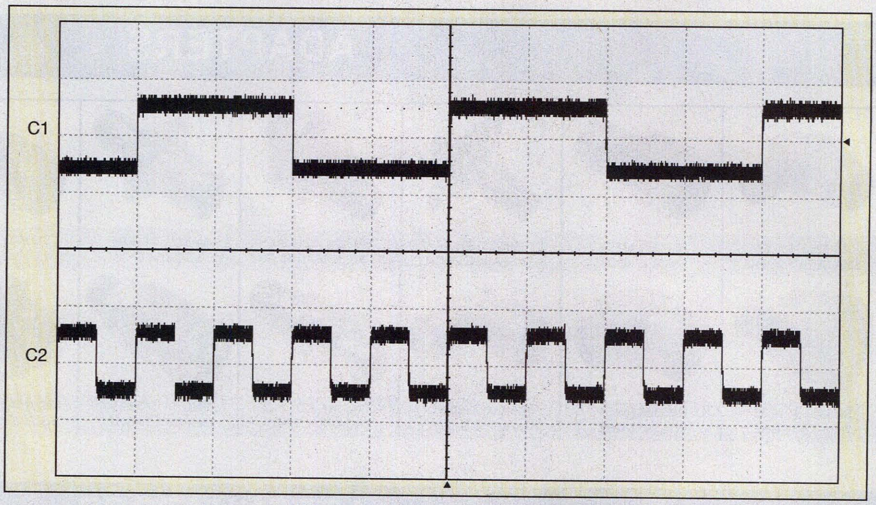

3. The I and Q data schemes are shown for the feed to the UQPSK modulator.

To optimize available transmit power from a satcom system, an UQPSK modulator is proposed here, where the power level of the low-data-rate channel can be reduced to achieve the same carrier-to-noise (E_b/N_o) ratio for both channels. This can be achieved by unbalancing the amplitudes of the carrier's signal components in the I and Q channels of a conventional QPSK modulator. The amplifier power following the modulator is shared between the I and Q channels in proportion to the amplitudes of the I and Q signal components of the modulated carrier.

Figure 1 shows a block diagram of the proposed UQPSK modulator. In a conventional QPSK modulator, the carrier source signal is divided equally by a 3-dB/90-deg. branch line hybrid coupler to yield two equal-amplitude carriers in quadrature. Both carriers are modulated with I and Q data streams using binary-phase-shift-keying (BPSK) modulation. The BPSK-modulated carriers are combined in an in-phase Wilkinson power combiner to produce a QPSK-modulated carrier. When data of different bit rates are to be modulated, an UQPSK modulator can be used.

In the case of an UQPSK modulator, for optimum utilization of power, an attenuator is added to the low-data-rate channel to reduce the power. A phase shifter is added to the high-data-rate channel to compensate for the phase shift introduced by the attenuator in the low-data-rate channel. The resulting output is a UQPSK-modulated signal. The mainlobe bandwidth will be determined by the high-data-rate channel. **Figure 2** shows

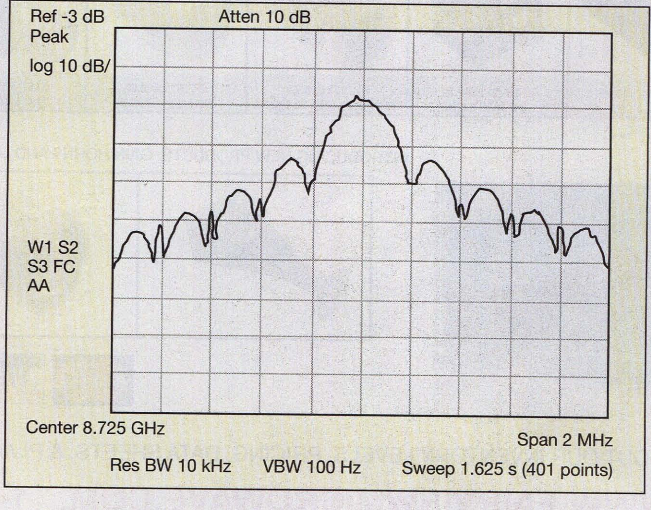

4. The modulated spectra for the I data are shown here.

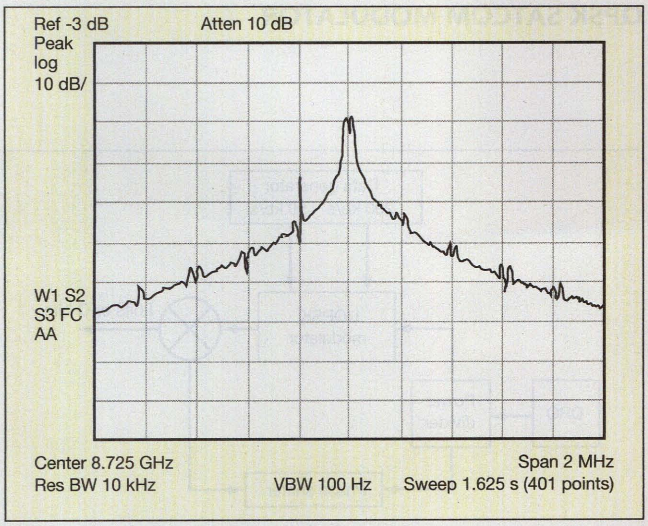

5. The modulated spectra for the Q data are shown here.

a plot of the I and Q data, along with the simulated UQPSK spectrum.

The UQPSK modulator was realized using a 3-dB/90-deg. branch line coupler, two double-balanced mixers, a phase shifter, an attenuator, and an in-phase power combiner. A dielectric resonator oscillator (DRO), generating a carrier signal at 8725 MHz, served as the carrier source for the modulator. For demonstration purposes, 200- and 50-kb/s pulse streams were used to modulate the carrier signal. A data generator providing different bit rates (other than these two rates) was not readily available. The use of two different data generators would require that data to be synchronized with a clock.

In this experiment, the two data streams were generated from a single generator. Data at 200 kb/s was taken from the generator and divided by four using JK flip-flops to generate the 50-kb/s data. The two data streams of unipolar format were converted to bipolar format using a transistor-level converter circuit. The I data and derived Q data are shown in **Fig. 3.** The data streams were fed to the UQPSK modulator.

The carrier was fed to a 3-dB/90-deg. hybrid coupler, which generates two carriers of equal amplitude and 90-deg. phase difference for the modulator's I and Q channels. The data rate of the Q channel is one-fourth the data rate of the I channel. As a result, the power in the Q channel should be reduced proportionally to one-fourth the level of the power in the I channel. This is accomplished by means of 6-dB attenuation in the Q channel. To compensate for the phase shift introduced by the attenuator, a phase shifter was added to the I channel. These two carrier signals were then modulated by the I and Q data using double-balanced mixers [a model DML-2B-10G mixer from Merrimac Industries (www.merrimacind.com)]. Those modulated spectra are shown in **Figs. 4 and 5,** respectively. The BPSK modulated signals were fed to an in-phase power combiner to produce the

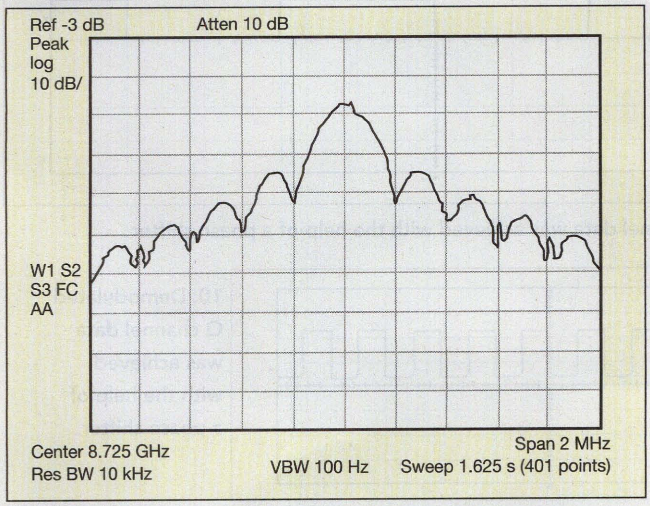

6. BPSK modulated signals were fed to an in-phase power combiner to produce a UQPSK-modulated output.

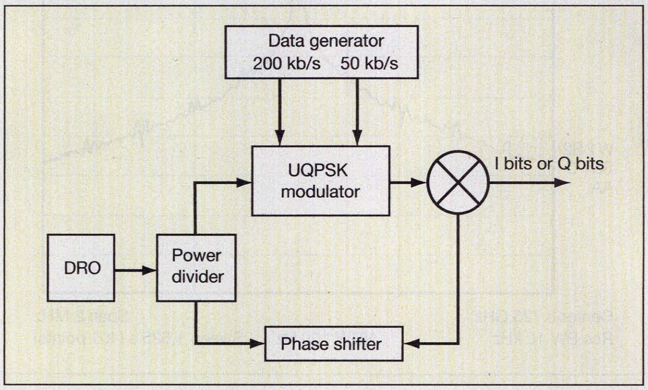

7. This block diagram details the different functions contained in the modulator/demodulator test setup.

UQPSK modulated output shown in **Fig. 6.**

Figure 7 shows a block diagram of the modulator/demodulator test setup, while **Fig. 8** features a photograph of the test setup. Since there was no standard UQPSK demodulator equipment available at the workplace, the modulated data was recovered as shown in **Fig. 7**.

To produce two carrier outputs from the DRO, a power-divider module was used. One of the power-divider's outputs was fed as an input to the UQPSK modulator. The UQPSK-modulated output and the other DRO carrier output from the power divider were fed to a mixer (not shown in **Fig. 8**) to bring back the original modulated data. A variable phase shifter (not shown in **Fig. 8**) was used in the carrier path. When the carrier phase was synchronized with the I channel carrier of the UQPSK signal, the I data stream was demodulated. When the phase of the carrier was shifted by 90 deg. using the variable phase shifter, the Q data stream was demodulated. Thus, by varying the phase of the phase shifter, the I and Q data streams could be demodulated; the resulting waveforms of that process are shown in **Figs. 9 and 10.**

In summary, an unbalanced QPSK modulator was demonstrated; it is a variant of a standard QPSK modulator. This unbalanced QPSK modulator is useful for transmitting different (unequal) data rates from two different satellite payloads, enabling effective utilization of on-board power. In addition, an arrangement was presented for data demodulation. Results are encouraging for fabricating all required functions on a single alumina substrate using microstrip transmission-line technology. MWRF

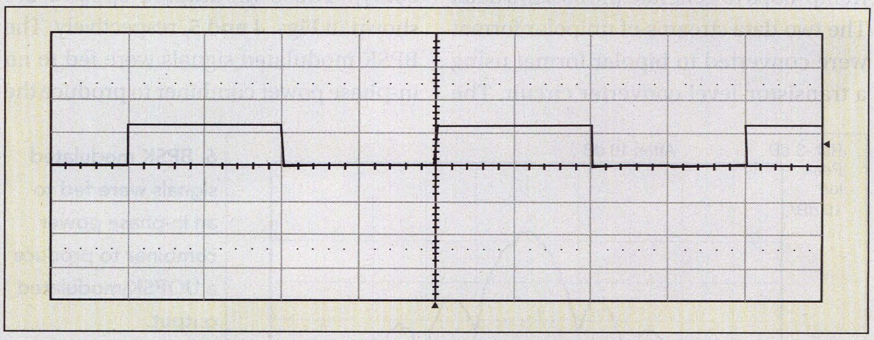

9. Demodulated I channel data was achieved with the help of a phase shifter.

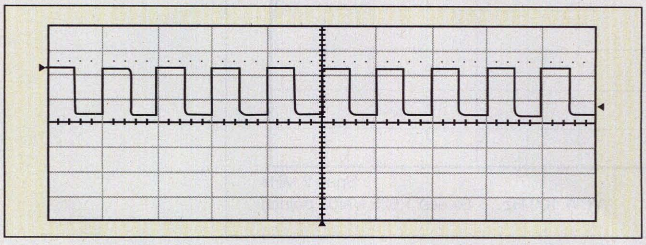

10. Demodulated Q channel data was achieved with the help of a phase shifter.

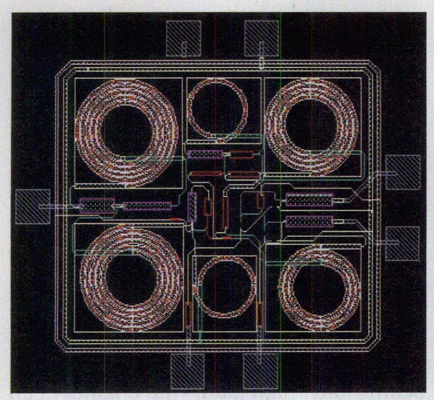

9. This chip photograph shows the basic layout of the dual-band receiver, fabricated in a commercial silicon CMOS foundry.

(continued from p. 57)

the forward body bias voltages are chosen at $V_{b1} = V_{b3} = 0.4$ V and $V_{b2} = 0.35$ V. Operating across the frequency ranges of 935 to 960 MHz and 1805 to 2483 MHz, the input reflection coefficients S_{11} for those frequency ranges are less than –14 and –11 dB, respectively, as shown in **Fig. 5**.

The double-sideband (DSB) noise figures range from 2.3 to 2.4 dB and 2.7 to 5.1 dB, respectively, across those two frequency bands, as shown in **Fig. 6**. The conversion gains for the two frequency ranges are 18.6 to 19.0 dB and 18.7 to 20.8, respectively **(Fig. 7)**. The input third-order-intercept points (IIP3) for the front end are –8.2 dBm at 935 MHz and –9.8 dBm at 2100 MHz **(Fig. 8)**. **Figure 9** shows the layout for the front end, with an active area of 0.61 x 0.53 mm^2. The power consumption is only 2.1 mW. **Table 2** summarizes the performance of the front-end device.

The total measured conversion gain of the receiver is 18.6 to 20.8 dB and the DSB noise figure ranges from 2.3 to 5.1 dB. The IIP3 is –8.2 dBm at 935 MHz and –9.8 dBm at 2100 MHz. Power consumption is a mere 2.1 mW with a 1-V supply. MWRF

ACKNOWLEDGMENT

The authors wish to thank the Open Fund Project of the Key Laboratory of Hunan University (No. 12K012).

REFERENCES

1. J. Liu, H. Liao, and R. Huang, "0.5 V ultra-low power wideband LNA with forward body bias technique," Electronics Letters, Vol. 45, No. 6, 2009, pp. 289-290.
2. T.T.N. Tran, et al., "Ultra-low-power series input resonance differential common gate LNA," Electronics Letters, Vol. 47, No. 12, 2011, pp. 703-704.
3. W. Dake, et al., "A 0.4-V Low Noise Amplifier Using Forward Body Bias Technology for 5 GHz Application," IEEE Microwave and Wireless Components Letters, Vol. 17, No. 7, 2007, pp. 543-545.
4. A. Chyuen-Wei, Z. Yuanjin, and H. Chun-Huat, "A Multi-band CMOS Low Noise Amplifier for Multi-standard Wireless Receivers," in ISCAS 2007 IEEE International Symposium on Circuits and Systems.
5. W. Hongrui, Z. Li, and Y. Zhiping, "A Wideband Inductorless LNA With Local Feedback and Noise Cancelling for Low-Power Low-Voltage Applications," IEEE Transactions on Circuits and Systems I: Regular Papers, Vol. 57, No. 8, 2010, pp. 1993-2005.
6. W. Chao-Shiun, L. Wei-Chang, and W. Chorng-Kuang, "A multi-band multi-standard RF front-end IEEE 802.16a for IEEE 802.16a and IEEE 802.11 a/b/g applications," in IEEE 2005 International Symposium on ISCAS.
7. N. Mingchen, et al. "A wide-band RF front-end for multi-standard application," in 9th International Conference on Solid-State and Integrated-Circuit Technology, ICSICT 2008.
8. L. Chen-Ming, et al., "A Low-Power Self-Forward-Body-Bias CMOS LNA for 3-6.5-GHz UWB Receivers," IEEE Microwave and Wireless Components Letters, Vol. 20, No. 2, 2009.

Editor's Note: For the complete list of references, please go to www.mwrf.com for the online version of this article.

Software Simplifies ANTENNA DESIGN

FOR THE PAST 10 years, the automated synthesis of microwave devices has been growing more popular in computer-aided-engineering (CAE) applications. With access to information and various automated design algorithms and export models, for example, an engineer can quickly evaluate different antenna topologies. He or she can then choose an appropriate topology for the design task at hand. In a four-page application note titled "Design Flow for Base Station Antenna," AWR Corp. shows how software like its Antenna Magus product can be used to hasten early design stages. Such software also makes it easier to export specific designs into electronic-design-automation (EDA) tools.

AWR Corp., 1960 E. Grand Ave., Ste. 430, El Segundo, CA 90245; (310) 726-3000, www.awrcorp.com.

The note uses a wide-area-network (WAN) base-station antenna as a design example. Here, the goal is to ensure adequate signal coverage for several homes in an area using just one base station. Typically, designers would consider various antenna topologies with which they are familiar and determine if one would be suitable. If not, they would begin an online product search and potentially reach out to antenna manufacturers with which they have partnered. With software like Antenna Magus, however, they could begin by simply considering a selection of antenna topologies—all of them familiar—and decide if one would be a good choice.

Such software serves as an information resource. It allows engineers to search for and explore a variety of options, get more information on them, and compare them. To help the designer derive antenna requirements from system specifications, utilities like a free-space path-loss calculator are included. In the example, the calculation shows that a transmit antenna with 18-dBi gain in the directions of required coverage is needed, given the requirement of –60-dBm power from a 16-dBi receive antenna at 1 km from a 5-mW transmitter. To provide the required coverage, a high-gain fan-shaped beam would be ideal. Using the keywords "fan beam" and "high gain," the engineer can quickly access six technology options with performance information that can be easily compared.

The note closes with another example, which illustrates how today's software tools allow an antenna design to be created and exported. The software performs some tasks automatically, such as calculating the effective dielectric constant of a two-layer dielectric and finding the correct feed spacing for a good match. The user specifies bottom-substrate height and top-substrate parameters and the antenna is rapidly designed. Such software options are very helpful for finding a first-order design in a rapid fashion, assessing its performance, and exporting parameterized models.

Master Testing Of IEEE 802.11ad PHY

CURRENTLY, FEW DEVICES and technologies use the 60-GHz band. In addition, it is only lightly regulated while allowing for rapid data-transfer rates compared to existing options in the 2.4- and 5.0-GHz bands. It may therefore prove a solution to the lack of bandwidth for data-hungry consumer applications. The IEEE 802.11ad standard, which resides in this band, provides very high throughput to 7 Gb/s over a short range using approximately 2 GHz of spectrum. In a four-page application note titled, "Solutions for 802.11ad PHY Layer Testing," Agilent Technologies pinpoints some design challenges and explains how they can be overcome.

IEEE 802.11ad is a backwards-compatible extension to IEEE 802.11-2007. The new specification adds a media-access-control (MAC)/physical layer (PHY) to provide short-range, high-capacity, point-to-point links at 60 GHz. To support a range of price/performance points to 6.75 Gb/s, it mixes single-carrier and orthogonal-frequency-division-multiplexing (OFDM) modulation techniques. At the MAC or data-link layer, it is compatible with the other IEEE 802.11x standards. Yet its PHY characteristics set it apart—and complicate testing.

IEEE 802.11ad measurement obstacles include the creation and analysis of 60-GHz signals with 2-GHz modulation bandwidth. Because that modulation bandwidth is much greater than that of other wireless communications systems, it requires different measurement tools and techniques. Some devices also lack a metallic connection, which means designers may not be able to connect the device to test equipment.

Thanks to applications like short-range radar and military communications, tools for millimeter-wave circuit design and simulation, network analysis, signal analysis, and power measurement have been available for a number of years. Although IEEE 802.11ad applications require a much wider modulation bandwidth, they can still be served by existing solutions. Of course, such solutions must be flexible enough to adapt to the standard's changing requirements. Agilent suggests its SystemVue Electronic System Level (ESL) design software and 60-GHz PHY test solution. The firm then goes on to detail the aspects of these products that make them well suited for IEEE 802.11ad testing, which includes their simulation and signal-generation and analysis capabilities. In doing so, it efficiently explains why IEEE 802.11ad presents test challenges and how those issues can be successfully addressed.

Agilent Technologies, Inc., 5301 Stevens Creek Blvd., Santa Clara, CA 95051; (408) 345-8886, www.agilent.com.

ULRICH L. ROHDE
Chairman

AJAY K. PODDAR
Chief Scientist

Synergy Microwave Corp., 201 McLean Blvd., Paterson, NJ 07504; (973) 881-8000, FAX: (973) 881-8361, e-mail: sales@synergymwave.com, www.synergymwave.com.

DROs DROP PHASE NOISE

With the aid of a unique coupling mechanism, these fundamental-frequency dielectric-resonator oscillators operate through 10 GHz with extremely low phase noise.

PHASE NOISE can be a limiting factor in modern communications systems, especially those that rely on phase-based modulation. Phase noise can increase the bit error rate (BER) of a telecommunications link, in addition to degrading both the stability of beams in particle accelerators and the sensitivity of radar systems. Fortunately, when properly designed, dielectric resonator oscillators (DROs) can deliver stable signals at microwave through millimeter-wave frequencies with excellent phase-noise characteristics. In particular, a new line of compact DROs from Synergy Microwave Corp. (www.synergymwave.com) features low phase-noise levels at fundamental-frequency outputs through 10 GHz and higher, for use in commercial, industrial, and military applications **(Fig. 1)**.

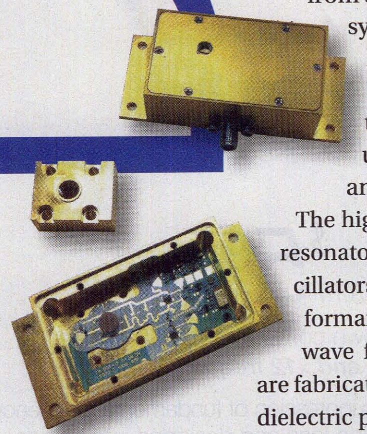

1. This photograph shows an actual 10-GHz DRO circuit and its surface-mount housing.

The high quality factor (Q) of a dielectric resonator makes it possible to achieve oscillators with excellent phase-noise performance at microwave and millimeter wave frequencies. Dielectric resonators are fabricated on ceramic materials with high dielectric permittivity, high Q, and high temperature stability. They have much smaller size compared to cavity resonators; therefore, they are frequently employed in the design of frequency-stable RF circuits (especially in high-frequency oscillators).

When high data rates must be transferred—as with multiple-quadrature amplitude modulation (M-QAM) schemes in Long-Term-Evolution (LTE), local multipoint distribution service (LMDS), and fixed-frequency point-to-point digital radios and satellite-communications (satcom) links—such systems rely on free-running or phase-locked signal sources with low phase noise. Such spectrally pure sources are also invaluable for radar systems and in research laboratories. A wide range of military, industrial, medical, and test-and-measurement markets demand stable frequency sources with low phase-noise performance and low thermal drift. DROs have provided low-noise solutions in the frequency range from 3 to 18 GHz, with spectral purity that compares favorably to other competing solutions (such as multiplied lower frequency fundamental sources).

A typical DRO circuit uses high-Q dielectric resonator (DR) and active device in a series/parallel feedback configuration to achieve the negative resistance required for stable oscillations. The DR is typically a piece of a dielectric material, usually manufactured in a circular shape such as a disk or cylinder. It boasts very high (much higher than 1) relative dielectric constant, ε_r, that acts like a resonant cavity by means of reflections at the dielectric/air interface. The DR can resonate in a number of modes and frequencies depending on the type of material, dimensions, and the proximity and shapes of enclosures.

Figure 2 shows a typical DR in a polar coordinate system used for providing insight into possible resonant conditions for a given physical dimension. These include L, the length of the DR, and a, the radius of the DR. It can be shown that by matching the tangential fields at the resonator (dielectric/air)

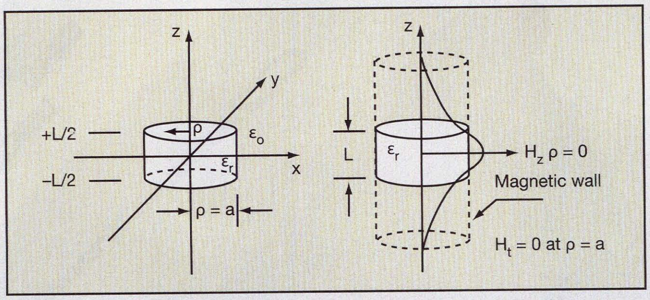

2. These diagrams show a typical disk dielectric-resonator $TE_{01\delta}$ mode (left) and H_z field distribution (right).

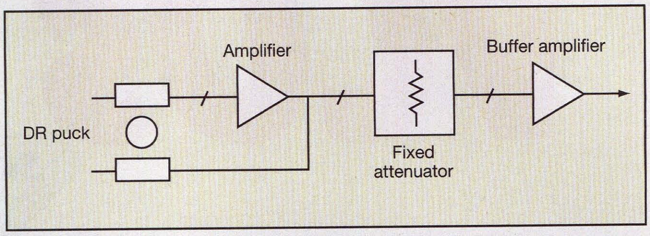

3. This simple block diagram shows the basic components of a dielectric resonator oscillator.

interface, at | z | = L/2 it is possible to derive Eqs. 1 and 2:

$$A\cos(\beta L/2) = Be^{-\alpha(L/2)} \quad (1)$$

and

$$-(jA/Z_d)\sin(\beta L/2) = (B/Z_a)e^{-\alpha(L/2)} \quad (2)$$

with:

$Z_d = \omega\mu_0/\alpha$, (where Z_d is the wave impedance within the dielectric) (3)

$Z_a = j\omega\mu_0/\alpha$, (where Z_a is the wave impedance within the air) (4)

where α and β are the imaginary and real propagation constants, respectively. From Eqs. 1 and 2,

$$-jZ_a \sin(\beta L/2) = Z_d\cos(\beta L/2) \rightarrow \tan(\beta L/2) = \alpha/\beta \quad (5)$$

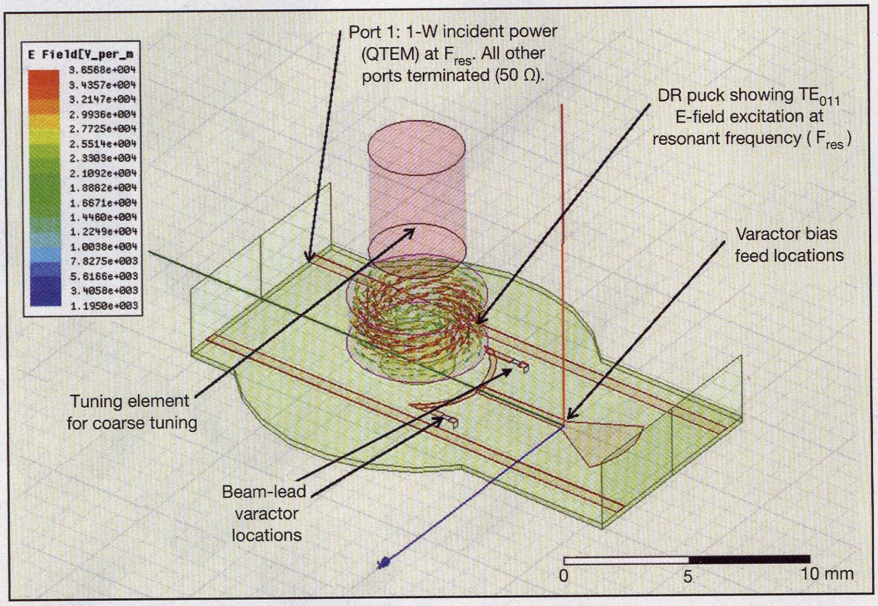

4. This is a three-dimensional (3D) model for a varactor-tuned dielectric resonator oscillator.

By solving transcendental Eq. 5, the resonant frequency, f_0, the length, L, and the radius, a, of the DR are found by Eq. 6:

(See Eq. 6, this page.)

where:

L = the length of the DR;
a = the radius;
ε_r = the relative permittivity of the dielectric material; and
c = the speed of light in a vacuum.

Transcendental equation Eq. 6 produces two possible solutions for the resonant wavelength, λ, but only one is valid in yielding a deterministic solution within the dielectric ($\lambda\varepsilon_r$) and the air ($\lambda\varepsilon_o$).

Designing and fabricating low-noise-noise oscillator circuits based on DRs is not trivial, given the nonlinear natures of the active devices needed for the oscillators as well as the resonators. Synergy Microwave Corp. has studied the nonlinear behavior of these two key components for DROs and has developed a new line of low-noise DROs with outstanding phase-noise characteristics. These include the model DRO1000-8, which offers mechanical and electrical frequency tuning around a center frequency of 10 GHz.

Figure 3 shows a typical block diagram of the 10-GHz DRO. One of the design challenges for this source involved maintaining low phase noise even with electronic varactor tuning, while also minimizing the cost of the oscillator by achieving a structure that could be assembled repeatably in production. To achieve this consistency in design and manufacturing, comput-

$$\tan\left[\frac{L}{2}\left(\varepsilon_r\left(\frac{2\pi f_0}{c}\right)^2-\left(\frac{2.405}{a}\right)^2\right)^{0.5}\right]=\left[\frac{\left(\frac{2.405}{a}\right)^2-\left(\frac{2\pi f_0}{c}\right)^2}{\varepsilon_r\left(\frac{2\pi f_0}{c}\right)^2-\left(\frac{2.405}{a}\right)^2}\right]^{0.5} \quad (6)$$

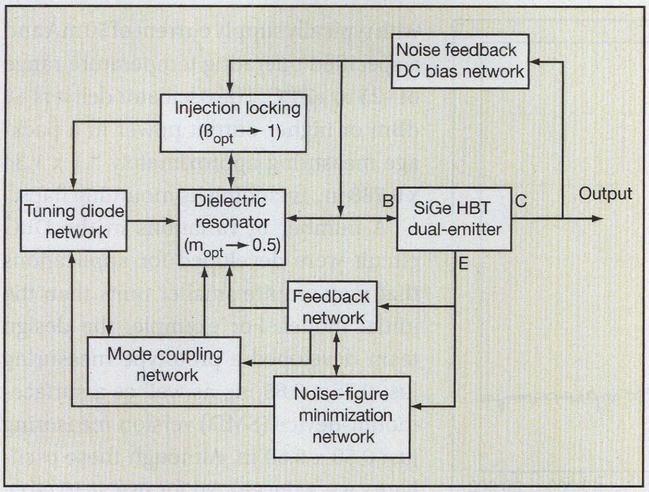

5. This block diagram shows some of the typical components in a dielectric-resonator-oscillator (DRO) circuit.

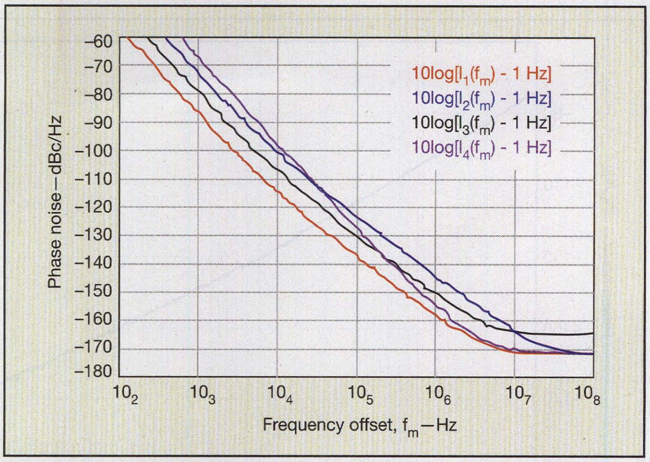

6. These plots show how various parameters, such as loaded resonator quality factor (Q), can impact the phase-noise performance of a microwave DRO.

er-aided-engineering (CAE) simulation tools were used, such as ANSYS =HFSS from ANSYS (www.ansys.com) and ADS Momentum software from Agilent Technologies (www.agilent.com).

Figure 4 shows a three-dimensional (3D) model for the varactor-tuned DRO. The complete DRO design was evaluated and optimized using harmonic-balance circuit simulation along with electromagnetic (EM) co-simulation. This approach allows designers to achieve a optimum dynamic loaded Q-factor for a typical DR coupling arrangement in conjunction with the oscillator core, which is one of the preconditions for achieving lowest phase noise. The active device has been selected carefully with respect to noise figure and flicker noise, with optimum bias level conditions.

Equation 7 provides an expression for an oscillator or other source's phase noise (see ref. 1):

$$\pounds(f_m) = 10\log\left\{\left[1+\frac{f_0^2}{(2f_mQ_0)^2m^2(1-m)^2}\right]\left(1+\frac{f_c}{f_m}\right)\left(\frac{FkT}{2P_0}+\frac{2kTRK_0^2}{f_m^2}\right)\right\} \quad (7)$$

$$m_{opt} \rightarrow 0.5 = \left[\frac{1}{1+\beta}\right]_{\beta=\beta_{opt}} \Rightarrow \beta_{opt}(\phi = \phi_{opt}) \rightarrow 1 \quad (12)$$

(low phase noise)

where:

m = the ratio of the loaded and unloaded Q.

The coupling coefficient, β, and the ratio parameter m can be described by Eq. 8 as:

$$\frac{d}{dm}\left[10\log\left\{\left[1+\frac{f_0^2}{(2f_mQ_0)^2m^2(1-m)^2}\right]\left[1+\frac{f_c}{f_m}\right]\left[\frac{FkT}{2P_0}+\frac{2kTRK_0^2}{f_m^2}\right]\right\}\right] = 0 \Rightarrow m_{opt} = 0.5 \quad (11)$$

$$m = \frac{Q_L}{Q_0} \Rightarrow \frac{Q_L}{Q_0} = \frac{1}{1+\beta} \quad (8)$$

Dynamic loaded Q can be given by Eq. 9:

$$Q_L = \frac{\omega_0}{2}\left[\frac{\partial\phi}{\partial\omega}\right] \Rightarrow \frac{\partial Q_L}{\partial\omega} = \frac{\omega_0}{2}\left[\frac{\partial^2\phi}{\partial\omega^2}\right]_{\omega=\omega_0,\phi=\phi_{opt}} \Rightarrow 0 \quad (9)$$

For maximum dynamic loaded Q, $(\partial/\partial\omega)[Q_L(\omega)]_{\omega} = \omega_0 \rightarrow 0$, therefore, the minimum phase noise can be found by differentiating Eq. 7 with respect to ratio parameter m, and equating to zero for a minimum value of phase noise as shown in the next several equations:

$$\frac{\partial}{\partial m}\left[\pounds(f_m)\right]_{m=m_{opt}} = 0 \Rightarrow (\phi = \phi_{opt}) \quad (10)$$

(See Eqs. 11 and 12, this page.)

where:

$\pounds(f_m)$ = the ratio of the sideband power in a 1-Hz bandwidth at f_m to total power in dB;
f_m = the sideband frequency;
f_0 = the offset frequency;
f_c = the flicker corner frequency;
Q_L = the loaded quality factor;
Q_0 = the unloaded quality factor;
F = the noise factor;
k = Boltzman's constant;
T = the temperature (in degrees Kelvin);
P_0 = the average output power;
R = the equivalent noise resistance of the tuning diode; and

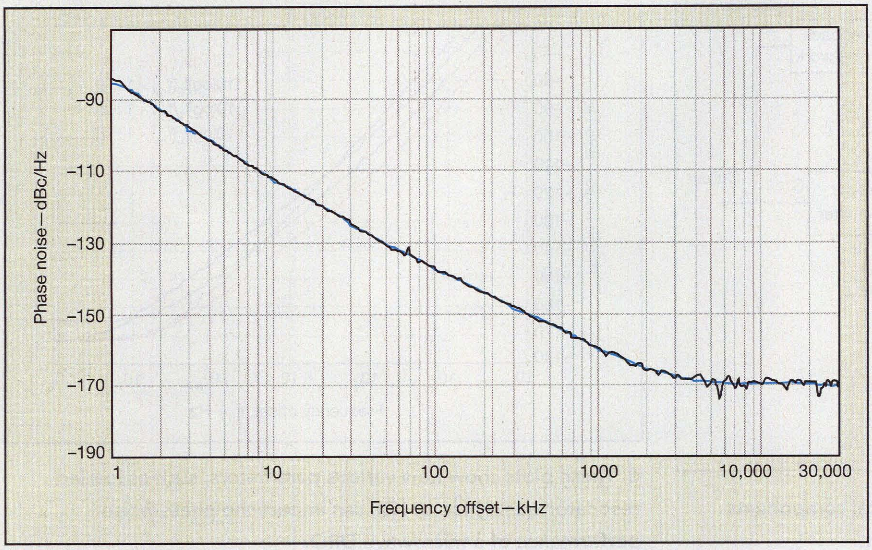

7. This is an actual phase-noise plot for a model 100-8 10-GHz DRO, made on an RF/microwave FSUP signal analyzer from Rohde & Schwarz (www.rohde-schwarz.com).

K_0 = the voltage gain.

From Eq. 12 for low-phase-noise applications, m_{opt} and β_{opt} should be dynamically controlled and must lie in the vicinity of 0.5 ($m_{opt} \approx 0.5$) and 1 ($\beta_{opt} \approx 1$), respectively, for the best phase-noise performance. **Figure 5** shows a typical block diagram of the DRO circuit used for validating the approach of achieving minimum phase noise performances.

Figure 6 illustrates the impact of possible impairments on the phase noise performance. The red trace identifies the measured phase noise performance of Synergy's new 10 GHz model number DRO100-8. The blue trace corresponds to a lower Q_L with identical oscillator core noise properties. The black and magenta traces correspond to identical Q_L but significantly higher effective noise figure or flicker corner frequency when the active device is not selected or biased optimally. A combination of these impairments together with nonlinear noise effects account for the much higher phase noise performance found in many competing DRO designs.

The model DRO100-8 DRO has a typical noise floor of –170 dBc/Hz, approaching state-of-the-art performance. The measured phase noise is -112 dBc/Hz offset 10 kHz from the carrier (**Fig. 7**). Mechanical and electrical tuning is available for frequency adjustment and phase locking. The frequency is set at the factory to 10 GHz and can be mechanically varied by approximately ±50 MHz. Tuning voltages of 1 to 15 VDC enable variations in the center frequency by ±1 MHz to compensate for frequency drift in phase-locked systems.

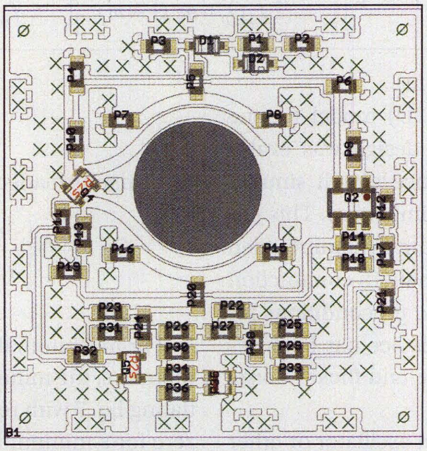

8. This is the typical layout for a 10-GHz DRO in a square housing measuring 0.5 x 0.5 in.

The DRO features temperature stability of typically better than 80 ppm. The oscillator's internal voltage regulation provides high immunity to power supply noise. The DRO100-8 handles supply-voltage variations between +7 and +10 VDC with typically supply current of 50 mA and a specified operating temperature range of –25 to +70°C. The oscillator delivers +8 dBm or higher output power in a package measuring approximately 3.1 x 1.34 x 0.788 in., including its mounting flaps.

A number of variations in the DRO circuit were developed for applications that may require smaller units than the initial model. For example, the design team developed a prototype measuring just 0.75 x 0.85 in., as well as a surface-mount-device (SMD) version measuring just 0.50 x 0.50 in. Although these oscillators were developed for use at 10 GHz, they are not limited to that frequency; they can be designed for any fixed frequency from 3 to 18 GHz without long development lead times. As an example, **Fig. 8** shows a prototype 10-GHz DRO layout for a 0.75 x 0.75 in. package. The measured phase-noise performance is better than –100 dBc/Hz offset 10 kHz from the carrier.

As with crystal oscillators, DROs can be prone to vibrational noise since the DR cannot be fully mechanically secured. To minimize such noise, vibrations must be damped before they reach the DR. The DRO100 features rugged construction with extensive damping of the DR to minimize vibration noise and microphonic effects, thus preventing unwanted modulation. The DRO's low phase noise makes it well suited for use in high-data-rate communications systems; as reference oscillators for phase-noise-measurement systems; in radar, cable-television (CATV), optical SDH/SONET communications, and satcom systems; and in a variety of other high-frequency electronic systems requiring low-noise sources. MWRF

SYNERGY MICROWAVE CORP., 201 McLean Blvd., Paterson, NJ 07504; (973) 881-8000, FAX: (973) 881-8361, e-mail: sales@synergymwave.com, www.synergymwave.com.

REFERENCE

1. U.L. Rohde, A.K. Poddar, and G. Boeck, Modern Microwave Oscillators for Wireless Applications: Theory and Optimization, John Wiley & Sons Inc., 2005.

JACK BROWNE | Technical Contributor

Sampling An Array Of Test Probes And Fixtures

Often overlooked, RF/microwave probes, probe stations, and fixtures provide the means of moving test signals from devices and circuits under test to measurement equipment.

TEST PROBES and fixtures for RF/microwave applications are as diverse as the components, devices, and materials they evaluate. These measurement "accessories" must inject and extract signals to and from a device under test (DUT) while remaining as close to electrically "invisible" as possible. Tracking current trends in RF/microwave test probes and fixtures is typically a matter of understanding the performance levels of the DUTs which they must handle. In turn, those performance levels are driven by the applications the DUTs serve, generally for higher power levels in smaller package sizes.

Last February, this magazine provided an "RF Essentials" article on probes and fixtures for RF/microwave testing, explaining some of the basic requirements for the different types of probes and fixtures for coaxial and on-wafer measurements (http://mwrf.com/semiconductor/probes-and-fixtures-ease-microwave-testing). Probe and fixture products are available from a wide range of suppliers, including companies known for testing and those that are component suppliers (which may have developed probes and fixtures for their own requirements).

In sorting through the capabilities of any set of test probes and fixtures, it is also important to realize that calibration software is a vital complement to any probe or fixture. This minimizes electrical contributions to a test system that will typically include a signal source and an analyzer—such as an RF/microwave scalar network analyzer (SNA) or a vector network analyzer (VNA). Calibration techniques are generally known for the type of measurement standards they employ, including shorts and opens, Among the leading calibration techniques for fixtures, probes, and VNAs are the short, open, load, through (SOLT), line-reflect-match (LRM), and line-reflect-line (LRL) approaches.

1. The LMS-2709(S) Laboratory Microprobe Station is stable and repeatable enough to function effectively with microwave probes to 220 GHz. [Photo courtesy of Jmicro Technology (www.jmicrotechnology.com).]

One of the best-known names in high-frequency test probes and fixtures, Cascade Microtech® (www.cmicro.com), supplies a wide range of products—from probes and probe cards to full on-wafer probe systems. The company's founders, Reed Gleason and Eric Strid, created the first microwave wafer probe in the early 1980s and have built a company around the high quality of their probes and probe systems; Cascade currently offers more than 50 different probe models for wafer, package, and board-level characterization. An essential requirement for any test probe system is its capability to move signals from the waveguide or coaxial environment of the test equipment to an electrical environment that may be much different for the DUT, including semiconductor wafers and miniature surface-mount packages.

As an example, Cascade's Infinity Probe® line, which was introduced in 2002, is available with standard models operating to 220 GHz and special models available for on-wafer measurements to 500 GHz. The on-wafer devices they contact can have a variety of different arrangements for how signal (S) and ground (G) points are fabricated. Hence, the Infinity Probes incorporate membrane contact tips with different pitches (50 to 250 μm) and numerous ground and signal configurations, such as GSG, SG, GSGSG, and GSSG. The firm's Waveguide Infinity Probe uses a membrane GSG contact tip to reduce stray electromagnetic (EM) fields near the probe tip for improved crosstalk performance between the probe tips and usable performance through 500 GHz.

Earlier this year, Cascade introduced its CM300 on-wafer measurement system, a scalable platform for device characterization and modeling. It works with test automation software to speed and improve the repeatability of on-wafer mea-

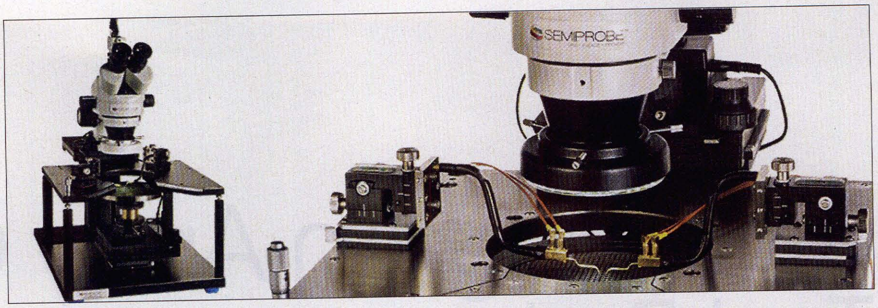

2. The "Probe Systems For Life™" line of probe stations use interchangeable function modules to quickly alter measurement capabilities. [Photo courtesy of SemiProbe LLC (www.semiprobe.com).]

surements, even when testing over wide temperature ranges. According to Debbora Ahlgren, Cascade's Vice President of Marketing, "With the CM300, our customers benefit from highly configurable and scalable solutions. By allowing them to create more precise model parameters and achieve reliable, repeatable contact over temperature and time, the CM300 helps them achieve faster time-to-market on new devices and technologies." The CM300 system can be used for high-volume measurements on devices with contact pads as small as 30 μm.

Jmicro Technology (www.jmicrotechnology.com) is another leading supplier of RF/microwave probes and probe stations, with the firm's LMS-2709(S) Laboratory Microprobe Station serving industrial and academic customers for over five years. The compact test station **(Fig. 1)** is suitable for college and industrial laboratories for testing both active and passive components and devices with the aid of additional test equipment, such as test signal sources and vector network analyzers (VNAs). The standard vacuum chuck on the LMS-2709(S) can handle semiconductors, thick-film, and thin-film circuits as large as 2 x 2 in. (5.08 x 5.08 cm) with as much as 1 x 1 in. (2.54 x 2.54 cm) stage movement. Precision x-y-z positioning manipulators help align test probes to better than 0.0003 in. (0.01 mm) positioning accuracy. The LMS-2709(S) measures 12.5 x 12.5 in. (31.75 x 31.75 cm), is less than 20 in. (50.8 cm) high, and weighs about 32 lbs (14.51 kg).

SemiProbe LLC (www.semiprobe.com) is yet another supplier of high-quality RF/microwave probe systems, with a patented adaptive architecture that promises to combat obsolescence. The company's unique "Probe Systems For Life™" series of DC/RF/microwave wafer-probing systems, such as the PS4L probe station **(Fig. 2)**, can be modified at any time to suit any application for testing packaged or on-wafer devices. A PS4L probe station can be purchased as a manual system and upgraded to a fully programmable probe station at any time, using different interchangeable function modules. It can even be equipped with different stages for evaluating wafers with diameters from 2 to 12 in. and features enough stability for use with test probes from DC through 220 GHz.

Probe stations such as the PS4L require precision test probes from another supplier, like the Picoprobe® test probes from GGB Industries (www.ggb.com). These test probes are available in a wide range of frequencies, from active high-impedance models operating from DC to 500 MHz to microwave probes such as the model 40A with coverage of DC to 40 GHz using 2.92-mm coaxial K connectors. It is available with a number of tip materials, including nickel and tungsten, and contact pitches ranging from 50 to 2540 μm. GGB's Picoprobes employ individually spring-loaded contacts to achieve better than –80-dB measurement repeatability with high return loss and low insertion loss.

Along with supporting RF/microwave probe systems and test fixtures, several companies are well known for their precision impedance tuners to assist with load-pull testing of different on-wafer and packages devices. Both Focus Microwaves (www.focus-microwaves.com) and Maury Microwave (www.maurymw.com) offer a variety of precision tuners that can greatly benefit testing with a VNA and RF/microwave probe or test fixture, and both companies can provide test fixtures for a wide range of product package styles, including for MMICs and components in TO-packages.

When a high-frequency measurement involves a single device or circuit board for characterization, a suitable test fixture can provide an effective means of bringing test signals to and from the circuit under test. Inter-Continental Microwave (www.icmicrowave.com) has a long history of developing quality RF/microwave test fixtures for handling packaged transistors, diodes, ICs, and even passive components (such as capacitors). In addition to its extensive lines of standard test fixtures, the company offers fast turnaround time on fixtures designed and built according to a customer's requirements.

Some of Inter-Continental Microwave's fixtures, such as the model WK-7000 Universal Substrate Test Fixture, attempt to handle as many different DUTs as possible. Offering a frequency range of DC to 40 GHz, the WK-7000 is designed for use with microstrip substrates and to accommodate DUTs with many different physical parameters. It employs interchangeable transition assemblies for upgrading to higher frequency ranges as needed. Numerous versions are available, with built-in DC bias and for testing over wide temperature ranges.

Additional suppliers of RF/microwave test probes and fixtures include Altair Microwave, Inc. (www.altairmicrowave.com), Electro-Photonics LLC (www.electro-photonics.com), Keycom (www.keycom.co.jp), MicroTest (www.microtst.org), NPS, Inc. (www.nps-i.co.jp/e/), Southern Microwave, Inc. (www.southernmw.com), and Wentworth Laboratories (www.wentworthlabs.com). Finally, some components suppliers, such as Synergy Microwave Corp. (www.synergymwave.com), will often supply test fixtures for its products, including its various types of dielectric resonator oscillators (DROs) and voltage-controlled oscillators (VCOs). MWRF

POWER AMPLIFIER SOLUTIONS

[Broad Selection - COTS and Custom Products]

DEFENSE ELECTRONICS

MODULES	SKU	Start (MHz)	Stop (MHz)	Pout (Watt)	Size (Inch)	Gain (dB)
	1094	20	520	100	6.4x3.4x1.1	50
	1163	20	520	125	7.0 x4.0 x1.5	54
	1193	20	1000	100	7.0 x4.0 x1.5	53
	1119	500	2500	50	7.4x3.6x1.1	46
	1189	500	2500	100	7.4x3.6x1.06	50
	1164	800	3000	50	6.4x3.4x1.1	50
	1132	960	3000	160	12x10x1.1	54
	1146	1000	3000	100	6.8x4.4x1.1	10
	1131	2500	6000	35	6.9x3.6x1.1	48
	1191	2500	6000	100	8.0x6.5x1.0	60

SYSTEMS	SKU	Start (MHz)	Stop (MHz)	Pout (Watt)	Size	Gain (dB)
	2101	20	500	500	R5U	56
	2126	20	500	1000	R5U	60
	2162	20	1000	1000	R5U	60
	2066	500	1000	1000	R5U	60
	2157	1000	2000	1300	R3U+R5U	62
	2142	1000	2500	500	R5U+R3U	56
	2154	20	3000	250	C19U	54
	2135	300	3800	50	R3U	48
	2153	700	3800	200	R3U	54
	2141	100	6000	400	R14U	56

- *Amplifier products from 10 KHz to 6 GHz*
- *LDMOS and GaN technologies - optimized size, weight, efficiency*
- *Selection of COTS models available from inventory at Richardson RFPD*
- *Multi-function HPA solutions built per customer specification*

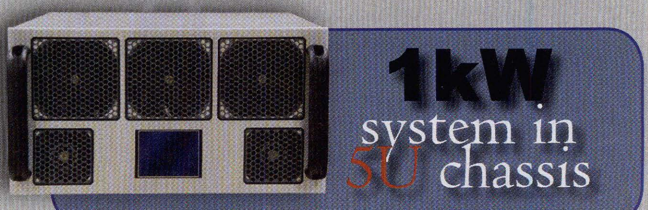

Certified to ISO 9001:2008
TÜVRheinland

www.EmpowerRF.com

EMPOWER
RF SYSTEMS, INC.

Miniature Mixer Tackles K-Band

Model P1M29B3-2208F is a compact frequency mixer from Spacek Labs that translates K-band signals (typically 26 to 40 GHz) to intermediate-frequency (IF) bandwidths to 13 GHz. The double-balanced mixer, which is optimized for spurious rejection of better than −30 dBc for an RF input level of −10 dBm, is available as a passive mixer or can be specified as an active mixer with amplification on any of the ports. As an active mixer, it provides 10-dB conversion gain with 3.5-dB maximum noise figure. The PM series mixer measures just 1.0 x 12.6 x 0.3 in.

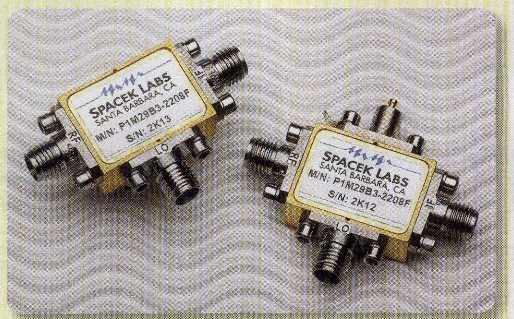

SPACEK LABS, INC., 212 E. Gutierrez St., Santa Barbara, CA 93101; (805) 564-4404, FAX: (805) 966-3249, ***www.spaceklabs.com.***

Portable Testers Read PIM Levels

A line of portable passive-intermodulation (PIM) testers from AWT Global provides the flexibility of two built-in test carriers with adjustable level range of +15 to +44 dBm for each carrier. Suitable for testing outdoor wireless cells and in-building distributed antenna systems (DASs), the PIM+ series of portable PIM testers can be equipped with a variety of optional measurement capabilities, such as automatic return-loss, distance-to-fault (DTF), and distance-to-PIM (DTP) test functions. The portable testers, which are supplied with solid-state drives for storing data, are available for frequency ranges specific to cellular standards, such as the 700-, 850-, 900-, 1800-, 1900-, 2100-, and 2600-MHz mobile communications bands.

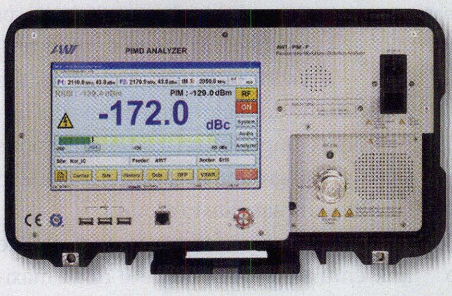

AWT GLOBAL, 2001 Rte. 46, Waterview Plaza, Ste. 310, Parsippany, NJ 07054; (973) 321-3423, FAX: (973) 402-8912, ***www.awt-global.com.***

SAW Oscillator Clocks To 1090 MHz

Model CCSO-914X is a surface-acoustic-wave (SAW) clock oscillator that can be supplied in single-frequency bands from 250 to 1090 MHz. Based on a SAW resonator and proprietary circuitry, the modular clock oscillator features −153 dBc/Hz phase noise offset 10 kHz from the carrier, with a noise floor of −173 dBc/Hz. The low-noise, low-jitter oscillator, which can run on +3.3- and +5-VDC supplies, generates a true sinewave output with minimum output power of +8 dBm and second harmonic levels of typically −20 dBc. It is designed for an operating temperature range from −40 to +85°C. The SAW clock oscillator is supplied in a surface-mount-technology (SMT) package measuring just 9 × 14 mm. It is priced at $36.96 in single-piece quantities.

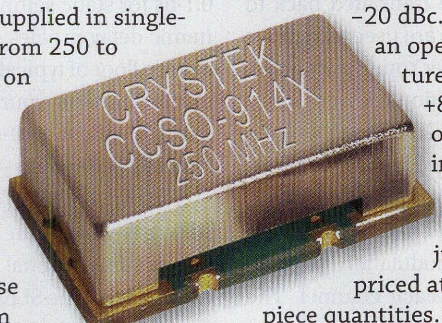

CRYSTEK CORP., 12730 Commonwealth Dr., Fort Myers, FL 33913; (800) 237-3061, (239) 561-3311, FAX: (239) 561-1025; e-mail: sales@crystek.com, ***www.crystek.com.***

Amplifier Gains 0.7 To 2.7 GHz

Model SKY67130-396LF is a broadband amplifier from Skyworks Solutions optimized for use from 0.7 to 2.7 GHz. Fabricated with an indium gallium phosphide (InGaP) heterojunction-bipolar-transistor (HBT) process and housed in a 2 x 2 mm, 8-pin package, it can be used with supply voltages from +2.7 to +5.5 VDC. It exhibits typical noise figure of 2.6 dB at 2.6 GHz, with 13-dB gain at that frequency and +4-dBm output power at 1-dB compression. The input and output third-order intercept points at 2.6 GHz are typically +26 and +39 dBm, respectively. The amplifier typically draws 22 mA from a +3.3-VDC supply. It is unconditionally stable to 24 GHz and is designed for operating temperatures from −40 to +85°C. It is suitable for wireless-local-area-network (WLAN) and cellular-communications-infrastructure applications.

SKYWORKS SOLUTIONS, INC., 20 Sylvan Rd., Woburn, MA 01801; (781) 376-3000, FAX : (781) 376-3100, e-mail : sales@skyworksinc.com, ***www.skyworksinc.com.***

Bandpass Filters Pass Iridium Band

A series of compact inductive-capacitive (LC) bandpass filters from Trilithic have been developed for use in the Iridium telephony band from 1616.0 to 1626.5 MHz. They operate with maximum insertion loss of 2.6 dB while achieving at least 15-dB isolation of Global Positioning System (GPS) L1 and 70-dB isolation of GPS L2 signals.

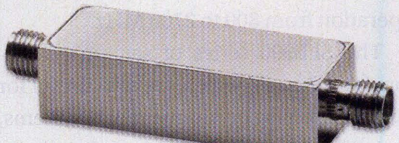

The filters also offer 45-dB isolation of signals in the 1710-to1850-MHz band and 55-dB isolation for frequencies beyond that band through 10 GHz. The filters, which are available in versions for printed-circuit-board (PCB) mounting and with coaxial connectors, measure just 0.5 x 0.5 x 2.0 in.

TRILITHIC, INC., 9710 Park Davis Dr., Indianapolis, IN 46235; (317) 895-3600, (800) 344-2412, FAX : (317) 895-3613, ***www.trilithic.com.***

JACK BROWNE | Technical Contributor

Systems Emulate Satellite Links

These programmable satellite-link emulators can be used to recreate signal-path conditions for testing, either between satellites and ground stations or in-flight communications systems and the ground.

SATELLITE-COMMUNICATIONS (SATCOM) systems count on dependable transmission and reception of microwave signals across the vast distances of space, or at least to and from orbiting satellites. Testing such systems is no trivial matter, since it involves including the effects of propagation and phase shifting across those distances. But the SLE900 Satellite Link Emulator line from dBm Corp. (www.dbmcorp.com) makes such satcom system testing possible at both intermediate frequencies (IFs) and microwave frequencies (using optional frequency converters).

The SLE900 series consists of three models: the SLE9072, with a 72-MHz-wide IF centered at 70 or 140 MHz; the SLE9125, with a 125-MHz-wide IF centered at 140 MHz; and the SLE9250, with a 250-MHz-wide IF centered at 1200 MHz. Optional tunable internal frequency up/downconverters can also be installed for L/S-band operation from 800 to 2700 MHz.

The SLE900 series of satcom emulators **(see figure)**, which are also useful for testing aircraft communications systems, blend the best of analog and digital signal processing to achieve desired signal-modifying effects. An IF input signal is first passed through an in-phase (I) and quadrature (Q) demodulator to reduce it to its I and Q signal components, and these baseband signals are then digitized by 12-b analog-to-digital converters (ADCs). Delay emulation is achieved in the digital realm, passing the digital signals through a first-in, first-out (FIFO) memory module. Digital signal processing (DSP) is used for additional signal impairments, such as the optional Rayleigh and Rician multipath fading and injection of additive white Gaussian noise (AWGN).

The SLE900 Satellite Link Emulator series operates at satcom intermediate frequencies (IF) and features a large touchscreen display for ease of control.

Once the desired impairments have been achieved in these digital I and Q signal components, they are applied to high-resolution (16-b) digital-to-analog converters (DACs) for their return to the analog realm. The analog I and Q signal components are "recombined" in a broadband I/Q modulator; a frequency-synthesized local oscillator (LO) is used to create frequency offsets and phase shifts as the I/Q signals are translated back to IF. At that stage, filters are used to remove the LO signals and other spurious content, and a variable attenuation provides emulation of path loss and flat fading.

The SLE900 Satellite Link Emulator series instruments can be configured with 1, 2, 3, or 4 independent channels, with the I/Q demodulation/modulation process applied separately to each channel. The emulators can effect quite a range of signal impairments as might be exhibited by a satcom system, including propagation delays, flat fading, path loss, phase shifts, and Doppler shifts. Propagation delays can be changed as part of the programmed control of the emulator, with phase continuity maintained during varying delay conditions.

The emulators can also deliver the time-varying delays found in satcom systems, which create frequency shifts and chip-period variations as caused by the movement of satellites or aircraft communications systems linked to the ground. The emulators can mimic the impairments imposed on communications signals from ground to satellite, satellite to satellite, and satellite to ground.

In terms of performance, the satellite link emulators can handle 0-dBm maximum input power and deliver 0-dBm maximum output power at a 0-dB attenuation setting. Attenuation can be set from 0 to 74 dB with 0.1-dB resolution and with a slew rate of better than 40 dB/ms as needed for dynamic attenuation profiles.

Delay resolution can be adjusted with 0.1 ns for static settings and 0.5 ps for dynamic delay profiles. The emulators have a noise floor of typically –145 dBm/Hz and exhibit in-band spurious levels of better than –45 dBc for a 0-dBm input level and typically better than –50 dBc.

Finally, the firm also offers SATGEN software, which can be used to program any required orbital and ground-station coordinates. The SLE900 also supports the Satellite Tool Kit (STK) software from Analytical Graphics (www.agi.com)—*JB*

DBM CORP., 32A Spruce St., Oakland, NJ 07436; (201) 677-0008, FAX: (201) 677-9444, info@dbmcorp.com, *www.dbmcorp.com.*

SDR Board Eases Radio System Design

This demonstration board offers a head start to radio designers seeking to evaluate the use of advanced linear digital modulation schemes in their communications systems.

SOFTWARE-DEFINED RADIOS (SDRs) are often associated with military users, but they also bring enormous versatility to commercial and industrial applications. To shorten the learning curve for those hoping to adopt SDR technology in their own systems, CML Microcircuits (www.cmlmicro.com) is offering its very compact model DE9941 SDR 1 Demonstration Board, which makes use of the company's model CMX998 Cartesian Feedback Loop Transmitter, model CMX994 Direct-Conversion Receiver, and model CMX7164 Multimode Wireless Data Modem integrated circuits (ICs). The credit-card-sized demonstration board can be used to send and receive wireless data from 452 to 467 MHz using a wide range of secure modulation schemes, including quadrature amplitude modulation (QAM), frequency-shift-keying (FSK), and Gaussian minimum-shift-keying (GMSK) modulation **(see figure)**.

The DE9941 SDR 1 Demonstrator Board can transmit and receive signals with 4/16/64-state QAM linear modulation, as well as 2/4-level FSK and GMSK. The board, which includes a 1-W power amplifier for transmission, is designed to be compliant with EN 302 561 radio requirements. The DE9941 incorporates a voltage-controlled oscillator (VCO) and phase-locked loop (PLL) for synthesized operation from 452 to 467 MHz. The SDR 1, which operates from a single +3.6-VDC, 2-A supply, measures a mere 83 x 55 mm and includes a single serial C-Bus interface. The demonstrator can connect directly to the firm's model PE0002 Evaluation Kit Interface Card for ease of connection to personal computers (PCs).

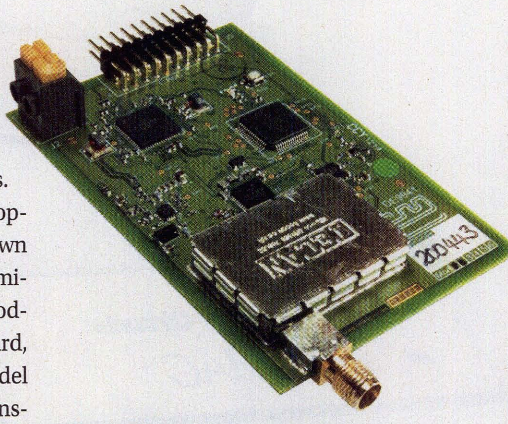

The model DE9941 SDR 1 is a software-defined-radio evaluation board that includes transmitter, receiver, and modem ICs along with supporting hardware.

The DE9941 SDR Demonstration Board has three CML Microcircuits radio ICs: the aforementioned models CMX998, CMX994, and CMX7164. The CMX998 transmitter covers a frequency range of 30 MHz to 1 GHz and supports a wide range of linear modulation schemes, including QAM, quadrature phase shift keying QPSK, π/4 differential QPSK (DQPSK), eight-state phase-shift keying (8PSK) and orthogonal frequency division multiplex (OFDM). The broadband transmitter has low −148 dBc/Hz noise level and 360-deg loop phase-shift control.

The CMX994 receiver works with high-linearity downconversion mixers and several stages of baseband filtering for removal of out-of-band signals. The filters are followed by variable-gain baseband amplification. The bandwidths of the second-stage filters can be scaled for multiple-channel-bandwidth applications, such as 6.25-, 12.50-, and 25.00-kHz channels.

The receiver IC also incorporates a broadband in-phase/quadrature (I/Q) demodulator with frequency range of 100 to 940 MHz for direct-conversion applications. In addition, the IC boasts a broadband low-noise amplifier (LNA) with wide gain-control range. The receiver can support low-frequency operation to 50 MHz, and can operate with its own local-oscillator (LO) circuitry or an external LO. On-board LO generation is provided by an integer-N phase-lock loop (PLL) and voltage-controlled oscillator (VCO) with negative-resistance amplifier. The LO can operate in divide-by-2/4/6 modes for multiple-frequency-band operation.

The CMX994 receiver's outputs are differential I/Q signals which are applied to the analog-to-digital converters (ADCs) in the CMX7164 modem IC. The half-duplex model CMX7164 modem supports a wide range of modulation modes in multiple-channel arrangements. Together, the modem, transmitter, and receiver ICs combine to form a versatile SDR demonstrator board designed to operate with a single low-voltage support for ease of integration in demonstration or prototype evaluation systems. It is a painless means for evaluating the benefits of SDR radio functionality for a wide range of systems.—*JB*

CML MICROCIRCUITS (USA), INC., 465 Corporate Square Dr., Winston-Salem, NC 27105; (336) 744-5050, (800) 638-5577, FAX: (336) 744-5054, e-mail: us.sales@cmlmicro.com, *www.cmlmicro.com*.

Infocenter

*Domestic Edition only **International Edition only This index is provided as an additional service by the publisher, who assumes no responsibility for errors or omissions.

MARKETING & ADVERTISING STAFF

VICE PRESIDENT & MARKET LEADER
BILL BAUMANN
T: (212) 204-4365
bill.baumann@penton.com

BRAND DIRECTOR, e|DESIGN
CENTRAL U.S.
TRACY SMITH
T: (913) 967.1324 F: (913) 514.6881
E: tracy.smith@penton.com

BRAND CHAMPION
NORTHEAST
DAVID MADONIA
T: (212)-204-4331
E: dave.madonia@penton.com

SOUTH
BILL YARBOROUGH
T: (713) 636-3809 T: (713) 523-8384
E: bill.yarborough@penton.com

NORTHERN CALIFORNIA, NEVADA, NORTHWEST
JAMIE ALLEN
T: (415) 608-1959 F: (913) 514-3667
E: jamie.allen@penton.com

ONLINE SALES DEVELOPMENT DIRECTOR
STEPHANIE CAMPANA
T: (312) 840-2403-8437
stephanie.campana@penton.com

EUROPEAN SALES REP
MARK DURHAM
T: +44 (0)7958 564137
E:mark.durham@penton.com

TAIWAN, R.O.C.
CHARLES C.Y. LIU
T: (886)-2-2727-7799 F: (886)-2-2728-3686

JAPAN
HIRO MORITA
T: 81-3-3261-4591 F: 81-3-3261-6126

KOREA
JO YOUNG SANG
T: 011-82-2-739-7840
F: 011-82-732-3662

CUSTOMER SERVICE - SUBSCRIPTIONS
New/Renew/Cancel/Change Address/Missing and Back Issues
T: 866-505-7173 F: 847-763-9673
E: microwaves&rf@halldata.com

Subscription Assistance and Information: Microwaves & RF (ISSN 0745-2993) is published monthly, except semi-monthly in December. **Microwaves & RF** is sent free to individuals actively engaged in high-frequency electronics engineering. In addition, paid subscriptions are available. Subscription rates for U.S. are $95 for 1 year ($120 in Canada, $150 for International). Published by Penton Media, Inc., 9800 Metcalfe Ave., Overland Park, KS 66212-2216. Periodicals Postage Paid at Shawnee Mission, KS and at additional mailing offices.
POSTMASTER: Send change of address to Microwaves & RF, Penton Media Inc., P.O. Box 2095, Skokie, IL 60076-7995. For paid subscription requests, please contact: Penton Media Inc., P.O. Box 2100, Skokie, IL 60076-7800. Canadian Post Publications Mail agreement No. 40612608. Canadian GST# R126431964. Canada return address: Bleuchip International, P.O Box 25542,London, ON N6C6B2.

Back issues of **MicroWaves** and **Microwaves & RF** are available on microfilm and can be purchased from National Archive Publishing Company (NAPC). For more information, call NAPC at 734-302-6500 or 800-420-NAPC (6272) x 6578. Copying: Permission is granted to users registered with the Copyright Clearance Center, Inc. (CCC) to photocopy any article, with the exception of those for which separate copyright ownership is indicated on the first page of the article, provided that a base fee of $1.25 per copy of the article plus 60 cents per page is paid directly to the CCC, 222 Rosewood Dr., Danvers, MA 01923. (Code 0745–2993/02 $1.25 +.60) Copying done for other than personal or internal reference use without the expressed permission of Penton Media, Inc., is prohibited. Requests for special permission or bulk orders should be addressed in writing to the publisher.

50-V GaN HEMTs Power LTE Networks

These internally matched, high-efficiency 100- and 200-W power transistors are suitable for linear amplifiers in LTE cellular and telecommunications applications through 2.7 GHz.

COST-EFFECTIVELY BOOSTING radio signals at high power levels is critical to the long-term financial health of cellular communications. Cree, Inc. (www.cree.com) looks to have made some significant steps in the right direction with the introduction of its new +50-VDC gallium-nitride (GaN) high-electron-mobility-transistor (HEMT) devices.

Cree's new 50-V GaN HEMT devices include 100-W models CGHV22100F and CGHV22100P in flange- and surface-mount ceramic-metal housings **(see figure)**, respectively, for applications from 1.8 to 2.2 GHz. Also included are 100-W models CGHV27100P and CGHV27100F for applications from 2.5 to 2.7 GHz. In addition, the company also announced the availability of several 200-W models.

Models CGHV22100F and CGHV22100P provide typical gain of 20 dB from 1800 to 2200 MHz, with gain levels of 18.7 dB at 1800 MHz, 20.7 dB at 2000 MHz, and 22.0 dB at 2200 MHz when delivering +44 dBm output power into a Cree amplifier test fixture. The 100-W GaN transistors offer good linearity, based on adjacent-channel-leakage-ratio (ACLR) performance of –37.8 dBc at 1800 MHz, –37.1 dBc at 2000 MHz, and –35.1 dBc at 2200 MHz. At +44 dBm output power, the drain efficiency is 35.4% at 1800 MHz, 31.7% at 2000 MHz, and 30.6% at 2200 MHz.

Models CGHV22200F and CGHV2200P are flange- and surface-mount packaged devices, respectively, with 16.6 dB gain at 1.8 GHz, 19.2 dB gain at 2.0 GHz, and 18.1 dB gain at 2.2 GHz. These 200-W GaN transistors offer drain efficiency of 31.5% at 1.8 GHz and +47 dBm output power, 31.9% at 2.0 GHz and +47 dBm output power, and 34.8% at 2.2 GHz and +47 dBm output power. For +47-dBm output power, they achieve ACLR of –37.4 dBc at 1.8 GHz, –37.4 dBc at 2.0 GHz, and –35.6 dBc at 2.2 GHz.

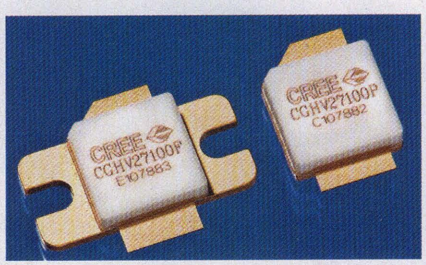

The 100- and 200-W 50-V LTE GaN HEMTs are supplied in a choice of rugged flange-mount (left) or surface-mount ceramic-metal packages.

Models CGHV27100F and CGHV27100P are flange- and surface-mount-packaged GaN HEMTs, respectively, rated for 100 W output power from 2.5 to 2.7 GHz. Meanwhile, models CGHV27200F and CGHV27200P are GaN HEMTs with 200-W output-power capability from 2.5 to 2.7 GHz **(see table)**. The 100-W devices deliver 18.0-dB typical gain with –37 dBc ACLR and 33% drain efficiency at 25 W average output power. At +44-dBm output power, these GaN power transistors provide 18.1-dB gain at 2.5 GHz, 18.0-dB gain at 2.6 GHz, and 17.9-dB gain at 2.7 GHz. At that output-power level, the drain efficiency is typically 34.0% at 2.5 GHz, 33.5% at 2.6 GHz, and 32.0% at 2.7 GHz, while the ACLR is typically –37.0 dBc at all three test frequencies (2.5, 2.6, and 2.7 GHz).

The 200-W transistors achieve 16-dB typical gain from 2.5 to 2.7 GHz, with -37 dBc ACLR and 29% drain efficiency at 40 W average output power across that 200-MHz bandwidth. At +47-dBm output power, these devices offer 15.0-dB gain at 2500 MHz, 16.0-dB gain at 2600 MHz, and 16.0-dB gain at 2700 MHz. The drain efficiency at that output level is 29.0% at 2500 MHz, 28.5% at 2600 MHz, and 29.0% at 2700 MHz, while the ACLR is –6.5 dBc at 2500 MHz, –37.5 dBc at 2600 MHz, and –37.0 dBc at 2700 MHz.—*JB*

CREE, INC., 4600 Silicon Dr., Durham, NC 27703; (919) 407-5639, *www.cree.com/rf*.

The 50-V GaN HEMTs at a glance.

Model	Frequency range	Output power	Gain
CGHV22100F	1.8 to 2.2 GHz	100 W	20.7 dB at 2.0 GHz
CGHV22100P	1.8 to 2.2 GHz	100 W	20.7 dB at 2.0 GHz
CGHV27100F	2.5 to 2.7 GHz	100 W	18.0 dB at 2.6 GHz
CGHV27100P	2.5 to 2.7 GHz	100 W	18.0 dB at 2.6 GHz
CGHV22200F	1.8 to 2.2 GHz	200 W	19.2 dB at 2.0 GHz
CGHV22200P	1.8 to 2.2 GHz	200 W	19.2 dB at 2.0 GHz
CGHV27200F	2.5 to 2.7 GHz	200 W	16.0 dB at 2.6 GHz
CGHV27200P	2.5 to 2.7 GHz	200 W	16.0 dB at 2.6 GHz

Get a piece of the ARRA pie...

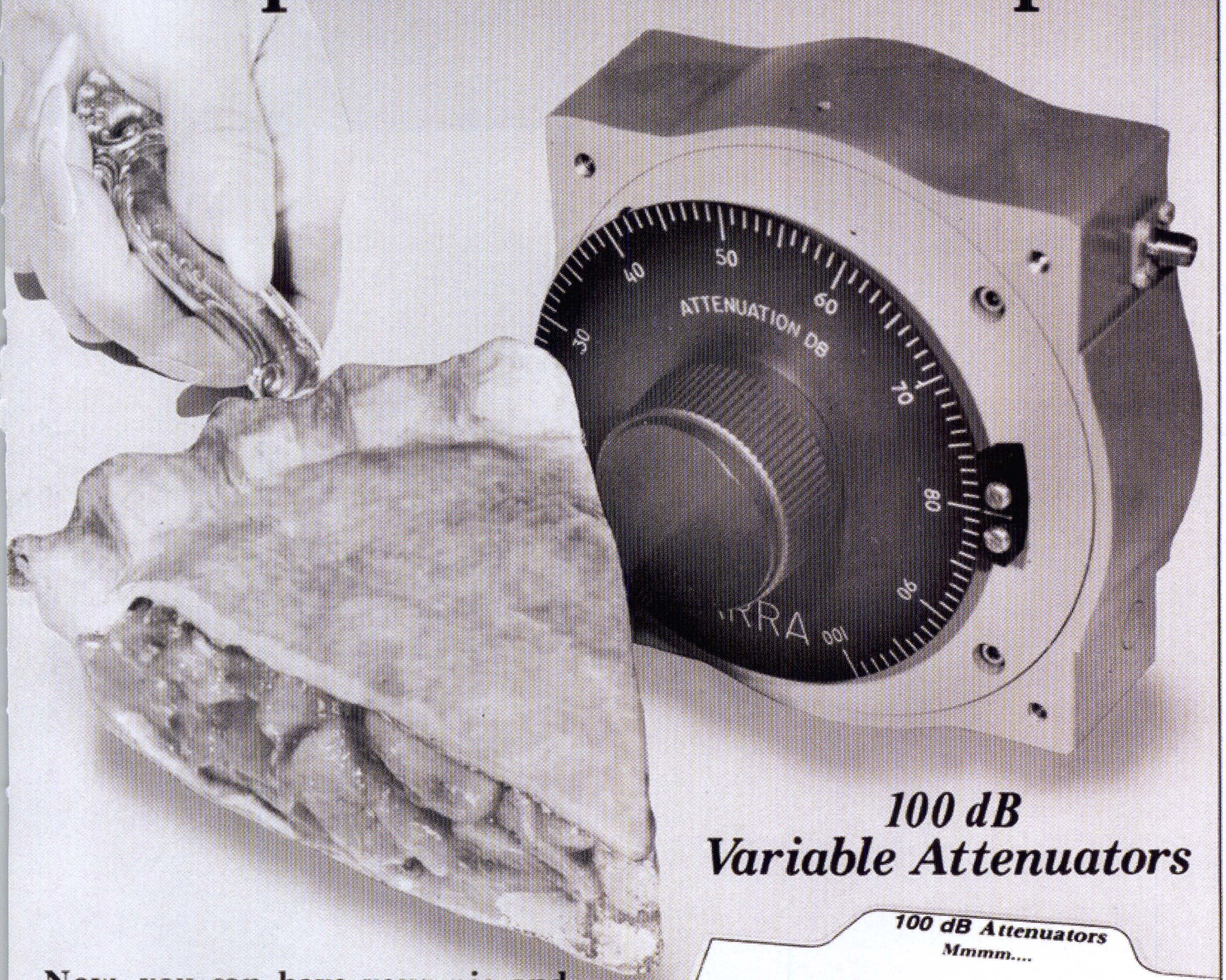

100 dB Variable Attenuators

100 dB Attenuators
Mmmm....

Freq Range	Atten vs Freq dB	Model #
500 - 1000 MHz	1.5	2952 - 100
900 - 1300 MHz	0.75	2-3952 - 100
1000 - 2000 MHz	1.5	3952 - 100X
2000 - 4000 MHz	1.5	4952 - 100X
4000 - 8000 MHz	1.5	5952 - 100X

Insertion loss - 6 dB
VSWR - 1.5
Power - 15 cw
Temperature -30 to +120 C

Now, you can have your pie and eat it too! Only from ARRA! Four models that cover the 500 to 8000 MHz frequency range! Available in lower attenuation ranges. ***Customerized to your requirements with little or no additonal charge.*** Top performance. Super dial accuracy.

- Direct reading dial
- Extremely high reliability
- Non-contacting movable parts (our special recipe)
- High power version available (up to 200 W)
- Usage will not change calibration
- Attenuation will not vary with temperature
- Excellent phase characteristics
- Type N standard SMA connectors available

Applications include:
•TACAN •DME/IFF •Lab standards •Altimeter
Or any other requirements needing high attenuation and accurate dial reading.

Visit our website at www.arra.com
E-Mail: sales@arra.com

Some of the best attenuator recipes you can find are cooking at ARRA right now! Send for your copy today and get a piece of the ARRA pie.

...the last word in variable attenuators

ARRA INC.
15 Harold Court • Bay Shore NY 11706-2296

Tel 631-231-8400 Fax 631-434-1116